PHYSIOLOGICAL REVIEWS
Vol. 79, No. 4, October 1999
Printed in U.S.A.

Measurement of Intracellular Calcium

AKIYUKI TAKAHASHI, PATRICIA CAMACHO, JAMES D. LECHLEITER, AND BRIAN HERMAN

Departments of Cellular and Structural Biology and of Physiology, and Department of Molecular Medicine, Institute of Biotechnology, University of Texas Health Science Center at San Antonio, San Antonio, Texas

Takahashi, Akiyuki, Patricia Camacho, James D. Lechleiter, and Brian Herman. Measurement of Intracellular Calcium. *Physiol. Rev.* 79: 1089–1125, 1999.—To a certain extent, all cellular, physiological, and pathological phenomena that occur in cells are accompanied by ionic changes. The development of techniques allowing the measurement of such ion activities has contributed substantially to our understanding of normal and abnormal cellular function. Digital video microscopy, confocal laser scanning microscopy, and more recently multiphoton microscopy have allowed the precise spatial analysis of intracellular ion activity at the subcellular level in addition to measurement of its concentration. It is well known that Ca^{2+} regulates numerous physiological cellular phenom-

ena as a second messenger as well as triggering pathological events such as cell injury and death. A number of methods have been developed to measure intracellular Ca^{2+}. In this review, we summarize the advantages and pitfalls of a variety of Ca^{2+} indicators used in both optical and nonoptical techniques employed for measuring intracellular Ca^{2+} concentration.

I. INTRODUCTION

Calcium acts as a universal second messenger in a variety of cells. The beginning of life, the act of fertilization, is regulated by Ca^{2+} (31, 378, 423). Numerous functions of all types of cells are regulated by Ca^{2+} to a greater or lesser degree. More than 100 years ago, Ringer and co-workers (316–321) demonstrated that Ca^{2+}-containing perfusate was required for the normal contraction of frog heart. In the 1940s, it was found that an injection of Ca^{2+} into a muscle fiber induced contraction, but K^+, Na^+, or Mg^{2+} did not (145, 147, 184). Heilbrunn (144, 146) emphasized the potential roles of Ca^{2+} in various cellular functions; however, it took a long time until his ideas were broadly accepted. In the 1960s, Ebashi and Lipmann (95, 99) discovered an intracellular Ca^{2+} storage site, the sarcoplasmic reticulum, in muscle fibers. Subsequently, they clarified the exact mechanism of muscle contraction and the role of the Ca^{2+}-binding protein troponin in contraction of striated muscle of higher vertebrates (96–98). After that, it was shown that Ca^{2+}-binding proteins existed in a variety of cells and acted as linkers between Ca^{2+} the messenger and various cellular phenomena (182, 183, 202), which facilitated analysis of the potential functions of Ca^{2+} in a variety of cells. Cells themselves control intracellular Ca^{2+} concentration ($[Ca^{2+}]_i$) strictly with several Ca^{2+} regulatory mechanisms, such as Ca^{2+} channels, Ca^{2+} pumps, and Ca^{2+} exchangers.

Since the 1920s, scientists have attempted to measure $[Ca^{2+}]_i$, but few were successful. The first reliable measurements of $[Ca^{2+}]_i$ were performed by Ridgway and Ashley (314) by injecting the photoprotein aequorin into the giant muscle fiber of the barnacle. Subsequently, in the 1980s, Tsien and colleagues (127, 254, 401, 402, 405, 427) produced a variety of chemical fluorescent indicators. These reagents have provided trustworthy methods for measuring $[Ca^{2+}]_i$. Since the development of these monitors, investigations of Ca^{2+}-related intracellular phenomena have skyrocketed.

As might have been predicted, the interests of many researchers shifted from $[Ca^{2+}]$ analysis at the cellular level to that of the subcellular level. It has been found that $[Ca^{2+}]$ is not even distributed throughout the whole cell and that intracellular heterogeneity of $[Ca^{2+}]$ (such as Ca^{2+} waves and Ca^{2+} sparks) is observed in a variety of cells (e.g., oocyte, heart muscle cell, hepatocyte, and exocrine cell) (53, 64, 118, 187, 216, 302, 331, 390, 391). With the advent of the confocal laser scanning microscope (CLSM) in the 1980s (42, 424, 425), measurement of intracellular Ca^{2+} has accelerated significantly. Confocal laser scanning microscopy, and more recently multiphoton microscopy, allows the precise spatial and temporal analysis of intracellular Ca^{2+} activity at the subcellular level in addition to measurement of its concentration. This is due to the fact that the emitted fluorescence detected by the CLSM and multiphoton microscopes are limited to a specific focal plane. These optical techniques have enabled scientists to document the spatial movement of $[Ca^{2+}]$ in cells (32, 223).

Because of the importance of Ca^{2+} in biology, numerous techniques/methods for analyzing the mechanisms of cellular and/or subcellular Ca^{2+} activity have been established. Unfortunately, however, there is no one best technique/method with which one can measure Ca^{2+}. Although each method for analyzing Ca^{2+} activity has certain advantages over the others, each also suffers drawbacks. In this review, we summarize the advantages and pitfalls of some standard Ca^{2+} indicators, the methods used to measure Ca^{2+}, including some recent microscopic techniques, and procedures used for measuring cellular and/or subcellular Ca^{2+} activity in living cells.

II. CHEMICAL FLUORESCENT INDICATORS

A. Selection Criteria of Chemical Fluorescent Indicators

The most widely used Ca^{2+} indicators are chemical fluorescent probes because, in general, their signal (light) is quite large for a given change in $[Ca^{2+}]$ compared with other types of Ca^{2+} indicators. Most of the classical members of this group were produced by Tsien and colleagues (127, 254, 401, 402, 405).

There are several different fluorescent Ca^{2+} indicators, and it is important to select the most suitable probe for a given experiment (Table 1). They can be divided into various groups based on several different criteria. One way of dividing these probes into two groups is to separate them based on whether they are ratiometric versus nonratiometric (single wavelength) indicators. The former includes indo 1 and fura 2, whereas the latter includes fluo 3, the calcium green class, and rhod 2. The use of ratiometric indicators allows for correction of differences of pathlength and accessible volume in three-dimensional specimens.

Another important criteria for division is the excitation/emission spectra. The absorption spectra [e.g., ultra-

TABLE 1. *Fluorescent Ca^{2+} indicators*

Indicator	Forms	Absorption Wavelength, nm		Emission Wavelength, nm		Lifetime		K_d	F_{max}/F_{min} (R_{max}/R_{min})	Notes	Reference No.
		Ca^{2+} free	Ca^{2+} bound	Ca^{2+} free	Ca^{2+} bound	Ca^{2+} free	Ca^{2+} bound				
Quin 2	A, E	353	333	495	495	1.3	11.6	60 nM	5–8	Strong chelating effect	153, 209, 400, 405
Indo 1	A, E, D	346	330	475	401	0.3	1.7	230 nM	(20–80)	Dual-emission ratiometry (405/485 nm)	127, 180, 298, 384
Fura 2	A, E, D	363	335	512	505	1.72	2.1	224 nM	(13–25)	Dual-excitation ratiometry (340/380 nm), much compartmentalization and binding to proteins	106, 127, 189, 329, 386, 415, 427
Mag-indo 1	A, E, D	349	328	480	390			35 μM	(12)	Low affinity	399
Mag-fura 2 (furaptra)	A, E	369	329	511	508			25 μM	(6–30)	Low affinity	155, 198, 311, 379
Mag-fura 5	A, E	369	330	505	500			28 μM		Low affinity	65, 167
Indo 1FF	A, E	346	330	475	401			33 μM	(5–10.6)	Low affinity	111
Fura 2FF	A, E	360	335	505	505			35 μM		Low affinity	124
Indo PE3	A, E	346	330	475	408			260 nM		Leakage resistant	
Fura PE3	A, E	364	335	508	500			250 nM	(18)	Leakage resistant	159, 347, 415
Bis-fura 2	A	366	338	511	504			370 nM		Brighter signal, dual-excitation ratiometry (340/380 nm)	271
C_{18}-fura 2	A	365	338	501	494			150 nM	(22–26)	Near membrane	105, 106
FIP18	A, E	346	335	502	495			450 nM		Near membrane	
FFP18	A, E	364	335	475	408			400 nM	(7)	Near membrane	106, 415
Benzothiaza-1	A, E	368	325	470	470			660 nM		Dual-excitation ratiometry (340/380 nm), moderate affinity	
Benzothiaza-2	A, E	368	325	470	470			1.4 μM		Dual-excitation ratiometry (340/380 nm), moderate affinity	
BTC	A, E	464	401	533	529	0.7	1.4	7 μM	(4–10)	Dual-excitation ratiometry with relatively long wavelength (400/480 nm)	163–165, 172, 437
Fluo 3	A, E	503	506	526	526	0.79	2.33	400 nM	40–100	The most popular visible wavelength indicator (suited to CLSM and flow cytometry)	185, 254, 281, 336
Fluo 3FF	A, E	506	515	526	526			41 μM		Low affinity	74
Fluo-LR	A, E	506	506	525	525			550 nM		Leakage resistant	
Fluo 4	A, E	491	494	none	516			345 nM	>100	Stronger absorption than fluo 3, large quantum yield, faster loading than fluo 3-AM	
Fluo 5N	A, E	491	494	none	516			90 μM		Low affinity	
Mag-fluo 4	A, E	490	493	none	516			22 μM		Low affinity, less Ca^{2+}/Mg^{2+} selectivity than fluo 5N	
Calcium green-1	A, E, D	506	506	531	531	1.05, 0.46	3.60, 3.53	190 nM	~14	Large quantum yield	100, 208, 336
Calcium green-2	A, E	506	503	536	536			550 nM	60–100	Large quantum yield, larger increase of emission fluorescence upon binding Ca^{2+} than calcium green-1	116, 312, 369
Calcium green-5N	A, E	506	506	532	532			14 μM	~38	Low affinity	310, 408, 437
Calcium orange	A, E	549	549	575	576	1.24	2.33	185 nM	~3	Suitable for $[Ca^{2+}]$ measuring by lifetime imaging (broad measurable range)	92, 100, 208
Calcium orange-5N	A, E	549	549	582	582			20 μM	~5	Low affinity	271, 437
Calcium crimson	A, E, D	590	589	615	615	2.56, 2.1	4.1, 4.9	185 nM	~2.5	Suitable for $[Ca^{2+}]$ measuring by lifetime imaging (broad measurable range)	100, 152, 208
Oregon green BAPTA 488-1	A, E, D	494	494	523	523			170 nM	~14	pH insensitive	40, 396
Oregon green BAPTA 488-2	A, E	494	494	523	523			580 nM	~100	pH insensitive, larger increase of emission fluorescence upon binding Ca^{2+} than Oregon green BAPTA-1	88
Oregon green BAPTA 488-5N	A, E	494	494	521	521			20 μM	~44	pH insensitive, low affinity	74, 88
Fura red	A, E	472	436	657	637			140 nM	(5–12)	Dual-excitation ratiometry (420/480 nm), dual-emission ratiometry with fluo 3 or calcium green	89, 206, 225
Rhod 2	A, E	556	553	576	576			1 μM	14–100	Accumulation to mitochondria, relatively high K_d	132, 254, 388
X-rhod 1	A, E	576	580	none	602			700 nM		Accumulation to mitochondria, higher Ca^{2+} sensitivity than calcium crimson	
Rhod 5N	A, E	547	549	none	576			320 μM		Accumulation to mitochondria, low affinity	
X-rhod 5N	A, E	576	580	none	580			350 μM		Accumulation to mitochondria, low affinity	
Mag-rhod 2	A, E	547	549	none	577			70 μM		Accumulation to mitochondria, low affinity, Mg^{2+} indicator	
Mag-X-rhod 1	A, E	575	578	none	603			45 μM		Accumulation to mitochondria, low affinity, Mg^{2+} indicator	
Calcium green C_{18}	A	509	509	530	530			280 nM	~8	Near membrane	231
Fura-indoline-C_{18}	A	612	498	711	694			260 nM		Near membrane	

This table is based on *The Handbook of Fluorescent Probes and Research Chemicals* (6th ed.) by Molecular Probes, Texas Fluorescence Lab 1998 catalog and other published papers. A, E, and D in the forms column represent the active form or acid, ester, and dextran conjugate, respectively. K_d, dissociation constant; F_{max}/F_{min}, ratio of maximum fluorescence to minimum fluorescence; R_{max}/R_{min}, ratio of maximum fluorescence ratio to minimum fluorescence ratio.

violet (UV) or visible wavelength (blue, green, and red)] of the indicator should be examined closely and optimally matched to the maximal output of the excitation light source. In particular, when using single- or multi-photon excitation lasers, the excitation wavelength is fixed so that indicators need to be selected such that the maximum probe absorbance occurs at the available wavelengths of the laser in the system. Recently, it has become popular to use multiple dyes to analyze different parameters simultaneously (e.g., $[Ca^{2+}]$ and pH or $[Ca^{2+}]$ and membrane potential) or to measure $[Ca^{2+}]$ in targeted subcellular components such as mitochondria (36, 59, 60, 221, 232, 238, 239, 300, 360, 413, 438). Hence, the emission spectra of Ca^{2+} indicators are the most essential factor in selection of dyes for multiple staining. Calcium indicators are categorized into several groups according to their emission: *1*) blue-emission group: quin 2, indo 1, benzothiaza, and fura 2; *2*) green-emission group: fura 2, BTC, fluo 3, calcium green, and Oregon green 1,2-bis(2-aminophenoxy)ethane-*N*,*N*,*N*′,*N*′-tetraacetic acid (BAPTA); *3*) yellow- and orange-emission group: calcium orange, calcium crimson, and rhod 2; and *4*) red- and near infrared-emission group: calcium crimson and Fura red.

Another consideration in selection of indicators is their chemical form. Calcium indicators are provided commercially in various forms such as salt (acid), ester, and dextran conjugates. The methods for incorporating the indicator into cells is dependent on the chemical form of the indicator (see sect. IV).

One of the most important considerations in choosing an indicator is its Ca^{2+}-binding affinity, which is reflected in the dissociation constant (K_d). Calcium indicators are thought to shift their absorption or emission spectrum or change their emitted fluorescence intensity in response to Ca^{2+} at a concentration range between $0.1 \times K_d$ to $10 \times K_d$. However, Ca^{2+} sensitivity is generally most reliable in a $[Ca^{2+}]$ range below and very near the K_d (246). Although high affinity (low K_d) Ca^{2+} indicators may emit bright fluorescence, they may also buffer intracellular Ca^{2+}. Moreover, because a high-affinity Ca^{2+} indicator becomes saturated at relatively low $[Ca^{2+}]$, errors in $[Ca^{2+}]$ estimation can occur. Recently, low-affinity (high K_d) fluorescent Ca^{2+} indicators have been produced. One of the uses of low-affinity indicators is to measure Ca^{2+} levels in subcellular organelles. For example, regulation of Ca^{2+} in the sarcoplasmic reticulum or endoplasmic reticulum is thought to be one of the important regulators of Ca^{2+}-dependent physiological phenomena, but levels of $[Ca^{2+}]$ in these organelles are quite high and it has been difficult to measure them with the conventional high-affinity Ca^{2+} indicators because of their buffering effects and the large separation between the K_d of the indicator and organelle $[Ca^{2+}]$. Recently, monitoring of $[Ca^{2+}]$ in organelles with low-affinity Ca^{2+} indicators has been reported (124, 155, 399). These low-affinity Ca^{2+} indicators can also be used to measure rapid changes in $[Ca^{2+}]$. Because of their low affinity for Ca^{2+}, the kinetics of the reactions are rapid enough to analyze Ca^{2+} alterations accompanying muscle contraction with high temporal resolution, as has recently been described (65, 104, 198).

B. Ultraviolet-Wavelength Excitation Fluorescent Indicators

The first popular chemical fluorescent Ca^{2+} indicators were the UV-excitable indicators. Subsequently, several visible wavelength-excitable Ca^{2+} indicators have been produced, but UV-excitation indicators are still widely used as a quantitative ratiometric Ca^{2+} indicators. The UV-based ratiometric Ca^{2+} indicators suffer from the disadvantage that they require UV excitation. Ultraviolet irradiation is known to be more cytotoxic compared with long-wavelength irradiation (41). Moreover, some intracellular constituents emit intrinsic fluorescence when excited in the UV portion of the electromagnetic spectrum, which may interfere with precise evaluation of $[Ca^{2+}]$. For example, because the excitation and emission peak of NADH are 340 and 440–470 nm, respectively (139, 292), it is necessary to estimate if fluorescence from these substances contaminates the true UV-excited Ca^{2+} indicator fluorescence. In addition, there are several optical problems associated with the use of UV-excitation sources, i.e., common microscopic objectives are not chromatically corrected for use with UV light. Although this is not so severe a problem in wide-field microscopy, corrections for chromatic aberrations are crucial for confocal imaging. Consequently, UV-based laser systems require specialized optical components (253, 280), which increases its cost and decreases overall signal intensity.

1. Quin 2

Quin 2 is one of the first-generation fluorescent Ca^{2+} indicators (400, 405). Following excitation at 339 nm, quin 2 shows a five- to sixfold increase in emission fluorescence when bound to Ca^{2+}. In contrast, the emitted fluorescence decreases when excited at 365 nm, which allows dual-excitation ratiometry (69). However, the absorption coefficient and the quantum yield of quin 2 are low and hence, at concentrations needed to measure observable fluorescence, quin 2 buffers cellular Ca^{2+}. Therefore, quin 2 has most recently been used not as a simple indicator for measuring $[Ca^{2+}]_i$ but as a buffer of intracellular Ca^{2+}. For example, in certain situations, it has been hard to determine the function of a specific regulator of Ca^{2+} (e.g., Ca^{2+} channel on the plasma membrane) due to the intrinsic Ca^{2+}-buffering capacity by other cellular Ca^{2+} regulators. To study specifically the influx or efflux of Ca^{2+} at the plasma membrane, deliber-

ate overloading of cells with quin 2 has provided increased intracellular Ca^{2+}-buffering capacity (108, 260) and reduction of the interference by other intrinsic Ca^{2+}-buffering capacity (176, 393, 410, 411). Quin 2 has also been used as an intracellular Ca^{2+} chelator (66, 123, 153, 433).

2. Indo 1

Indo 1 is one of the most popular Ca^{2+} indicator (127). This indicator was synthesized in a similar design of BAPTA, which is a more pH-insensitive chelator than EGTA between pH 6.0 and 8.0 (141, 435) and has high selectivity for Ca^{2+} over Mg^{2+} (401). Indo 1 has several advantages over quin 2, including *1*) greater selectivity for Ca^{2+} over other divalent cations such as Mg^{2+}, Mn^{2+}, and Zn^{2+}; *2*) a shift in emission wavelength upon binding Ca^{2+}; and *3*) increased fluorescence quantum efficiency and lower affinity for Ca^{2+} relative to quin 2, resulting in less buffering of cellular Ca^{2+} and easier observation of intracellular Ca^{2+} kinetics (127). Indo 1 is one of the ratiometric Ca^{2+} indicators. Indo 1 exhibits a Ca^{2+}-induced wavelength shift in emission rather than excitation, which allows an increase in the speed of $[Ca^{2+}]$ measurements using separate cameras or photodetectors. The absorption maximum of indo 1 is 330–350 nm. The fluorescence emission at 400–410 nm increases and that at 485 nm decreases when indo 1 combines with Ca^{2+} (Fig. 1). Thus the ratio of the emitted fluorescence intensities at 410 and 485 nm allows accurate estimation of $[Ca^{2+}]_i$ independent of optical path length or total dye concentration. Such ratio measurements also correct for uneven dye loading, dye leakage, photobleaching, and changes in cell volume, e.g., during contraction in muscle cells (43, 252, 416) (Fig. 2). However, one of the most famous disadvantages of indo 1 is its rapid photobleaching. It has been reported that the rate of photobleaching does not affect the emission ratio much if the UV illumination is not excessive (416). However, rapid photobleaching has the potential to decrease signal-to-noise ratio (416). In addition, it has been reported that UV illumination induces photodegradation of indo 1 (342). Ultraviolet illumination generates a Ca^{2+}-insensitive fluorescent compound from indo 1 whose emission spectrum is quite close to Ca^{2+}-free indo 1, resulting in underestimation of $[Ca^{2+}]$ measurements (342). Moreover, the intracellular milieu can change indo 1's emission spectrum (161, 289). Also, autofluorescence due to NADH, whose excitation and emission are 340 and 440–470 nm, respectively, overlaps with the spectrum of Ca^{2+}-free indo 1.

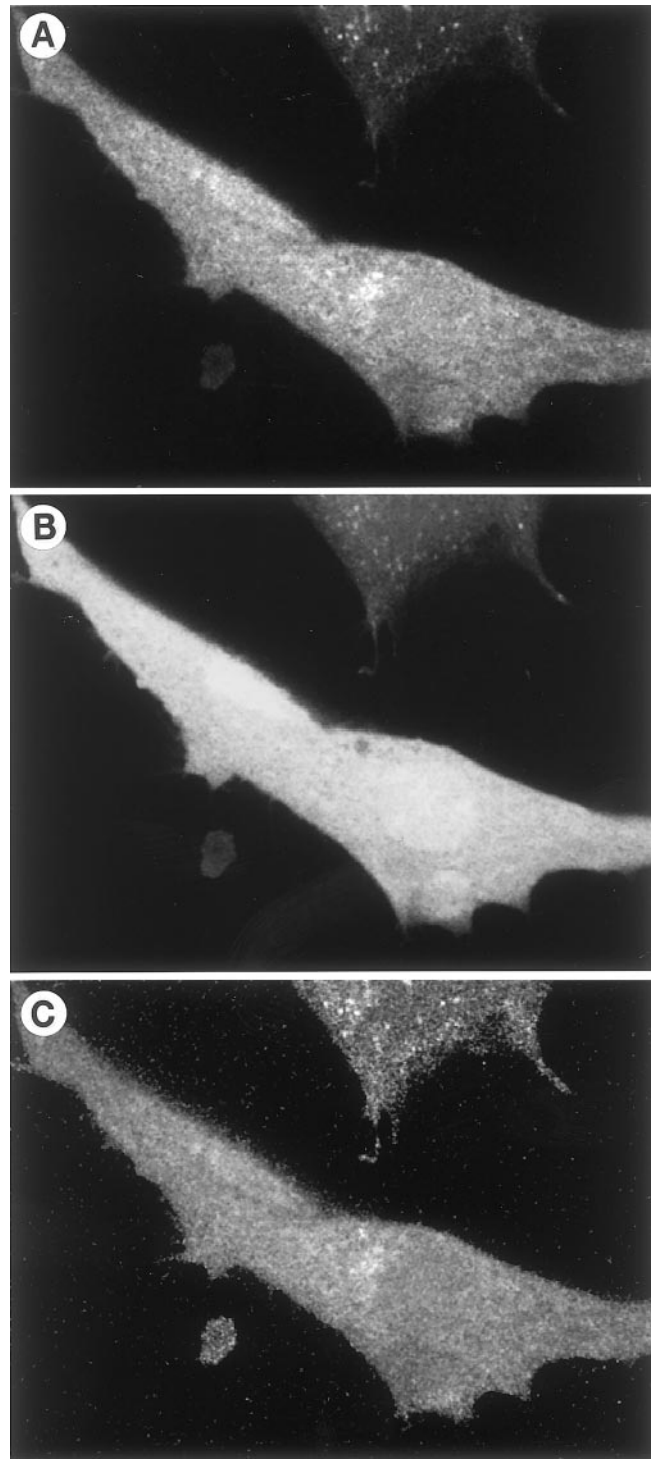

FIG. 1. Two-photon excitation microscope images of indo 1-labeled cells. Images of indo 1-loaded BHK cells were obtained using two-photon excitation laser scanning microscopy (TPLSM). Excitation wavelength was 700 nm, and emission fluorescence was divided into 2 channels. *A*: obtained from channel 1 using 380- to 420-nm band-pass filter. *B*: obtained from channel 2 using 470- to 490-nm band-pass filter. *C*: ratiometric image from channels 1 and 2.

3. Fura 2

Fura 2 is also a UV-excited Ca^{2+} indicator that allows ratiometric measurement. However, unlike indo 1, upon binding Ca^{2+}, fura 2 undergoes a shift in absorption rather than the emission peak (127). The maximal absorption peaks are 335 and 363 nm at maximal and minimal $[Ca^{2+}]$, respectively, and the emission peak of both Ca^{2+}-bound

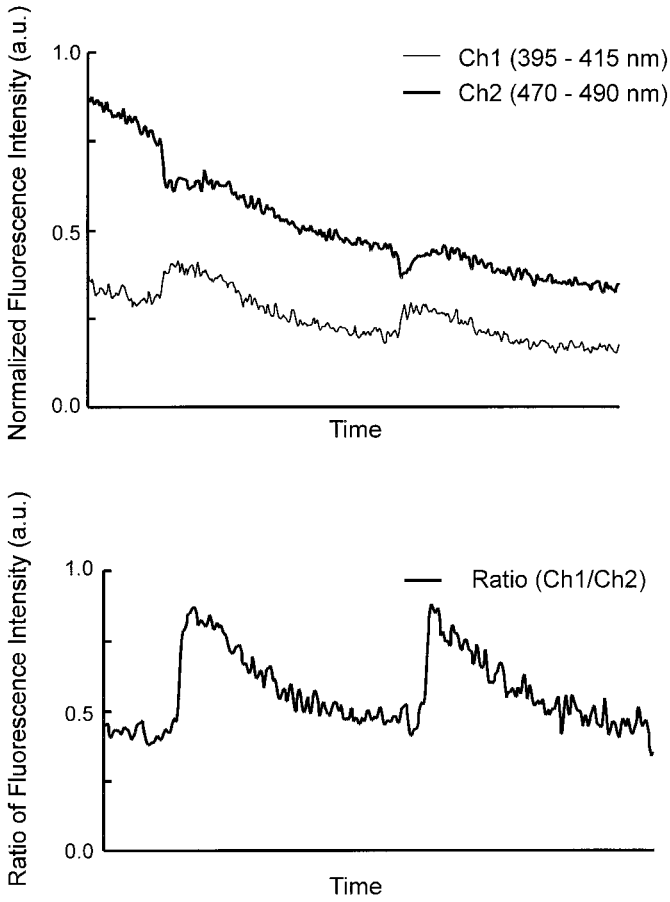

FIG. 2. Ratiometric measurement of $[Ca^{2+}]$ using indo 1. Beating cultured heart muscle cells loaded with indo 1 were excited at 351 nm and scanned with ultraviolet (UV) confocal laser scanning microscopy (CLSM). *Top panel*: raw data of fluorescence intensity. *Bottom panel*: ratio between 2 channels during excitation-contraction coupling. Although fluorescence intensities obtained in both channels decreased gradually because of photobleaching, ratio measurement faithfully demonstrated reliable changes in $[Ca^{2+}]$ during cardiac myocyte contracture.

and Ca^{2+}-free forms of fura 2 is 500 nm (306, 427). For ratiometric measurements, excitation at 340 and 380 nm has usually been preferred (127), because the absorption peak of Ca^{2+}-free fura 2 is quite close to its isobestic point, and Ca^{2+}-free fura 2 emits greater than Ca^{2+}-bound fura 2 when excited by wavelengths longer than 370 nm. Although fura 2 is a good probe for use in wide-field microscopy, it is unfortunately not suited to Ca^{2+} measurements using CLSM or flow cytometry, because it is difficult to alter the excitation wavelength rapidly using this type of instrumentation. Compartmentalization and protein binding of fura 2-AM may be more pronounced than indo 1-AM (121, 166, 199, 329). This provides the potential for using fura 2 for monitoring $[Ca^{2+}]$ within certain subcellular components (122, 124), but may also affect its apparent Ca^{2+} sensitivity because the emission from fura 2 bound to protein or inside compartments does not reflect cytosolic $[Ca^{2+}]$ precisely. It has been reported that fura 2 also degenerates into a Ca^{2+}-insensitive but fluorescent compound induced by UV illumination, resulting in inaccuracy of ratiometric measurement of $[Ca^{2+}]$ (27).

4. Indo 1FF, fura 2FF, Mag-indo 1, Mag-fura 2, and Mag-fura 5

Indo 1FF and fura 2FF belong to the low Ca^{2+} affinity class of Ca^{2+} indicators (111, 124). They are sometimes quite useful for particular Ca^{2+} measurements because of their high K_d. For example, they are used for measurements of rapid changes of $[Ca^{2+}]$ as well as measuring very high Ca^{2+} levels in internal compartments (124, 133). It has been demonstrated that indo 1FF shows a blue shift in the emission spectra and changes in Ca^{2+} affinity dependent on the concentrations and types of environmental proteins (111). Mag-indo 1, Mag-fura 2 (furaptra), and Mag-fura 5 were produced as indicators to monitor the cytosolic Mg^{2+} concentration (270, 311). Unlike most Ca^{2+} indicators, which have low affinity for Mg^{2+}, these indicators display low affinity for Ca^{2+} but high affinity for Mg^{2+} (K_d values for Mg^{2+} of Mag-indo 1, Mag-fura 2, and Mag-fura 5 are 2.7, 1.9, and 2.3 mM, respectively, which are several times greater than that of fura 2; Refs. 198, 403) (162). The affinity for Ca^{2+} of these indicators is orders of magnitude lower than indo 1 or fura 2. Mag-fura 2 has been reported as a useful indicator for measuring fast response of $[Ca^{2+}]$ in stimulated frog skeletal muscle because Mg^{2+} reaction during electrical stimulation is two to three orders of magnitude slower and smaller than Ca^{2+} (198, 200). Care must be taken to consider local Mg^{2+} levels when using some of these indicators, because the potential exists that any observed spectral change in response to $[Ca^{2+}]$ may be interfered with by a change in $[Mg^{2+}]$ (157).

5. Fura PE3 and indo PE3

These are derivatives of fura 2 and indo 1, respectively, and their absorption and the emission spectra are almost identical to the original fura 2 and indo 1. However, they are structurally designed to be retained within the cytoplasm much longer than the parent compounds through the addition of a positive charge (415). Some reports have demonstrated that they are more reliable and useful than the original fura 2 and indo 1 because of their lower amount of dye leakage and compartmentalization (159). However, they have a greater tendency to crystallize and precipitate compared with fura 2 and indo 1, which results in a reduction in loading efficiency or dye precipitates in the cell (415). Moreover, fura PE3 may be a little more pH sensitive than fura 2 because of changes in electron-withdrawing effects (415). Although fluores-

cence of fura 2 can be quenched by Mn^{2+}, that of fura PE3 is quenched only by Ni^{2+}.

6. Bis-fura 2

Bis-fura 2 is also a derivative of fura 2 (271). It was produced by linking two fura fluorophores with one Ca^{2+}-binding site. The properties of bis-fura 2 that distinguish it from fura 2 are the following: *1*) the emitted fluorescence intensity is about twice that of fura 2, which allows reduction of dye concentration; *2*) the K_d is larger than that of fura 2, which expands the measurable [Ca^{2+}] range especially in the range above 500 nM of Ca^{2+}; and *3*) it has more negative charges, which facilitate better dye retention within the cytosol. One of disadvantages of bis-fura 2 is that it has been provided commercially only as a cell-impermeable form that requires invasive loading methods (337).

7. C_{18}-fura 2, FFP18, and FIP18

C_{18}-fura 2 and FFP18 are relatively novel Ca^{2+} indicators based on fura 2 (105, 106), and FIP18 is based on indo 1. C_{18}-fura 2 was synthesized by conjugating fura 2 to a lipophilic alkyl chain. After microinjection, this indicator is located at the inner plasma membrane, which allows estimation of local changes in [Ca^{2+}] at sites near the inner plasma membrane. However, the K_d of C_{18}-fura 2 is 150 nM, which is too low to detect great change in [Ca^{2+}] near the plasma membrane. FFP18 and FIP18 are more recent indicators for measurement of near-membrane [Ca^{2+}] (75). The K_d of FFP18 is three times greater than that of C_{18}-fura 2, which enables more accurate measurements at higher [Ca^{2+}] (75, 106, 415). In addition, it is less lipophilic than C_{18}-fura 2, resulting in faster diffusion out of the microinjection pipette into cells (106). FFP18 and FIP18 exist as AM forms, resulting in less invasive and easier incorporation of the indicators into cells (75). The calibration of intracellular indicators loaded as an AM form can be performed using extracellular perfusate containing Ni^{2+}, which does not cross the plasma membrane and quenches the indicators in the outer leaflet of the plasma membrane facing the perfusate (75). However, because of relatively dim fluorescence and slow diffusion, it takes a much longer time to obtain adequate fluorescence using either AM forms or microinjection compared with original fura 2 (75, 105). In addition, it is necessary to add Ni^{2+} in the external perfusate to quench fluorescence of the external indicators, which may limit experimental conditions. It has been also reported that all of FFP18 does not always associate only with the plasma membrane but may also associate with the nuclear membrane or membranes of peripheral sarcoplasmic reticulum (106).

8. BTC

N-[3-(2-benzothiazolyl)-6-[2-[2-[*bis*(carboxymethyl)-amino]-5-methylphenoxy]ethoxy]-2-oxo-2H-1-benzopryan-7-yl}-N-(carboxymethyl)-glycine (BTC) is also a dual-excitation ratiometric Ca^{2+} indicator (165). The excitation maximum shifts from 464 to 400 nm upon binding Ca^{2+}. The higher excitation wavelength compared with that of fura 2 or indo 1 should lower cellular cytotoxicity and autofluorescence when using this probe. Moreover, the K_d is 7.0 μM, which is much greater than that of fura 2 and indo 1. This lower Ca^{2+} affinity enables more accurate measurement of higher levels of [Ca^{2+}] (163, 172) and/or analysis of prompt changes in [Ca^{2+}] (312). When the AM form of BTC is incorporated into cells such as cultured neurons, it is quickly hydrolyzed in the cytosol and shows little compartmentalization (164). On the other hand, it has been reported that BTC is not suitable for analysis of [Ca^{2+}] in muscle fibers during contraction because of delayed response (although it is still better than fura 2), artifacts due to contractile motions, and effects on emission output by changes in interaction between BTC and myoplastic constituents (437). Because BTC also undergoes photodegradation the same as fura 2 or indo 1, Hyrc et al. (164) have emphasized the necessity of minimizing the light exposure time (164).

C. Visible-Wavelength Excitation Fluorescent Indicators

The visible-wavelength Ca^{2+} indicators have some advantages over UV-based Ca^{2+} indicators: *1*) their emissions are in regions of the electromagnetic spectrum where cellular autofluorescence and background scattering are less severe; *2*) the cytotoxicity of visible light is less than that of UV; and *3*) excitation with visible light enables one to monitor changes in [Ca^{2+}] while manipulating the observed change in [Ca^{2+}] using UV-sensitive caged compounds (119, 224, 396). Caged compounds are photosensitive chelators of ions or substances such as Ca^{2+} (406, 412), H^+ (350), ATP (279), and inositol trisphosphate (IP_3) (119). They exist in an inactivate form due to a combination with radicals such as those of the nitrophenyl group. Thus they are "chemically caged." They are activated (released from their cage) upon illumination (360 nm), which results in the breaking of the bounds between the nitrophenyl group and the substances. In the case of caged Ca^{2+} compounds, the affinity for Ca^{2+} is reduced by irradiation, resulting in release of Ca^{2+} in microseconds to milliseconds (129, 130). Use of these caged compounds requires caution because the caged form of the compound may buffer ions, and they may also quench the fluorescence of Ca^{2+} indicators at low [Ca^{2+}] (439).

1. Fluo 3

Fluo 3 is one of the most suitable Ca^{2+} indicators for CLSM and flow cytometry. Fluo 3 was synthesized from BAPTA by combination with a fluorescein-like structure (254). The absorption and emission peaks of fluo 3 are 506 and 526 nm, respectively. It can be excited with an argon-ion laser at 488 nm, and its emitted fluorescence (at wavelengths >500 nm) increases with increasing $[Ca^{2+}]$ (186, 254). Fluo 3 is reported to undergo a 40- to 200-fold increase in fluorescence upon binding Ca^{2+} (140, 254). Because the range of increase in $[Ca^{2+}]$ in many cells after stimulation is generally 5- to 10-fold, fluo 3 is a good probe to use with high sensitivity in this region. In known in vitro conditions, the K_d of fluo 3 has been estimated to be 400 nM (22°C, pH 7.0–7.5), but this value may be significantly influenced by pH, viscosity, and binding proteins in in vivo conditions (140) (see sects. v*B* and vi*G*). The most important disadvantage of fluo 3 may be the fact that it does not display a shift in its absorption or emission spectra upon binding Ca^{2+}, which makes it impossible to perform ratiometric measurements of $[Ca^{2+}]$ using just fluo 3. Ratiometric measurements may be made by using either fura red which is a longer wavelength Ca^{2+} indicator (see below), a Ca^{2+}-insensitive red fluorescent dye such as rhodamine and Texas red, or seminaphthorhodafluors (SNARF) as long as pH remains constant (87, 110, 225, 315). Although indo 1 is a popular ratiometric Ca^{2+} indicator that allows ratiometry with the emission intensities at two wavelengths, it has been difficult for many commercial CLSM to use UV excitation required for indo 1. This is gradually becoming less of a problem as UV-based confocal systems and multiphoton approaches are allowing use of UV-excitation probes in confocal situations, but they are still expensive in general. Double-labeled cells coloaded with fluo 3 and red spectral dye (e.g., fura red) and excited at 488 nm allow the use of visible-light CLSM to evaluate $[Ca^{2+}]$ via ratiometry. This ratiometric method has made the use of caged compounds much easier and flow cytometry more reliable (224, 281). However, differences between fluo 3 and the other dyes in photobleaching rates, compartmentalization, or responses to changes in intracellular environment might result in the measured changes in the ratio independent of changes in $[Ca^{2+}]$ (i.e., at constant $[Ca^{2+}]$) (224, 225, 341). In addition, when the AM forms are used, the calibration is often troublesome (110, 344). More recently, analogs of fluo 3, fluo 4, and fluo 5N (low affinity for Ca^{2+}) have been produced.

2. Calcium green

Calcium green, like fluo 3, is also a long-wavelength Ca^{2+} indicator. The absorption and emission spectra are quite similar to those of fluo 3, but the fluorescence of calcium green-1 at saturated $[Ca^{2+}]$ is fivefold higher than that of fluo 3. Thus lower concentrations of calcium green-1 can be used to measure resting and stimulated $[Ca^{2+}]$ accurately (100). Calcium green is classified into three types according to its Ca^{2+} affinity (the K_d values are 190 nM, 550 nM, and 14 μM). Although the affinity of calcium green-1 for Ca^{2+} is much higher than fluo 3 or calcium green-2, calcium green-5N has low affinity for Ca^{2+} so that it is useful for measurement of rapid changes in $[Ca^{2+}]$ or small changes in $[Ca^{2+}]$ at lower $[Ca^{2+}]$ (104). Calcium green-2 presents greatest maximum fluorescence (F_{max})-to-minimum fluorescence (F_{min}) ratio in the calcium green group (116). Calcium green has been also used for ratiometric measurements by dual loading with other dyes (62, 285, 368, 369).

3. Oregon green BAPTA

Oregon green BAPTA is a relatively new Ca^{2+} indicator based on BAPTA. Because the excitation peak is slightly blue-shifted compared with some of the fluorescein derivatives (e.g., calcium green), Oregon green BAPTA is more efficiently excited at 488 nm (40, 85). In addition, it has been reported that Oregon green provides greater photostability and less pH sensitivity in the physiological pH range than fluorescein (pK_a values of Oregon green and fluorescein are 4.7 and 6.4, respectively) (381, 414). In some types of cells (e.g., BHK cells and rat hepatocytes that we have investigated), the fluorescence of Oregon green BAPTA in the cytosol shows a rapid decrease, partially due to excretion by the plasma membrane anion transport system compared with calcium green or fluo 4 (Fig. 3) (see sect. iv*G*).

4. Calcium orange and calcium crimson

Calcium orange and calcium crimson are Ca^{2+} indicators based on tetramethylrhodamine and Texas red, respectively. The absorption and emission spectra are similar to the rhodamine and Texas red (absorption and emission peaks of calcium orange are 549 and 576 nm, respectively, and those of calcium crimson are 590 and 615 nm, respectively) (100), which enables dual-staining with blue or green fluorescent probes. Their K_d values are both 185 nM based on in vitro steady-state fluorescence intensity measurements, which are smaller than other visible-wavelength excitation indicators. However, they have attracted a great deal of attention because quantitative estimates of Ca^{2+} over a large range of $[Ca^{2+}]$ can be provided with these probes using time-resolved fluorescence lifetime imaging microscopy (TRFLM) (152, 208) (see sect. vii*A*).

5. Fura red

Fura red is structurally and chemically similar to fura 2. However, the excitation/emission spectra are shifted to

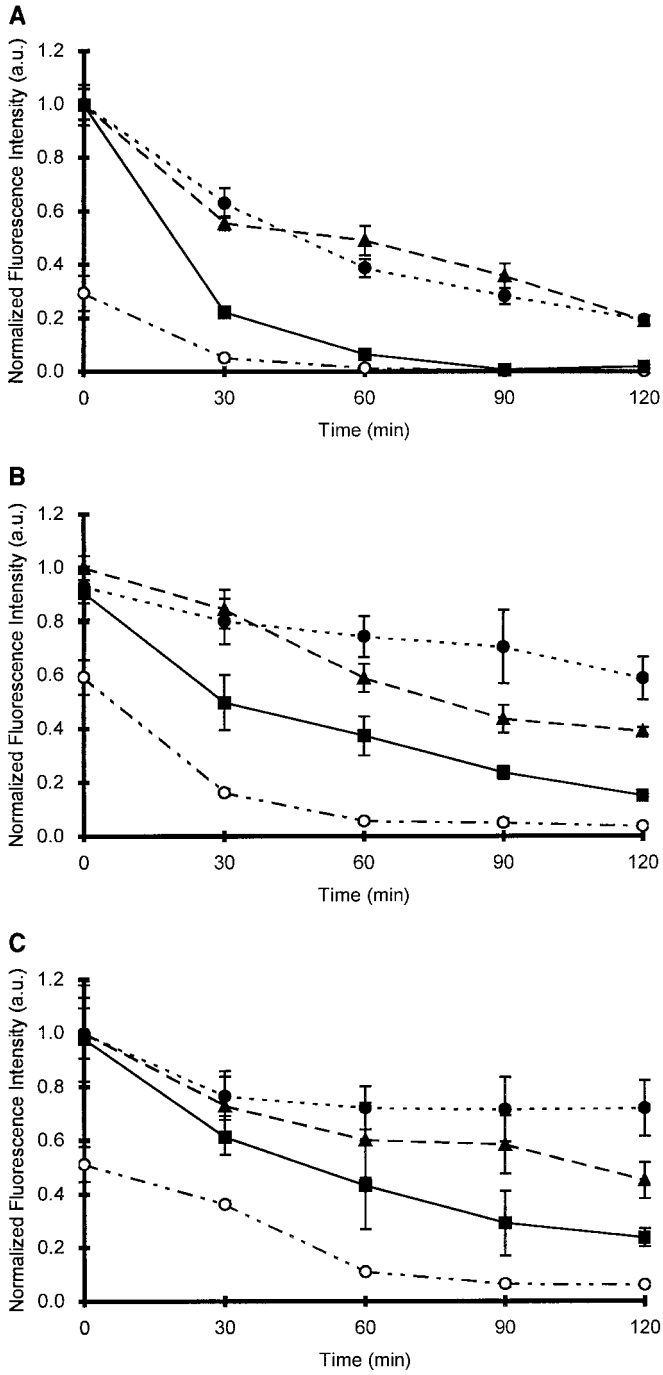

FIG. 3. Dye leakage of Ca^{2+} indicators from cytosol of BHK cells. Dye leakage from cytosol of BHK cells was compared among fluo 4, calcium green-1, and Oregon green BAPTA-2. BHK cells were loaded with AM forms of indicators (10 μM) for 30 min at 37°C and were then placed on a microscope stage at room temperature. Cells were bathed in medium (DMEM with 10% bovine calf serum) or phosphate-buffered solution with 10% bovine calf serum. Emitted fluorescence intensities were obtained using CLSM under identical conditions. Excitation wavelength was 488 nm, and fluorescence was collected between 510 and 550 nm. Open circle in each of graphs represents no probenecid added. Solid squares, triangles, and circles represent conditions where loading solution included 2.5 mM probenecid and external solution on microscope included 0, 2.5, and 5 mM probenecid, respectively. *A*: Oregon green BAPTA-2. *B*: calcium green-1. *C*: fluo 4.

the red, which eliminates interference from autofluorescence in most cells. Like fura 2, fura red offers ratiometric $[Ca^{2+}]$ measurement by excitation at 420 and 480 nm (emission range is wavelength longer than 550 nm) (206). When excited at a long wavelength such as 488 nm, fura red exhibits a decrease in emission upon Ca^{2+} binding. With the use of this property, simultaneous labeling with fura red and fluo 3 has been used for ratiometric measurements of $[Ca^{2+}]_i$ (86, 87, 110, 225, 371). Because the emitted fluorescence of fura red is much dimmer than that of fluo 3 (the fluorescence quantum efficiency is only 0.013 in the Ca^{2+}-free form; Ref. 186) and fura red is one of the Ca^{2+} indicators having the highest affinity for Ca^{2+} (K_d is 140 nM at pH 7.2, 22°C), the intracellular (and hence loading) concentrations have to be two or three times of that of fluo 3 (225, 344), which may result in Ca^{2+} buffering, limitation of measurable $[Ca^{2+}]$ range, and a requirement for higher excitation intensities (110).

6. *Rhod 2*

Rhod 2 is a rhodamine-based Ca^{2+} indicator produced by Tsien and co-workers (254). Recently, this indicator has been used for measurement of mitochondrial $[Ca^{2+}]$ in various kinds of cells (14, 160, 360, 398). Because the mitochondria exhibits a large potential difference (inside negative) across its membrane, the AM form of rhod 2, which is a multivalent cation, is effectively accumulated, hydrolyzed, and trapped in mitochondria as is the case with rhodamine-123 or tetramethylrhodamine methyl ester (TMRM) (177, 178, 219). It has been shown that by modulating the loading condition (e.g., temperature, time, preloading), rhod 2 can be selectively accumulated in the mitochondria of certain cells (398) and that the fluorescence of rhod 2 faithfully reports mitochondrial $[Ca^{2+}]$ (14, 160, 360). Because the excitation/emission spectra of rhod 2 is shifted to the red compared with Ca^{2+} indicators based on fluorescein, rhod 2 enables the measurement of both cytosolic and mitochondrial $[Ca^{2+}]$ in a single cell in combination with shorter wavelength Ca^{2+} indicators (14, 179). In addition, rhod 2 is often used for in situ measurement of $[Ca^{2+}]$ of brain cells (256, 388, 389). This may be partially due to the fact that the excitation/emission range of rhod 2 is long enough to reduce contamination of the observed emitted fluorescence by intrinsic autofluorescence signals (228). Moreover, it has been reported that rhod 2 penetrates deeper into brain slices and stains tissues more homogeneously than fluo 3 and that there is less fluorescence from damaged cells on the edge of the brain slice (203).

7. *Dextran conjugates*

For several fluorescent indicators, compartmentalization is a severe problem. One of the most effective techniques to decrease compartmentalization is to link

the indicator to a dextran, which is a hydrophilic polysaccharide of >10,000 molecular weight. The conjugates of the indicator and dextran cannot cross the plasma membrane and require some invasive techniques for introduction into the cells (e.g., microinjection or scrape-loading). Once inside the cell, the indicator-dextran conjugate is retained in the cytosol and provides more precise estimation of the cytosolic ion concentration over extended periods of observation (44, 117, 345). Sometimes mixtures of Ca^{2+} indicator dextran and Ca^{2+}-insensitive dextran (e.g., calcium green dextran and rhodamine or Texas red dextran) are injected into cells together to enable ratiometric measurement of cytosolic [Ca^{2+}] much like the ratiometric measurements one can make with fluo 3 and fura red (62).

8. Calcium green C_{18} and Fura-indoline-C_{18}

These are lipophilic Ca^{2+} indicator conjugates based on calcium green-1 and Fura red-like C_{18}-fura 2. They also locate in the plasma membrane and indicate the changes in [Ca^{2+}] near the plasma membrane (231). However, calcium green C_{18} has a high negative charge, which aligns indicators in the plasma membrane in the outward orientation. It has been reported that ~90% of calcium green C_{18} is located in the plasma membrane of osteoblasts after loading with 5 μM calcium green C_{18} for 10 min at 37°C and that it is useful for monitoring Ca^{2+} efflux via the plasma membrane (231).

III. BIOLUMINESCENT CALCIUM INDICATORS

A. Ca^{2+}-Binding Photoproteins

Bioluminescence is the production of light by biological organisms. Several Ca^{2+}-binding photoproteins have been described, e.g., aequorin, obelin, mitrocomin, and clytin, and some of them have been used to measure [Ca^{2+}] (351, 407). Because these photoproteins emit visible bioluminescence by an intramolecular reaction in the presence of Ca^{2+}, they offer simplicity in terms of required instrumentation and are not affected by photobleaching due to excitation illumination. The most serious problems with these probes have been the methods required for loading and detection of the bioluminescence and calibration. For example, each aequorin molecule gives off only one photon when it binds to Ca^{2+}; therefore, the bioluminescence observed is not always of sufficient intensity for detection, sometimes necessitating complicated detection systems (34, 131).

1. Obelin

Obelin is a Ca^{2+}-activated photoprotein extracted from the hydroid *Obelia geniculata* (12, 54). When obelin binds to at least three molecules of Ca^{2+}, it emits bioluminescence (261). The onset of the luminescence after binding the photoprotein to Ca^{2+} is much faster than that of aequorin (3 ms by obelin vs. 10 ms by aequorin), which makes it more useful for experiments requiring high temporal resolution (377). However, the disadvantage of obelin is that it shows much less Ca^{2+} sensitivity than aequorin, especially at [Ca^{2+}] $<10^{-5.5}$ M (261).

2. Aequorin

Aequorin, isolated from the jellyfish *Aequore forskålea* (353, 355), is the most popular bioluminescent Ca^{2+} indicator. Since Ridgway and Ashley (314) recorded Ca^{2+} transients in the giant barnacle muscle fiber with aequorin in 1967, it has been used widely as a Ca^{2+} indicator. The aequorin complex consists of apoaequorin protein of molecular mass 21,000 Da, the luminophore coelenterazine, and molecular oxygen (168, 355). Aequorin contains three Ca^{2+}-binding sites and becomes luminescent when Ca^{2+} binds to at least two of these sites. When Ca^{2+} binds to aequorin, the molecular oxygen in aequorin is released, and the coelenterazine is oxidized to coelenteramide, resulting in the emission of blue light (465 nm). Aequorin can be regenerated from apoaequorin and coelenterazine in the presence of oxygen (352, 354). The emitted luminescence increases monotonically as [Ca^{2+}] increases between 10^{-7} and 10^{-4} M, and the normalized intensity (L/L_{max}) varies in proportion to approximately [Ca^{2+}]$^{2.5}$ when [Ca^{2+}] is near 10^{-6} M (5, 34). This can sometimes result in overestimation of [Ca^{2+}] at higher [Ca^{2+}] levels if the [Ca^{2+}] is not homogeneously distributed throughout the cells. With the use of this feature, the existence of two high [Ca^{2+}] compartments has been demonstrated in vascular smooth muscle cells loaded with aequorin and fura PE3 (1). Note, however, that the cytosolic resting [Ca^{2+}] in some cells is unfortunately quite close to the limit of the measurable [Ca^{2+}] range of original aequorin. Magnesium depresses the Ca^{2+} sensitivity of aequorin, but pH does not affect the sensitivity of aequorin for Ca^{2+} in the physiological pH range (pH 6.6–7.4). It is thought that the distribution of the loaded aequorin is limited to the cytosol and that it does not get into organelles. Since the late 1980s, the usefulness of aequorin has been enhanced by some technological developments. Several kinds of homogeneous recombinant aequorin have been produced from recombinant apoaequorins and coelenterazine (168, 169). In addition, various kinds of semisynthetic aequorins have been produced by replacing the coelenterazine moiety with several analogs of coelenterazine, which has provided a wide range of Ca^{2+} sensitivity (355, 356).

3. Specifically targeted recombinant aequorin

This method has made aequorin a quite useful probe for measuring [Ca^{2+}] within organelles. Rizzuto and coworkers (322, 323, 325, 332) fused the cDNA for aequorin

in frame with that encoding a mitochondrial presequence. The hybrid cDNA was transfected into cells, and stable clones expressing mitochondrially targeted aequorin were successfully obtained. This method offers the ability to monitor Ca^{2+} homeostasis in specific organelles of intact cells. The targeting strategy has been widely used with various kinds of presequences to monitor [Ca^{2+}] in subcellular constituents such as nucleus (16–18, 47, 48), sarcoplasmic reticulum (313, 326), endoplasmic reticulum (7, 51, 191, 264, 326), Golgi apparatus (304), secretary granules (307), mitochondria (322–325, 332), gap junction (115), and cytosol (16, 46, 197). The important advantages of using targeted recombinant aequorin are that the cells remain intact under physiological conditions and the recorded signal of aequorin luminescence reports on [Ca^{2+}] in only the organelle to which it was targeted. Although [Ca^{2+}] of various subcellular compartments was successfully monitored using targeted aequorin, measurements of [Ca^{2+}] in high [Ca^{2+}] domains such as sarcoplasmic reticulum or endoplasmic reticulum were more difficult because of rapid consumption of aequorin (45). Recently, it has been reported that low Ca^{2+} affinity aequorin reconstituted with synthetic coelenterazine (356) provides a lower rate of aequorin consumption and allows reliable monitoring of [Ca^{2+}] in high [Ca^{2+}] compartments for longer experimental periods (22, 229, 263, 326).

B. Green Fluorescent Protein-Based Ca^{2+} Indicators

Green fluorescent proteins (GFP) are photosensitive proteins synthesized by the jellyfish *Aequorea victoria*. These proteins absorb the blue luminescent emission of aequorin and give off green fluorescence in *A. victoria* (308). The cloning of GFP and ability to fuse its DNA to that of cellular constituents has led to the use of GFP as markers of gene expression and protein localization in living organisms (61, 170). Green fluorescent proteins have become one of the most popular and exciting new technologies in cell biological experiments. Recently, some groups have successfully synthesized Ca^{2+} indicators using GFP.

1. Chameleons

Miyawaki et al. (259) have expressed GFP-based Ca^{2+} indicators (called "chameleons") in the cytosol and endoplasmic reticulum of intact HeLa cells. They consist of two GFP mutants emitting fluorescence at different wavelengths: the Ca^{2+}-sensitive protein calmodulin and M13, which is the 26-residue calmodulin-binding peptide of myosin light-chain kinase. The hybrid protein (calmodulin-M13 complex) bridges the two GFP mutants. When Ca^{2+} binds to the calmodulin in this complex, the hybrid protein changes the conformation of the complex, resulting in decrease in the distance between the two GFP mutants and an increase in fluorescence resonance energy transfer (FRET). Tsien (404) demonstrated two combinations of donor and acceptor GFP mutants, blue fluorescent protein (BFP)-GFP and cyan fluorescent protein (CFP) yellow fluorescent protein (YFP). Their excitation wavelength and emission ratio are 380–510/445 and 440–535/480 nm, respectively. Among the various types of chameleons they synthesized, chameleon-1/E104Q which has BFP and GFP, shows a monophasic response to [Ca^{2+}] in the range of 10^{-7} to 10^{-4} M. By changing the two GFP mutants from BFP and GFP to enhanced CFP and YFP, the brightness, signal-to-noise ratio, and duration of recording were improved (yellow chameleon-2). However, neither chameleon-1 (yellow) nor chameleon-2 demonstrated large changes in ratio (both R_{max}/R_{min} are <2, which is much less than most chemical fluorescent Ca^{2+} indicators).

2. FIP-CB_{SM} and FIP-CA

Different GFP-based Ca^{2+} indicators, fluorescent indicator proteins (FIP), have been synthesized by Romoser and Persechini and co-workers (299, 330). Their synthesized GFP complex, FIP-CB_{SM}, contains an amino acid linker that includes the calmodulin-binding sequence from smooth muscle myosin light-chain kinase and two GFP mutants (BFP and red-shifted GFP, Ref. 77) (330). They also monitored [Ca^{2+}] of cytosol and nucleus with microinjected FIP-CB_{SM} by using the emitted intensity at 505 nm or the emitted ratio at 505/440 nm (380-nm excitation). However, unlike Miyawaki's indicator, their indicator displayed a decrease in FRET upon Ca^{2+} binding. When $(Ca^{2+})_4$-calmodulin complex is bound to FIP-CB_{SM} (K_d 0.4 nM), it alters the structure, resulting in an increase in the distance between two GFP mutants (from ~25 to ~65 Å). According to their report, the range of sensitivity is between <50 nM to 1 μM Ca^{2+}, and F_{max}/F_{min} (at 505 nm) and R_{max}/R_{min} (at 505/440 nm) are ~1.54 and 5.7, respectively. However, because FIP-CB_{SM} is an indicator of $(Ca^{2+})_4$-calmodulin complex, its Ca^{2+}-measuring capabilities may be limited by the calmodulin concentration in the cell. They also produced another Ca^{2+} indicator by fusion of FIP-CB_{SM} to an engineered calmodulin in which the NH_2- and COOH-terminal EF hand pairs are exchanged and the calmodulin-binding sequence of FIP-CB_{SM} is modified (299). This new FIP-CA series reported [Ca^{2+}] directly. The fluorescence intensity of the acceptor's emission peak (505 nm) decreased substantially when Ca^{2+} was bound. They reported that the K_d values for Ca^{2+} of FIP-CA_3 and FIP-CA_9 are 100 and 280 nM, respectively, in the presence of 0.5 mM Mg^{2+}. Their F_{max}/F_{min} (at 505 nm) and R_{max}/R_{min} (at 440/505 nm) are ~1.4 and 1.7, respectively.

3. Advantages and disadvantages

These GFP-based Ca^{2+} indicators have some advantages over chemical fluorescent probes or aequorin. Compared with aequorin, *1*) they can provide ratiometric [Ca^{2+}] measurements; *2*) the Ca^{2+}-dependent fluorescent response is reversible and requires no specific cofactors; and *3*) relatively bright fluorescence allows simplified photon-detection systems and comparatively high temporal resolution. Compared with chemical fluorescent probes, *4*) the sensitivity or Ca^{2+}-binding kinetics are independent of the concentration of the indicators; *5*) if they are incorporated into cells by microinjection, they are retained in the microinjected compartments (e.g., cytosol or nucleus) in the cell; and *6*) they can be precisely expressed in targeted intracellular components. Although rhod 2 can be localized well in some types of cells, it is difficult for most of the chemical fluorescent indicators to localize precisely only in the target organelle including endoplasmic reticulum and nucleus. The new GFP-based indicators have the potential to overcome these drawbacks of the chemical indicators and recombinant aequorin.

On the minus side, the GFP-based Ca^{2+} indicators have some disadvantages. One disadvantage is the small dynamic range of their fluorescence intensity or their ratio. As described above, most of their R_{max}/R_{min} values are <2, whereas those of fura 2 and indo 1 are ~20 and F_{max}/F_{min} of fluo 3 is >100. In addition, because of the spectral properties of donor and acceptor, the ratio of baseline fluorescence is not always zero even in the absence of FRET, which makes it more difficult to detect small changes in the ratio. Another potential disadvantage is that the fluorescence of GFP is partially pH sensitive (especially YFP) (196, 230, 247, 297, 395, 404, 420). The absorption and emission spectra of certain mutants of GFP have recently been found to be pH sensitive (297, 395, 419–421) (Fig. 4). It is thought that changes in the absorption and emission spectra are reversible in the physiological pH range and that they are due to changes in the degree of protonation/deprotonation of the GFP molecule, because native GFP are conformationally extremely stable (148, 419). Recently, it has been reported that GFP can serve as a pH indicator in neutral and acidic ranges (196). Indeed, Llopis et al. (230) have demonstrated that pH in cytosol and intracellular components in intact cells can be evaluated using GFP and YFP. They have shown that YFP is more suitable for cytosolic and mitochondrial pH measurements because YFP is more sensitive to change in pH near physiological levels (pK_a 7.1). Romoser et al. (330) also have mentioned the pH sensitivity of FIP-CA. Although the their K_d values for Ca^{2+} and the kinetics of reconformation are quite stable against the changes in pH, the fluorescence ratios are influenced by pH (especially in low [Ca^{2+}] range) due to differences in pH sensitivity of the two GFP mutants.

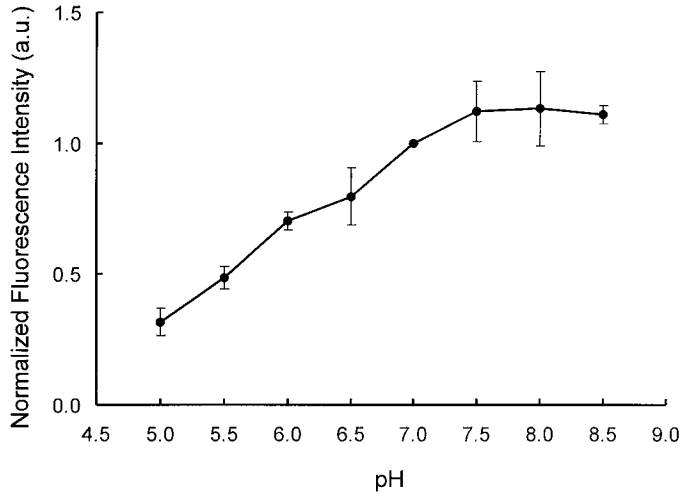

FIG. 4. pH sensitivity of green fluorescent protein (GFP). BHK cells expressing cytosolically localized GFP (F64L/S65T) were incubated in buffer containing 10 μM nigericin at various pH values. Cells were excited at 488 nm, and emission fluorescence was collected from 510 to 560 nm. Normalized fluorescence is presented as ratio to measured fluorescence at pH 7.0. GFP fluorescence varied dramatically at pH levels below 7.5.

IV. DYE-LOADING PROCEDURES

A. Ester Loading

Most chemical fluorescent indicators are cell impermeant. A few limited plant cells can be loaded directly with Ca^{2+} indicators (50). To load most cells with these indicators, however, it is necessary to adopt special invasive or biochemical techniques. Many of the fluorescent Ca^{2+} indicators are derivatized with an AM that is cell permeable (402, 405). Unlike the original active form, the AM form of the indicator can passively diffuse across cell membranes, and once inside the cell, esterases cleave the AM group off of the probe leading to a cell-impermeant indicator. It is thought that the final intracellular concentration of the hydrolyzed Ca^{2+} indicators is dependent on numerous factors (e.g., type of Ca^{2+} indicators and loaded cells, loading concentrations of Ca^{2+} indicators, number of the loaded cells, loading time, loading temperature, and preloading condition). It has been demonstrated that the final hydrolyzed concentration of quin 2 can be several hundred times that of the initial concentration of the ester in the loading solution (405). Because the AM have low aqueous solubility, some dispersing agents such as Pluronic F-127 or Cremophor EL (290, 338) are often used to facilitate cell loading. Pluronic F-127 is a nonionic dispersing agent that helps solubilize large dye molecules in physiological media (70, 218, 287, 306). If long loading times are required, 1 mg/ml BSA or 1–5% FCS should be added to the loading solution to maintain proper osmolality. However, FCS sometimes contains

nonspecific esterases and causes hydrolysis of the AM before entering the cell. In addition to the comparative ease of incorporating these dyes into cultured and/or isolated cells, ester loading methods have also allowed loading of indicators into whole organs (e.g., isolated whole heart) while maintaining physiological conditions (136, 217, 251, 357, 372). On the other hand, AM loading has various problems including compartmentalization and incomplete hydrolysis (see sect. VI, *D* and *E*).

B. Microinjection

The chemical fluorescent Ca^{2+} indicators are not always provided as the cell-permeable ester form. Moreover, some dextran conjugates and photoproteins are too large to permeate the plasma membrane. To load cells with these indicators, certain special techniques are required. Calcium indicators can be dissolved in a cytosolic-like solution and filled in a glass micropipette (34, 103). The micropipette is inserted into the cell, and the indicator is then injected into the cell intermittently (i.e., by N_2 gas). The advantage of this method is that it is possible to load the charged form of the indicator directly into the cytosol with certainty. However, this method is invasive and requires specialized instruments and practice. In addition, the number of cells that can be loaded with probes is limited (i.e., the best microinjectors can only load ~100 cells/h) relative to AM loading, and it is problematic to load specific cells in a tissue section.

C. Diffusion From Patch-Clamp Pipettes

Although microinjection works well with large cells, microinjection sometimes torments smaller cells by impaling them with the injection needle. For small cells (e.g., mast cells, adrenal chromaffin cells), some dyes have been often loaded via patch pipettes (6, 273, 285). This method has also been used for measurements of $[Ca^{2+}]_i$ in excitable cells (e.g., neurons, heart muscle cells) because it allows measurement of $[Ca^{2+}]_i$ and control of the membrane potential at the same time (21, 57, 387, 391). In addition to the possibility of simultaneous whole cell recording of membrane currents, pipette loading supplies Ca^{2+} indicators continuously and prevents decrease of intracellular dye concentration by dye leakage (268). Whereas indicators are put into the cell by positive external force in the microinjection method, they are loaded in the cell by diffusion in the patch pipette method. Accordingly, the rate that the indicators reach the steady state in the cytosol is dependent on the electric resistance within the pipette tip and the viscosity of the loading solution. The pipette loading procedure may result in cell dialysis and sometimes limit cell survival. Another limitation of this method is that few cells (but not always a single cell) can be loaded with the dye at the same time (390).

D. Chemical Loading Technique (Low Ca^{2+} Loading) and Macroinjection

The methods described below were developed to load indicators into a large number of cells in a tissue or organ. Because microinjection-based loading technique would require 50–100 times as many cells to be injected to obtain a satisfactory response with aequorin, microinjection is not a suitable way of loading aequorin into tissues or organs. Therefore, macroinjection, using a bigger pipette, enables the loading of dye into many cells at once. Macroinjection requires some other additional chemical treatments. The tissue is at first exposed to low-Ca^{2+} perfusate to cause a transient increase in plasma membrane permeability (266, 267), then the indicator-containing solution is pressure-injected into the tissue via a glass pipette. Finally, $[Ca^{2+}]$ of the perfusate is increased gradually to the normal range (192, 193). In this manner, a number of heart muscle cells surrounding the injected area in myocardium or isolated papillary muscle are also loaded with aequorin (192, 266). Although the macroinjection is easier than the microinjection, its reliability may be less.

E. Diffusion Through Gap Junction

This technique is to load Ca^{2+} indicators presumably through momentarily permeable gap junction sites (366). In a report by Lakatta's group (366), rat heart was retrogradely perfused with a low-Ca^{2+} solution containing collagenase and protease and then mechanically dissociated into single cells in a buffer solution containing indo 1 salt. It has been thought that during the exposure of enzymatic digestion, some gap junction sites retain their permeability, in part, to the external solutions, allowing indo 1 to diffuse into the cytosol through the gap junction (366). This approach also allows loading of Ca^{2+} indicators into numerous cells with little difficulty. However, there is a wide variation in the loaded dye concentration, necessitating careful calibration and estimation of $[Ca^{2+}]_i$.

F. ATP-Induced Permeabilization

External ATP elicits various responses in numerous cells. In some cell types [e.g., hepatocytes (63), mast cells (72), polymorphonuclear leukocytes (26), and some transformed cells (149, 195, 376)], extracellular ATP induces cation flux and increases the permeability of the plasma membrane via the ATP^{4-} receptor. The ATP^{4-}-induced permeabilization has been used to load various dyes

(<900 Da), including Ca^{2+} indicators into mouse macrophage and transformed macrophage-like cell lines (374, 375). Magnesium is added to inhibit ATP^{4-} permeabilization activity, providing a way to control the extent of cell loading. One limit of this method is the cell specificity of ATP-induced permeabilization. For example, although some transformed cell lines (e.g., Chinese hamster ovary cells, mouse fibroblasts, mouse melanoma cells, rat kidney cells) exhibit this ATP sensitivity, their nontransformed counterparts do not (149, 195).

G. Hyposmotic Shock Treatment

Hyposmotic shock treatment (HOST) was developed for incorporation of aequorin into various types of cells (including cultured and/or freshly isolated cells) (38, 39). Cells are first washed several times with cold Ca^{2+}-free solution to remove superficial Ca^{2+} that would consume much of the aequorin. Cells are then transferred to a tube containing a hyposmotic solution with aequorin for 2–5 min. During exposure of cells to the hyposmotic solution, the plasma membrane becomes permeable to the indicator, which can enter the cell (38). Although HOST allows incorporation of dyes into cells in high efficiency, hyposmotic shock may cause loss of cell viability and functional integrity.

H. Gravity Loading

When cells in suspension are used, the gravity-loading technique may be the easiest available to load aequorin (37). Cells are washed in cold Ca^{2+}-free solution three times and centrifuged at 50 *g* for 2 min between each wash. Then cells are incubated with aequorin for 10 min at 4°C, followed by centrifugation at 200 *g* for 30 s. The exact mechanism of dye loading is unknown, but it may be due to elevation of $[Ca^{2+}]_i$ during centrifugation (37). The efficiency of incorporation of aequorin using this manner has been reported as only 30% of that by HOST and as almost the same as scrape loading (37).

I. Scrape Loading

Scrape loading is used to load cultured cells with macromolecules (245). Cells are cultured on a culture dish and are scraped from the plate in buffer containing the indicator to be loaded. The cells are then washed several times and replaced on dishes and cultured. The scraping is thought to rip holes in the plasma membrane at areas of cell adhesion to its substrate. With the use of this method, cell-impermeable fluorescent indicators or labeled macromolecules can be loaded in cells at high levels (101, 120, 245). McNeil (244), who pioneered the scrape-loading technique, has also developed modifications of the method (e.g., scratch loading and bead loading). One of the disadvantages to this approach is the difficulty of loading dyes into freshly isolated cells because they are not attached as monolayers.

J. Lipotransfer Delivery Method

Indicator is delivered into cells by fusion of 40- to 50-nm membrane-permeant cationic liposomes containing the various types of dyes (20, 134). The delivery efficiency of liposomes is determined by the type of cationic reagent employed, the cell type, and culture conditions. Dye delivery by liposomes can also result in the delivery of exogenous lipid to cells that may alter its properties.

K. Fused Cell Hybrids

This method has been used to load photoproteins by fusing cells and human erythrocyte "ghosts" containing the photoprotein in a medium containing Sendai virus (56, 135). Human erythrocyte ghosts are prepared by suspension in a medium diluted 1:1 with water for 10 min at 0°C. After centrifugation, the swollen cells are resuspended in Chelex-treated TES solution with the photoproteins. The cells can be loaded with the photoprotein by fusion with the ghosts in a fusion medium with UV-inactivated Sendai virus.

L. Endocytosis and Retrograde Uptake

Recently, some loading techniques have been developed to monitor organelle pH (lysosome, Golgi network) using endocytosis and retrograde uptake of pH indicators (79, 286). These loading techniques may be applied for other ion indicators.

V. CALIBRATION AND ESTIMATION OF CALCIUM INDICATORS

For quantitative evaluation of $[Ca^{2+}]$ from fluorescence intensity measurements, calibration must be undertaken. It is especially important to remember that the K_d of Ca^{2+} for the fluorescent probe can be drastically affected by probe-environmental conditions. Thus it is important to estimate the K_d under the experimental conditions. There are two kinds of the calibration: in vitro calibration and in vivo (in situ) calibration.

A. In Vitro Calibration

Calcium concentration is related to the measured fluorescence intensity by

$$[Ca^{2+}] = K_d \times (F - F_{min})/(F_{max} - F) \quad \text{(single-wavelength measurement)} \quad (1)$$

or

$$[Ca^{2+}] = \beta \times K_d \times (R - R_{min})/(R_{max} - R) \quad \text{(ratiometric measurement)} \quad (2)$$

where F and R are the experimentally measured fluorescence intensities and the ratio of these intensities, respectively; F_{min} and R_{min} are the measured fluorescence intensity and ratio in the absence of Ca^{2+}, respectively; F_{max} and R_{max} are measured fluorescence intensity and ratio of Ca^{2+}-saturated dye, respectively; β is the ratio of the fluorescence intensities at the wavelength chosen for the denominator of R (e.g., 480-nm emission for indo 1 and 380-nm excitation for fura 2) in zero and saturating $[Ca^{2+}]$; and K_d is the dissociation constant of the indicator for Ca^{2+} (127).

Calibration curves are obtained by using a Ca^{2+}-buffering solution containing the Ca^{2+} indicator in an active (nonester) form. EGTA-Ca^{2+} buffer solutions are the most popular for the calibration of Ca^{2+} indicators. A series of calibration solutions containing various $[Ca^{2+}]$ are made by mixing two solutions (*solution A* containing 10 mM EGTA and *solution B* containing 10 mM Ca-EGTA) in various ratios. Both solutions contain the same concentrations of K^+ (100–140 mM), buffers (MOPS, HEPES, and so on), and other ions if necessary, and they are adjusted to the same pH and the same temperature. The $[Ca^{2+}]$ of the Ca^{2+}-buffering solution can be estimated by the ratio of the these two solutions and the K_d of EGTA for Ca^{2+} at each pH and temperature (400, 426). For example, the Ca^{2+} buffer can be prepared as follows to get a set of Ca^{2+} measurement standards.

1) Twenty milliliters of *solution A* (Ca^{2+} free) containing 100 mM KCl, 10 mM K-MOPS, 10 mM K_2H_2EGTA, and the Ca^{2+} indicator at 1–5 μM are adjusted to pH 7.2 by KOH and divided into two 10-ml aliquots.

2) One milliliter of a 1 mM $CaCl_2$ solution is diluted 10-fold by MOPS buffer (100 mM KCl and 100 mM K-MOPS).

3) Five-microliter aliquots of the 0.1 mM $CaCl_2$ solution are added to 10 ml of the 1 mM EGTA gradually while monitoring the pH. $CaCl_2$ addition will cause the pH to decrease and eventually stabilize.

4) Note the volume of 0.1 mM $CaCl_2$ required to attain stable pH.

5) *Solution B* (Ca^{2+}-saturating solution) should be prepared by adding the volume determined from *process 4* of 1 mM $CaCl_2$ to 10 ml of *solution A*, and the pH is adjusted 7.2 with KOH.

6) Make up 11 solutions by mixing *solution A* and *solution B* at various ratios (0–100%, 10% step). Concentrations of free Ca^{2+} in each solution can be calculated by the following equation and knowledge of the K_d of EGTA for Ca^{2+}

$$[\text{Free } Ca^{2+}] = K_d \times [\text{Ca-EGTA complex}]/[\text{free EGTA}] \quad (3)$$

Because free Ca^{2+} concentration is $\sim 10^6$ times smaller than total Ca^{2+} concentration, Ca-EGTA complex and free EGTA can be approximated to total Ca^{2+} concentration, which can be represented as the concentration of *solution B*. Free EGTA concentration can be practically shown by the concentration of *solution A*. Therefore, *Equation 3* can be altered to the following

$$[\text{Free } Ca^{2+}] = K_d \times [solution\ B]/[solution\ A] \quad (4)$$

Consequently, because the K_d of EGTA for Ca^{2+} (e.g., 150.5 nM at 20°C, pH 7.2) and the ratio of *solution A* to *solution B* are known, the concentration of free Ca^{2+} can be evaluated.

Because the K_d of EGTA for Ca^{2+} can be influenced by temperature, pH, ion strength, and concentrations of other heavy metal ions (107, 126, 138, 243), it is necessary to estimate the precise $[Ca^{2+}]$ of the buffering solution as a function of its specific contents before the calibration of the Ca^{2+} indicator.

B. In Vivo Calibration

It is known that the K_d of most Ca^{2+} indicators estimated using in vitro calibration is not the same as the actual K_d in the cell. This discrepancy is dependent on a fact that the K_d of the cell contained Ca^{2+} indicator is affected by the temperature, pH, viscosity, ionic strength, and other intracellular constituents (100, 112, 166, 199, 213, 214, 435) (see sect. VI*E*). Thus the K_d measured inside one type of cell may not be valid for other cells. In addition, intracellular environments also affect spectral properties of some Ca^{2+} indicators. It has been demonstrated that indo 1 and fura 2 exhibit different emission/absorption spectra in intracellular environments compared with buffers (19, 161, 288). The discrepancy may be caused in part by the absorption/scattering by intracellular constituents (288) and changes in the polarity (288, 289) and/or the viscosity (111, 362) of the environment. In addition, unless all of the AM are fully hydrolyzed, fluorescence from any residual AM may affect the amount of fluorescence observed from cells and hence the accuracy of quantitation (287). Because unhydrolyzed forms of Ca^{2+} indicators are Ca^{2+} insensitive, measurement of their fluorescent signal may lead to an underestimation of

$[Ca^{2+}]$. Therefore, it is better to calibrate the fluorescence intensity of the Ca^{2+} indicator in vivo if possible.

Nonfluorescent Ca^{2+} ionophores such as ionomycin and 4-bromo-A-23187 have been used to bring extracellular and intracellular Ca^{2+} levels close together (76, 227). With the use of EGTA-Ca^{2+}-buffered solutions containing these reagents at low concentration, in vivo calibration curves of Ca^{2+} indicators can be obtained (426, 427). However, these reagents are not without problems. *1*) Although Ca^{2+} ionophores at high concentration increase the permeability of not only the plasma membrane but also membranes of intracellular organelles (309, 427), it is difficult to equilibrate Ca^{2+} levels throughout all organelles. *2*) It is difficult for some Ca^{2+} ionophores to increase $[Ca^{2+}]_i$ high enough to saturate some of the low-affinity Ca^{2+} indicators. *3*) For some types of cells (e.g., heart muscle cells), elevation of $[Ca^{2+}]_i$ by Ca^{2+} ionophores causes changes in the shapes and volume of cells. As a result, intracellular dye concentrations or the fluorescence ratios may be altered. Depletion of ATP and glucose or addition of carbonyl cyanide *m*-chlorophenylhydrazone and rotenone is sometimes effective to avoid hypercontraction (222, 361). When the plasma membrane of cells is not easily permeabilized by these Ca^{2+} ionophores, nonionic detergents such as digitonin or Triton X-100 sometimes are used instead of Ca^{2+} ionophores (186) (see sect. VI*D*).

Another well-used in vivo calibration method is based on microinjection or intracellular dialysis with buffered solution (6, 422). Instead of equilibrating $[Ca^{2+}]_i$ by ionophores, $[Ca^{2+}]_i$ is controlled by buffered solutions with various $[Ca^{2+}]$ (different EGTA/Ca^{2+}-EGTA proportions) via micropipettes or microinjection needles. The R_{max}, R_{min}, and a third ratio to calculate K_d are evaluated when the intracellular dialysis is satisfyingly performed and the fluorescence ratio becomes steady (6). In the case of microinjection, the buffered solution is repeatedly given until no further change in the ratio is obtained (422). The calibration curve is obtained from mean values of numerous cells because it is hard to perform complete calibration in single cells. One of the disadvantages of this method is that the intracellular environment (e.g., viscosity, osmolarity, ionic strength, relative concentrations of intracellular proteins) will change after the injection or dialysis with buffered solutions (422). Another problem is that this technique cannot be used for calibration of nonratiometric indicators because the dye concentration may be changed by intracellular dialysis.

When cells are loaded with the AM form of Ca^{2+} indicators, compartmentalization and incomplete hydrolyzation are often found. These forms are insensitive to cytosolic $[Ca^{2+}]$ and should be subtracted from the whole fluorescence from the cells. Several Ca^{2+} indicators (e.g., indo 1, fura 2, fluo 3, and rhod 2) easily bind to Mn^{2+}, but they emit little when they are bound to Mn^{2+} (Mn^{2+} quenching). Accordingly, the interference by the fluorescence that is insensitive to cytosolic $[Ca^{2+}]$ can be estimated if $[Ca^{2+}]$ of the compartment is kept constant during the experiments (143).

C. Estimation of Fluorescence Intensity

As discussed in *Equations 1* and *2*, $[Ca^{2+}]$ can be estimated from measurements of the Ca^{2+} indicator fluorescence at minimal and maximal $[Ca^{2+}]$. In the case of ratiometric measurements, R_{max} and R_{min} can be obtained by using low concentrations of Ca^{2+} indicators because the ratio is theoretically independent of the dye concentration. In the case of single-wavelength measurements, however, F_{max} and F_{min} cannot be obtained unless the dye concentration is precisely estimated or in vivo calibration is performed in the same cell. Recently, estimation of fluorescence intensity of such nonratiometric Ca^{2+} indicators has been often reported not as $[Ca^{2+}]$, but as the pseudoratio ($\Delta F/F$) indicated by the following formula

$$\Delta F/F = (F - F_{base})/(F_{base} - B) \quad (5)$$

where F is the measured fluorescence intensity of the Ca^{2+} indicator, F_{base} is the fluorescence intensity of the Ca^{2+} indicator in the cell before stimulation, and B is the background signal determined from the average of areas adjacent to the cell (64, 226, 275, 383). Apart from dye saturation, $\Delta F/F$ is thought to approximately reflect $[Ca^{2+}]$ if there is no change in dye concentration, intracellular environment, or path length (383).

D. Aequorin

The bioluminescence of aequorin is usually shown as a fraction, L/L_{max}, where L represents the measured light intensity and L_{max} is the measured peak light intensity in saturating $[Ca^{2+}]$. It has been found that at 10^{-6} M Ca^{2+}, the luminescence intensity of aequorin is proportional to approximately $[Ca^{2+}]^{2.5}$ (5, 34). The L_{max} value is evaluated from the total luminescence of loaded aequorin, which can be released from the cell with Triton X-100 after completion of the experiments, in saturated $[Ca^{2+}]$ by taking advantage of the fact that a time constant for the decline in the luminescence intensity is 0.8 s (the rate constant is 1.2/s) in saturated $[Ca^{2+}]$ at 21°C (4). This procedure may be unnecessary if the volume of loaded aequorin can be estimated accurately (i.e., microinjection). As mentioned previously, however, aequorin is consumed when it is bound to Ca^{2+} during the experiments. The L_{max} value should be normalized as a function of time $[L_{max}(t)]$ accordingly, because consumption of aequorin occurs during the experiment. The $L_{max}(t)$ value is calcu-

lated from the whole record of the luminescence intensity or virtually estimated from the time constant of decrease in L_{max} obtained from the beginning and end of the experiments. Calcium concentration can be appraised from a calibration curve whose x- and y-axes represent log $[Ca^{2+}]$ and log (L/L_{max}), respectively, or by the following equation

$$L/L_{max} = \{(1 + K_R \times [Ca^{2+}])/(1 + K_{TR} + K_R \times [Ca^{2+}])\}^n$$

where n is the number of the Ca^{2+}-binding sites and K_R and K_{TR} represent, respectively, an equilibrium constant for Ca^{2+} binding to the R state and the transition between T and R states of aequorin in a model showed by Allen et al. (5).

Another calibration procedure for aequorin is based on the rate of aequorin consumption. Because the speed of aequorin consumption is dependent on $[Ca^{2+}]$, $[Ca^{2+}]_i$ can be estimated by a rate constant that is represented as a ratio of luminescence intensity above the background (photon count/s) to the product of the amount of remaining chromophores multiplied by the quantum yield (it should be equal to the total photon count after subtraction of background counts) (55, 67, 68, 429).

Normalization of targeted recombinant aequorin can be obtained in the same way as that of cytosolic aequorin, but the former requires longer times to quench all aequorin after addition of Triton X-100 compared with the latter (46, 325).

E. GFP-Based Ca^{2+} Indicators

Both Tsien and co-workers (259) and Persechini and co-workers (299, 330) demonstrated that the ratio of the fluorescence intensities at the wavelengths of the emission peaks for the GFP donor and acceptor could be used to monitor $[Ca^{2+}]$. Tsien's group (259) estimated $[Ca^{2+}]$ using the following equation

$$[Ca^{2+}] = K_d \times [(R - R_{min})/(R_{max} - R)]^{(1/n)} \quad (6)$$

where R is the ratio of emitted fluorescence of the acceptor to one of the donor at their respective emission maxima, R_{min} is the same ratio in the absence of Ca^{2+}, R_{max} is the same ratio of the Ca^{2+}-saturated dye, K_d is the apparent dissociation constant, and n is a cooperatively coefficient that corresponds to the number of interacting sites of the indicator. The Ca^{2+} indicators produced by Persechini's group (299, 330) underwent a decrease of FRET after binding of Ca^{2+}. They estimated $[Ca^{2+}]$ from the following equation

$$[Ca^{2+}] = K_d \times [(F_{max} - F)/(F - F_{min})]^{(1/n)} \quad (7)$$

where F is the measured fluorescence intensity of the acceptor's peak and F_{min} and F_{max} are the measured fluorescence intensity of the acceptor's emission peak in the absence and at saturating Ca^{2+}, respectively. These values were obtained using in vitro or in vivo calibration procedures as used with common chemical fluorescent indicators.

VI. POTENTIAL PROBLEMS OF CALCIUM INDICATORS AND THEIR SOLUTIONS

A. Intracellular Buffering

In general, the ion indicators function as chelators for a specific ion. Binding of the ion to the indicator then changes the fluorescence properties (absorption, lifetime, intensity, or spectra). This is exactly how a buffer works, and this can be experimentally problematic because high-affinity Ca^{2+} indicators such as fura 2 and calcium green-1 may buffer small changes in $[Ca^{2+}]$ when loaded into cells at high concentrations (156). For example, the Ca^{2+}-buffering power of fura 2 at commonly used concentrations is 10–20% of the intrinsic buffering power of the cytosol in smooth muscle cells (28). Therefore, low-affinity Ca^{2+} indicators are often preferred in measurements of $[Ca^{2+}]$ in such conditions (156). Some low-affinity indicators require high intracellular concentrations to obtain good signal detection (58).

Some early generation Ca^{2+} indicators (i.e., quin 2, fura 2) are now often used as a Ca^{2+} chelators for measurement of intrinsic intracellular Ca^{2+}-buffering capacity ("added buffer" approach) (58, 153, 274, 401). Because they have relatively high affinities for Ca^{2+} (K_d values are 60 and 224 nM, respectively), intentionally overloaded Ca^{2+} indicators behave as a major buffer for Ca^{2+}, competing with intrinsic buffering components in the cell. This buffering action occurs within milliseconds, whereas pump or sequestration mechanisms in some types of cells are on the time scale of seconds (274). The ratio of Ca^{2+}-bound indicator to Ca^{2+}-free indicator can be estimated, and n_{CB} (changes in the number of Ca^{2+}-bound indicators) can be evaluated by the changes in the fluorescence intensity. Hence, if the amount of increase in total Ca^{2+} can be calculated, the endogenous Ca^{2+}-buffering capacity can be estimated based on the assumption that Ca^{2+} that enters the cell diffuses throughout the cell immediately (before the pump or sequestration mechanism work) (108, 272, 274, 410). In addition, sufficiently loaded Ca^{2+} indicators dominate the intrinsic Ca^{2+} buffers and allow accurate quantification of Ca^{2+} efflux across the plasma membrane (176, 272, 274).

B. Cytotoxicity

Some indicators may be toxic to some types of cells. It is well known that some slow response potentiometric indicators affect redox metabolism in mitochondria as well as cell proliferation (364). For example, rhodamine-123 is usually not retained within mitochondria of normal cells when extensively washed, but it is retained within mitochondria of carcinoma and heart muscle cells, resulting in inhibition of their proliferation (29, 212, 348, 380). It has also been reported that fluo 3-loaded sea urchin eggs do not undergo normal development, whereas calcium green-loaded sea urchin eggs develop normally (378).

C. Autofluorescence

There are numerous cellular constituents that can fluoresce independently of the indicators. For example, connective tissue components such as collagen fibers or calcifications can give off autofluorescence, but the most serious problem for measuring $[Ca^{2+}]_i$ is autofluorescence from pyridine nucleotides (NADH, NADP), flavin adenine dinucleotide (FAD), and flavine mononucleotide (FMN). The former increases its fluorescence by reduction while the latter increases its fluorescence by oxidation (292, 358). The excitation and emission peak of NADH are 340 and 440–470 nm, respectively, and those of FAD are 450 and 530–550 nm, respectively (139, 292). For some short-wavelength indicators including UV-excited indicators (i.e., fura 2 and indo 1), it is necessary to estimate if autofluorescence from cellular constituents contaminates the true emission of the indicator. This problem is especially difficult to deal with in investigations using brain slices and muscular tissues (200, 291, 358). Consequently, many researchers have recently used long-wavelength indicators such as rhod 2 or fura red to reduce the autofluorescence (206, 255, 388).

D. Bleaching and Ca^{2+}-Insensitive Forms

Illumination of all fluorescent indicators leads to photodamage and photobleaching. Thus the goal of any measurement using these indicators is to delay these consequences for as long as possible. Excessive illumination causes a decrease in signal strength in proportion to the time and intensity of exposure to excitation illumination and can cause the formation of fluorescent but Ca^{2+}-insensitive species of the indicator (27, 342). Thus some balance between photobleaching and sufficient signal-to-noise ratio must be found in the excitation exposure time/intensity to obtain reliable Ca^{2+} measurements. Nonratiometric indicators are the most sensitive to photobleaching, but it is also important for ratiometric indicators to minimize photobleaching because the rates of photobleaching at the wavelengths of the two excitation or emission maxima are not always same, which can cause incorrect ratios resulting in errors in estimation of ion concentrations (23). In addition, Ca^{2+}-insensitive compounds may affect ratiometric measurements (27, 342). One way to diminish photobleaching is to remove oxygen from the indicator environments or to add an antioxidant in the perfusate (27), although this may not be optional for living cells.

In the case of loading indicators with ester forms, they respond precisely to the concentration of the specific ions after they are hydrolyzed. However, it has been demonstrated that incompletely hydrolyzed indicators are often insensitive to Ca^{2+} but emit more fluorescence than the ester form and display spectral differences relative to the Ca^{2+}-sensitive form (340).

E. Compartmentalization

One of the most important problems in the use of chemical fluorescent ion indicators is compartmentalization. Compartmentalization means that the indicator is trapped within some intracellular organelles and is not homogeneous in distribution throughout the cell. For the measurement of cytosolic $[Ca^{2+}]$, it is important not only to load high enough concentration of indicators into the cytosol, but also to minimize compartmentalization, because the level of Ca^{2+} in the compartment is not always the same as in the cytosol. The degree of compartmentalization is dependent on numerous factors (e.g., the loading condition, cell type, and type of indicator) (69, 236, 329). The same indicator can also be sequestered within different organelles in different types of cells. For example, it has been demonstrated that fura 2 accumulates well within mitochondria of endothelial cells (373), lysosomes of fibroblasts (236), and secretary granules of rat mast cells (6). This variation is dependent on the fact that there are several mechanisms of dye sequestration (89, 236). The sequestration of some indicators is partially mediated by organic anion transport systems (90). In addition, incomplete hydrolyzation of some of the indicators in the cytosol allows the ester-derived indicator to cross organelle membranes into the intracellular components, which themselves can have substantial esterase activity (128, 233). Differences in the affinity for cytosolic or organelle esterases may also result in variations in compartmentalization (373). Because the mechanisms of both the transport to organelles and the transformation to the active chelate form from the ester form are entirely biochemical phenomena, compartmentalization and the cytosolic dye concentration are much influenced by the temperature. Accordingly, by changing the loading or hydrolyzing temperature, compartmentalization can be reduced (251, 329).

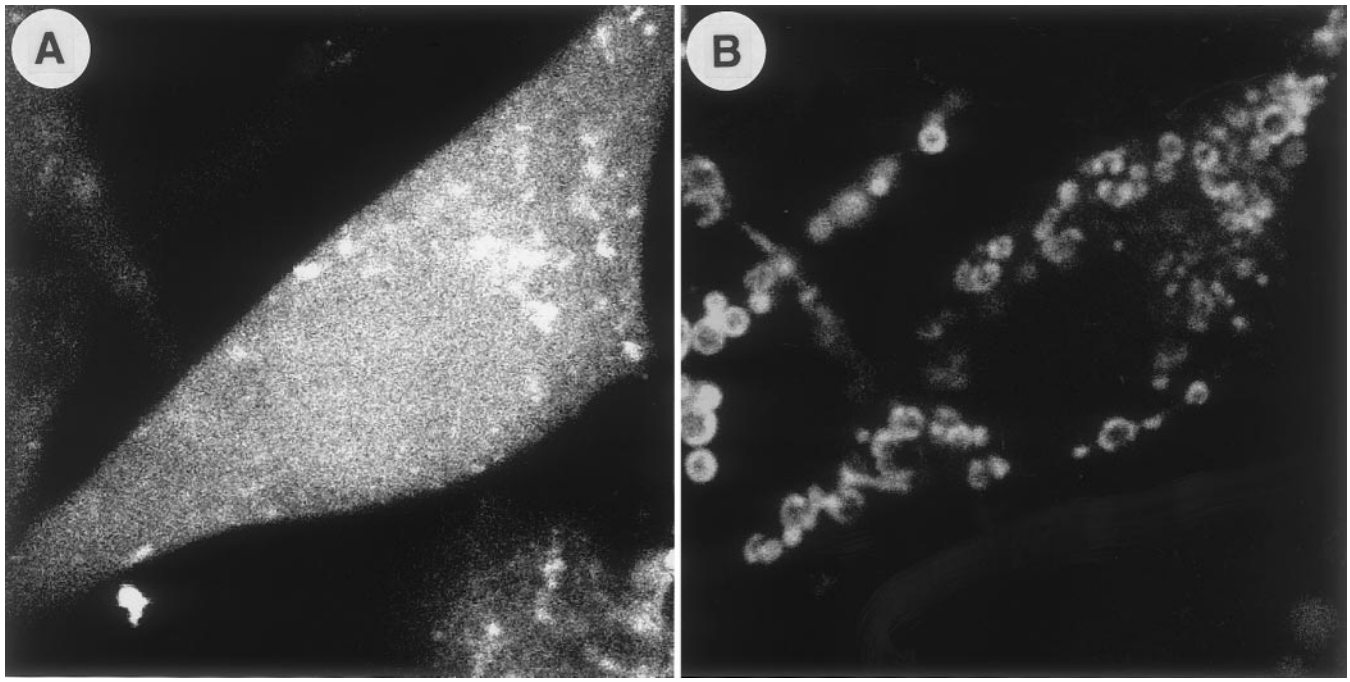

FIG. 5. Compartmentalization of fluo 3-AM. BHK cells were loaded with 10 μM fluo 3-AM for 30 min at 37°C. Ca^{2+} was monitored using CLSM. Excitation wavelength was 488 nm, and emitted fluorescence was detected between 510 and 550 nm. After addition of 20 μM digitonin in extracellular medium, cytosolic dye was released from cells and only compartmentalized indicator fluoresced. *A*: fluo 3-loaded cells before addition of digitonin. *B*: same cells after addition of digitonin.

Addition of digitonin or Triton X-100 provides information about how much the indicator is compartmentalized. Digitonin is a steroid-based nonionic detergent derived from the seeds of *Digitalis purpurea* (265). It complexes with cholesterol and other unconjugated β-hydroxysteroids in membranes (102, 339), resulting in an increase in the permeability of cell membranes to inorganic ions, metabolites, and enzymes without global changes in cell structures (109). Because the molar ratio of cholesterol to phospholipid in the plasma membrane is much greater than in organelle membranes, low concentrations of digitonin (10–100 μg/ml) selectively increase the permeability of plasma membrane, resulting in release of cytosolic indicator but retention of intracellular organelle indicator (186, 298, 440) (Fig. 5). Triton X-100 is also a nonionic detergent, which extracts intrinsic and integral proteins from membrane components, solubilizes hydrophobic proteins, and forms micelles with them while maintaining their structure and activity (71, 83, 346). It can be used to release compartmentalized indicator.

Recently, some researchers have attempted to measure $[Ca^{2+}]$ in organelles by taking advantage of compartmentalization. In particular, this is an effective method to measure mitochondrial $[Ca^{2+}]$. To evaluate mitochondrial $[Ca^{2+}]$, the fluorescence of the Ca^{2+} indicator in the cytosol can be quenched by Mn^{2+} (125, 258, 399). Several reports have shown that rhod 2 accumulates well into the mitochondria and demonstrates mitochondrial $[Ca^{2+}]$ in some types of cells (e.g., hepatocyte, heart muscle cell, astrocyte, oligodendrocyte, adrenal chromaffin cell, and lymphocyte) (14, 132, 160, 179, 254, 262, 276, 360, 398). Use of a combination of confocal microscopy, organelle-specific vital dyes, and nontargeted ion indicators has also allowed the measurement of organelle specific ion concentrations (91, 122, 155, 329, 399). The most popular example of this technique is estimation of mitochondrial $[Ca^{2+}]$ in cells double-stained with a Ca^{2+} indicator (e.g., fluo 3 or calcium green) and a potentiometric indicator (e.g., rhodamine-123 or TMRM). Mitochondrial $[Ca^{2+}]$ can be evaluated by measuring the fluorescence intensity of the Ca^{2+} indicator in areas (pixels) in which the potentiometric indicator is present (59). The dual-loading method enables measurement of changes in $[Ca^{2+}]$ and other functions (e.g., pH, membrane potential) in the targeted organelle simultaneously (60, 360). Calcium concentration in endoplasmic reticulum and/or sarcoplasmic reticulum has also often been measured using the similar technique (155, 156, 399). Although some Ca^{2+} indicators can be targeted to specific organelles successfully by altering the dye loading (or preloading) time, concentration, and/or temperature (59, 60, 329), some indicators have a propensity to accumulate into a specific organelle in some types of cells (14, 160, 179, 254, 262, 332, 360,

379). For example, Mag-fura 5, Mag-fura 2, and Mag-indo 1 are loaded easily into sarcoplasmic reticulum and/or endoplasmic reticulum compared with mitochondria in hepatocytes, gastric epithelial cells, gonadotropes, smooth muscle cells, fibroblasts, and astrocytes (52, 124, 133, 155, 156, 158, 379, 399). The tendency may be partially due to the differences in efficiency of hydrolyzation in each organelle (379). However, even if such indicators are loaded, most of them are still within the cytosol. Therefore, transient digitonin or saponin treatment has been often used for permeabilizing plasma membrane to release cytosolic dye, leaving entrapped dye within organelles (124, 155, 379). In such cases, in vivo calibration has been performed by controlling cytosolic [Ca^{2+}] and long-term exposure of bromo-A-23187 (379).

F. Binding to Other Ions and Proteins

Many of the chemical Ca^{2+} indicators bind to intracellular proteins and thus alter their fluorescent properties, including changes in the emission anisotropy, emission spectrum, the reaction kinetics, the diffusion constant, and the K_d for Ca^{2+} (25). For example, it has been reported that 80–90% of fura 2 in myoplasm is bound to soluble myoplastic proteins (e.g., aldolase, creatine kinase, and glyceraldehyde-3-phosphate dehydrogenase) (199). The degree of indicator-protein binding is dependent on the type of indicator employed and on the loading conditions (33, 166). It has been demonstrated that some Ca^{2+} indicators show changes in not only Ca^{2+} affinity but also fluorescence spectra when they are bound to intracellular proteins (19, 111, 161). When indo 1 binds to proteins, indo 1 shows a blue shift of emission spectra in the Ca^{2+}-bound form but not the Ca^{2+}-free form, resulting in an error in ratiometric [Ca^{2+}] measurements based on in vitro calibrations (19, 161).

In addition, all of these indicators are affected by other intracellular ions. In particular, the K_d values of some Ca^{2+} indicators are sensitive to pH to various degrees (100, 213, 214). For example, the K_d values of the three most popular Ca^{2+} indicators, indo 1, fura 2, and fluo 3, increase ~1.4–1.7 times and 7.1–11.8 times when pH changes from 7.4 to 6.5 and 5.5 (22°C), respectively (213, 214). Hence, much attention is needed in investigations that examine [Ca^{2+}] in acid environments (e.g., ischemia-reperfusion or measurement of [Ca^{2+}] in the lysosome). Although it is well known that Ca^{2+} indicators have various affinities for Mg^{2+}, they can also bind to other kinds of intracellular heavy metal ions such as Mn^{2+}, Co^{2+}, Zn^{2+}, Ba^{2+}, and Cd^{2+} (11, 258). Fura 2, Mag-fura 2, and indo 1 have much higher affinities to Mn^{2+} and Zn^{2+} than Ca^{2+} (13, 175, 359) [e.g., K_d values of fura 2 for Mn^{2+}, Zn^{2+}, and Ca^{2+} are 2.8, 3, and 145 nM, respectively (13, 207)]. Although Mn^{2+} and Co^{2+} strongly quench fluorescence of fura 2 and indo 1 (242, 258, 269), their spectral properties are similar whether they bind to Zn^{2+} or Ca^{2+} (127). The artifacts caused by these heavy metal ions can be identified and controlled using tetrakis-(2-pyridylmethyl)ethylenediamine (TPEN), which is a selective heavy ion chelator without disturbing [Ca^{2+}] and [Mg^{2+}] (11, 365, 409).

G. Dye Leakage

In many types of cells, indicators leak from cytosol to extracellular medium (242). This leakage is regulated in part by anion transport systems and can be inhibited or suppressed by probenecid and sulfinpyrazone (88, 89) (Fig. 3) or by low temperature (90, 242). The rate of dye secretion by anion transport system is partially dependant on the cell type. It has been reported that 40% of cytosolic fura 2 leaks from N2A neuroblastoma after 10-min incubation at 37°C, whereas only 15% of fura 2 leaks from J774 macrophages (89). Fura 2 leaks much faster from glial cells than neurons of leech central nervous system (268). Moreover, many papers have demonstrated the leakage of various Ca^{2+} indicators. Fura 2 is removed from the cytosol in smooth muscle cells (257), astrocytoma cells (242), pheochromocytoma-like cells (88), and pancreatic β-cells (9); indo 1 in pancreatic β-cells (10); and fluo 3 in lymphocytes (367). It has been thought that the rate of secretion is partially dependent on the electrical charge of the indicators. For example, it is known that the dye leakage of calcium green is less than that of fluo 3 because the former has one more positive charge compared with the latter. However, the use of probenecid or low temperature in these studies may limit the interpretation of these studies. Long exposure of cells to Pluronic F-127 also can sometimes facilitate dye leakage through the plasma membrane (241). Recently, more leakage-resistant indicators have been produced (e.g., fura PE3, indo PE3, and fluo LR). They are constructed by linking piperazine nitrogens to the parent indicator, which forms an ambient ion after protonation in the cell (415). Another way of preventing dye leakage is to conjugate the indicator with membrane-impermeant dextrans or other macromolecules (345) or to load indicators continuously via micropipettes during the experiment (268).

VII. TECHNIQUES FOR MEASURING CALCIUM

A. Optical Techniques for Measuring Ca^{2+}

Fluorescence microscopy allows analysis of the distribution and dynamics of functional molecules within single intact living cells. However, many molecules change concentration, distribution, and function simulta-

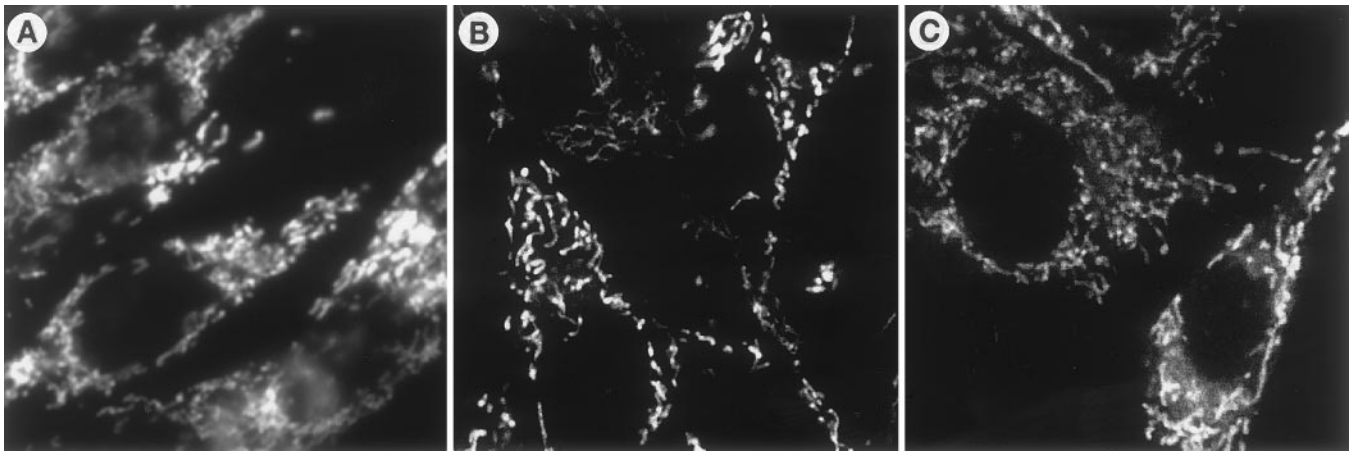

FIG. 6. Comparison of wide-field microscopy, CLSM, and TPLSM in visualization of mitochondria. BHK cells were loaded with MitoTracker Green. Spatial resolution (especially vertical) of image with wide field is much poorer than those with CLSM or TPLSM. *A*: wide-field microscope image (Olympus IX-70; Hamamatsu Photonics cooled charged-coupled device camera; ×100 oil immersion; numerical aperture, 1.35; excitation, 470–490 nm; emission, 510–530 nm). *B*: CLSM image (Olympus IX-70; Olympus Fluoview; ×60 water immersion; numerical aperture, 1.2; excitation, 488 nm; emission, 510–560 nm). *C*: TPLSM image (Olympus IX-70; customized Olympus GB-200; ×60 water immersion; numerical aperture, 1.2; Coherent Innova 300 plus Mira 900 Ti/Sapphire pulsed laser; excitation, 800 nm; emission, 510–560 nm).

neously or sequentially during numerous intracellular phenomena. To elucidate the mechanisms of these intracellular phenomena, multiparametric analysis is often required. Without multiparametric analysis, it may sometimes be difficult to determine whether an observed change in ion status is the cause or the effect of a particular biological process. In addition, the properties of some Ca^{2+} indicators are influenced by changes in the intracellular environment. For example, the K_d of some Ca^{2+} indicators is pH sensitive. Therefore, multiparametric analysis is often necessary to determine whether changes in other molecular species are occurring and whether they might alter the precision of the $[Ca^{2+}]$ measurements. We and others have developed a variety of instruments and techniques to resolve the problems discussed above and to improve experimental precision. Here, the properties and the purpose of some of these instruments as well as other useful implements are briefly described.

1. Multiparameter digitized video microscopy

Multiparameter digitized video microscopy permits single living cells to be labeled with multiple indicators whose fluorescence is responsive to specific cellular parameters of interest (150, 220). This system consists of the following equipment: an inverted fluorescence microscope equipped with differential interference contrast (DIC) and phase optics, an intensified charged-coupled device (CCD) camera or other type of camera, a videocassette recorder, a computer workstation with imaging boards for image processing, a xenon and mercury lamp, and a host computer to control the system. Two eight-position filter wheels under computer control are used to place interference and neutral density filters in the path of excitation light (221). Phase, DIC, and fluorescence images specific for each indicator are collected over time, digitized, and stored. Image analysis and processing then permits quantitation of the spatial and temporal distribution of the various parameters within the single living cells (36, 277).

2. Confocal laser scanning microscopy

In the case of the conventional nonconfocal microscope, spatial resolution is often limited by the blurring effect of out-of-focus fluorescent light. Background fluorescence reduces contrast and clarity of images. The vertical resolution is not very good, and the so-called focal plane is determined as the most contrasted plane by each investigator. Thus the observed fluorescence is the summation of the whole thickness of the material, which can lead to errors in quantitation especially in relatively thick cells. Analysis using specimens consisting of multilayer cells with wide-field microscopy has especially suffered from disturbance by the background intensity. This disadvantage is greatly reduced in confocal laser scanning microscopy (CLSM). The CLSM produces images by moving a scanning point across the specimen and collecting the emitted fluorescence through a pinhole that is located at the confocal point of the scanned focus. By excluding the out-of-focus fluorescence from the fluorophore, CLSM offers high vertical and horizontal spatial resolution (<1 μm) (87) (Fig. 6). Confocal laser scanning microscopy is able to produce thin and unblurred optical sections, offering the prospect of three-dimensional spatial recon-

struction of the parameters of interest. Because the resolution is much less than the thickness of the cell or some kinds of organelles, theoretically the fluorescence intensity of each pixel in the obtained image shows the concentration of the functional ion with precision. The most important mechanical limitations of the CLSM have been the lack of variation in the excitation wavelength and the temporal resolution. Because the light sources commonly employed in CLSM are argon or argon-krypton lasers, the usable range of excitation wavelengths is quite restricted. However, recently some UV-excitable CLSM have been produced (253, 280), and temporal resolution has been improved to video-frame rate (30 frames/s) or faster (15, 136, 188, 278, 392).

3. Two-photon excitation laser scanning microscopy

Two-photon excitation laser scanning microscopy (TPLSM) is a novel type of microscopy (81, 82). The concept of two-photon excitation is not a new idea. It was theoretically predicted in 1931 (114) but was not confirmed experimentally for more than 30 years (181). Two-photon excitation means that one fluorophore is excited by two individual photons simultaneously. Because the energy of the beam wave varies in inverse proportion to the wavelength, if the wavelength of excitation is doubled, then the energy decreases to one-half. Therefore, if two individual photons excite the target flourophore at the same time, the actual excitation power is theoretically equal to that of the one photon at one-half the wavelength. With the use of long-wavelength excitation, dyes normally excited in the UV range of the spectrum can be employed. Moreover, long-wavelength excitation results in less photodamage, cytotoxicity, and deeper penetration into the sample (383).

The TPLSM has high spatial resolution like the CLSM (80, 305, 428) (Fig. 6*C*). The mechanisms responsible for this high resolution are, however, quite different from that of CLSM. Because the probability of the simultaneous excitation by two individual photons is proportional to the square of the photon concentration, fluorophores far from the plane of focus cannot be excited with enough power with TPLSM, resulting in high spatial resolution (334). In the case of the CLSM, not only the focal plane but also the areas surrounding the plane of focus are excited, but the pinhole blocks emission light from the out-of-focus plane from reaching the detectors. The mechanism of localized excitation with TPLSM offers much less photobleaching than CLSM. In addition, CLSM using single-photon excitation is sometimes limited by scattering of background or solvent (430). In contrast, TPLSM is relatively free from these problems because the emission wavelength is usually hundreds of nanometers shorter than excitation wavelength and is spectrally well separated (430). Two-photon excitation laser scanning microscopy also usually requires no pinhole apparatus, which is necessary for CLSM, while keeping relatively high spatial resolution (428) (certainly TPLSM provides greater spatial resolution by employing a pinhole apparatus; confocal TPLSM). The simplified optical pathway results in increasing efficiency of detecting fluorescence.

Two-photon excitation laser scanning microscopy has another interesting property. The fluorescent responses of numerous molecules excited by two photons are not exactly the same as that by single-photon excitation at the half wavelength. It has been demonstrated that simultaneous absorption of two photons is influenced substantially by the degree of molecular symmetry and vibronic coupling in fluorophores and that the response of two-photon absorption is not same as that of single-photon absorption (3, 349, 431, 432). For example, when excited by two photons, octadecyl indocarbocyanines (DiI), rhodamine B, and fluorescein show a blue shift in the absorption spectra, whereas two-photon absorption spectra of indo 1 and GFP are close to their single-photon absorption spectra (431, 432). Accordingly, the TPLSM sometimes demonstrates different images from that obtained with single-photon excitation CLSM. For example, blue fluorescence, green fluorescence, and red fluorescence may be simultaneously excited using TPLSM (432) (Fig. 7).

4. Pulsed-laser imaging for rapid Ca^{2+} gradients

A pulsed-laser imaging system was developed by Kinoshita and colleagues (154, 194) and was applied to the investigations of rapid Ca^{2+} signaling in excitation-secretion or excitation-contraction coupling by Fernandez and co-workers (104, 262, 327). The concept of this system is that high temporal resolution can be obtained by piling up single images obtained at various time lags after repeated stimulation of an event if the event can be reproduced consistently. In this system, materials are transiently excited with a brief (300–350 ns) high-intensity (0.25 J) pulsed laser. The "snapshot" of the emitted fluorescence is obtained with a video camera for subsequent analysis. The delay of the pulsed excitation after the stimulating trigger is controlled by a host computer. This system allows submicron spatial resolution and millisecond temporal resolution.

5. Time-resolved fluorescence lifetime imaging microscopy

Evaluation of functional molecules with time-resolved fluorescence lifetime imaging microscopy (TRFLM) is completely different from conventional fluorescence microscopy (151, 152, 418). The fluorescence lifetime (τ) is the characteristic time that a fluorescent molecule remains in an excited state before returning to

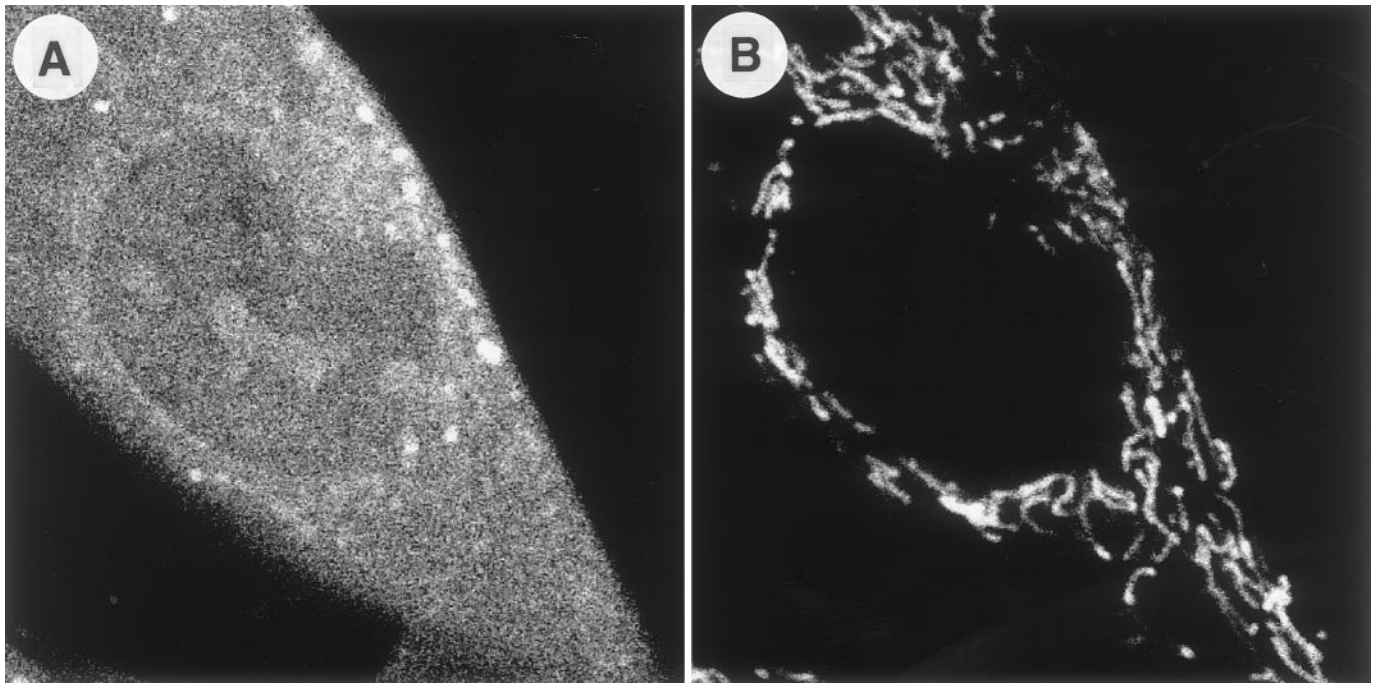

FIG. 7. Multiparametric measurements using TPLSM. An image of a BHK cell double-stained with benzothiaza-1 and TMRM was obtained using TPLSM. Excitation wavelength was 760 nm, and emitted fluorescence was divided into two channels using a 560-nm dichroic mirror. Image of channel 1 represented fluorescence intensity collected at 500–520 nm for visualization of benzothiaza-1, and image of channel 2 showed that at 610–650 nm for visualization of TMRM. Although actual excitation wavelength is only 380 nm, both channels can be simultaneously detected with sufficient fluorescence intensity. *A*: benzothiaza-1 image for $[Ca^{2+}]$ measurement. *B*: TMRM image for mitochondrial location and membrane potential.

the ground state. When a mixture of two fluorescent compounds of varying τ is excited with a short pulse (i.e., on the order of 1 ps), the excited molecules will emit fluorescence with a time dependence related to the length of each τ (Fig. 8). Although τ is not affected by scattering, decay characteristics of the background, path length, number of fluorophores (concentration of the probe), photobleaching, and other factors governing fluorescence intensity measurements, τ is quite sensitive to the chemical and environmental parameters of the fluorophore. For example, each Ca^{2+} indicator displays two τ values: that of the Ca^{2+}-bound state and the Ca^{2+}-free state (209). The τ values of each of these states remain constant as $[Ca^{2+}]$ changes, but the amplitude (contribution) to the mean τ changes as a function of $[Ca^{2+}]$. Thus much like ratiometric imaging, but using a nanosecond-gated multichannel plate image intensifier, TRFLM provides a two-dimensional image where each pixel value reflects mean τ of the fluorescence probe in cells. It has been demonstrated that various Ca^{2+} and pH indicators used with the conventional steady-state microscopy, including quin 2, indo 1, fura 2, fluo 3, calcium green, calcium crimson, calcium orange, SNARF, SNAFL, and 2′,7′-bis(carboxyethyl)-5,6-carboxyfluorescein, can be successfully used as a Ca^{2+} or pH indicator with TRFLM (152, 208, 209, 211, 335, 336, 385).

A limitation of some Ca^{2+} indicators that can be measured with TRFLM is that measurement of $[Ca^{2+}]$ using TRFLM is restricted by the τ values and F_{max}/F_{min}. For example, if the emission of the Ca^{2+}-free form is much dimmer than that of Ca^{2+}-bound form, the emitted fluorescence may be due to only the Ca^{2+}-bound form, and the measured τ may represent only τ of Ca^{2+}-bound form (208). In addition, the existence of probe bound to nonselective ions or existence of indicator complexes of different conformations with different τ values sometimes reduces the range. The range of accurately measurable $[Ca^{2+}]$ using a certain kind of the Ca^{2+} indicator and TRFLM is often shifted from that obtained with steady-state fluorescence measurements (336, 386). The TRFLM Ca^{2+} indicators include calcium green, fluo 3, or quin 2, which display small changes in mean τ upon binding Ca^{2+} and saturate (in terms of changes in mean τ) at 100–150 nM Ca^{2+} (208, 209, 336). Calcium crimson, calcium orange, and certain of the ratiometric indicators such as fura 2 are sensitive in terms of changes in lifetime over a relatively broad range of $[Ca^{2+}]$ (152, 386). Some of ratiometric Ca^{2+} indicators (e.g., quin 2 and fura 2) undergo phototransformation to Ca^{2+}-insensitive species and shift in emission spectra (27, 209, 342). Although it is hard to correct their effects on intensity-based ratiometry, TRFLM

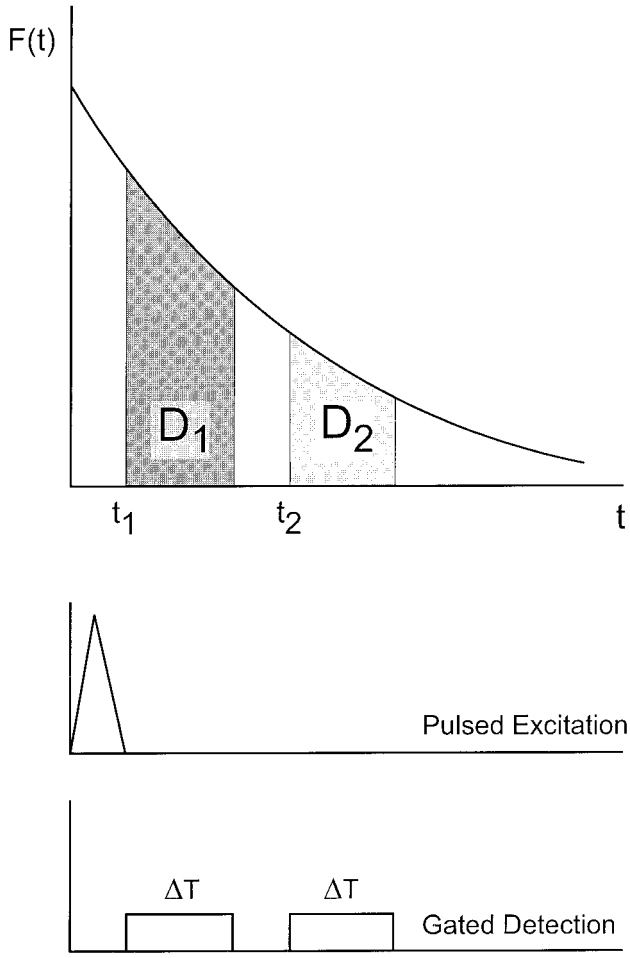

FIG. 8. Concept of fluorescent lifetime imaging. After pulsed excitation, emitted fluorescence is detected at differing times (t_1 and t_2) and for a specific duration (D_1 and D_2) relative to excitation pulse. Lifetime (τ) can be obtained by following equation with 4 parameters: $\tau = (t_2 - t_1)/\ln (D_1/D_2)$.

reveals the existence of such products and enables one to obtain accurate measurements of $[Ca^{2+}]_i$.

Another important advantage of lifetime-based $[Ca^{2+}]$ measurement over steady-state intensity-based measurements is that some of the problems in calibration described above can be avoided. The steady-state fluorescence intensity of some Ca^{2+} indicators is affected by the local environment, which makes the calibration and evaluation of $[Ca^{2+}]$ with intensity-based measurements quite complicated. The principle of estimating $[Ca^{2+}]$ with lifetime measurements is based on a fact that τ of the Ca^{2+}-bound indicator differs from that of the Ca^{2+}-free one. When $[Ca^{2+}]$ changes, the τ of the Ca^{2+}-bound or Ca^{2+}-free indicator does not change, but the contribution (amplitude) of the bound and unbound indicator in terms of mean τ changes. Importantly, some of the τ values of certain Ca^{2+} indicators are minimally affected by environmental factors (152). For example, although fluorescence intensity of calcium crimson decreases significantly with an increase in the concentration of proteins and cellular contents or a decrease in hydrophobicity, the τ values of the Ca^{2+}-bound and the Ca^{2+}-free form are hardly affected by them (152). The same advantages of lifetime-based measurement have also been demonstrated with a pH indicator, SNAFL-1 (335). This property reduces the discrepancy between in vitro calibration and in vivo calibration and makes the calibration much easier and the evaluation of ion concentrations much more accurate.

Time-resolved fluorescence lifetime imaging microscopy has many other potential applications. It can be also used to measure other types of ions and intracellular substances such as NADH (210).

6. *Photomultiplier tube*

The detectors for quantitative measurement of fluorescence through the microscope can be essentially categorized into two groups: photomultiplier tubes (PMT) and imaging devices (417). In the PMT, the light intensity is detected by a photocathode film that emits photoelectrons in response to absorption of light. The emitted photoelectrons near the photocathode are immediately accelerated toward the second emitter, the dynode, by a positive voltage gradient. This results in each electron being amplified many times, and the final electron gain after several repeated amplifying dynodes is more than 10^8 electrons.

Because the PMT per se does not have spatial resolution, images cannot be obtained without a scanning system, either a laser scanning or mechanical stage scanning system (171). Although other imaging devices such as the CCD camera provide spatial resolution, they have certain limitations in temporal resolution because the readout of these devices is relatively slow and the readout is associated with significant noise. Recently, intensified target videcons have been produced (2, 370). However, PMT allow more quantitative measurements with higher temporal resolution, high magnification of signal, and a good signal-to-noise ratio at a low price (35). In addition to their use in CLSM, PMT are widely used in conjunction with fiber optics for precise $[Ca^{2+}]$ measurements in localized areas (204, 333).

7. *Flow cytometry*

Flow cytometry is the measurement of fluorescence and/or light scattering emitted by whole cells, which are suspended in a flowing stream of solution. Single cells are hydrodynamically forced into the center of a surrounding sheath of fluid by passage through a narrow orifice (flow cell), which is specifically designed to generate laminar flow. The single-file stream of cells is guided into the path of a laser beam, which can be used for fluorophore excitation or for probing the size and structure of cells by light scattering. Light is detected with photomultipliers, which

convert the light into electrical signals for display and storage in a computer-based system. Fluorescent measurements are made using the appropriate excitation laser lines and barrier filters. Laser light, which is scattered by cells in the forward direction, is proportional to the cell size. Light scattered at right angles is proportional to granularity; the more complex the internal structure of the cell, the more light is scattered.

Information can be displayed in multiple formats depending on the system and the investigator needs. For example, when fluorescence is measured from the Ca^{2+} indicator indo 1, the ratio of the emission wavelengths can be displayed against the number of events (a frequency histogram). Alternatively, the fluorescent signal at two emission wavelengths can be plotted against each other so that the slope of the resulting display is equivalent to the ratio. Fluorescent signals can also be plotted as a function of forward or side scattering light, thereby allowing the user to test for correlation between cell size, structure, and fluorescent signal.

Fluorescence and light scattering can then be used to sort and/or isolate cells according to multiple cellular parameters. For example, it is possible to tag a specific cell type with a fluorescent antibody then record and sort the intracellular Ca^{2+} response from only that cell population. Flow cytometry clearly excels in the analysis of mixed cell population studies. When a cell type is particularly rare, cell sorting can be used to enrich the population of that cellular type. In another use, cells can be stimulated with an agonist of interest to identify the cells in that population that respond with an increase in intracellular Ca^{2+}. Cells responding to the agonist can then be sorted aseptically and subsequently be cultured to enrich the cell type [for example, see Tarnok (394)].

A potential problem with the measurement of agonist-induced Ca^{2+} mobilization using flow cytometry is a time lag between the addition of agonist to the cell suspension and the point at which a response can be measured. Typically, the sample tube containing the suspension of cells must be depressurized to add agonist and then repressurized to obtain proper cell flow. Depending on the system, cells must then travel for tens of centimeters before they cross the laser excitation beam. This can result in temporal gaps of 10–20 s, which may preclude an accurate measurement of the initial rise in intracellular Ca^{2+}. Several modifications to the flow cytometry equipment have been proposed to minimize the lapse in data acquisition (93, 190). A relatively cheap adaptation was recently reported by Burns and Lewis (49), which allows continuous data acquisition. This technique uses a small Teflon-coated magnet held above the cell suspension by a larger external magnetic bar. A drop of agonist is applied to the top of the stir bar, without exposing the suspended cells, and the sample tube is then pressurized. During data acquisition, the external magnet is removed so that the stir bar containing the agonist is dropped into the cell suspension. The only remaining time lag between agonist application and the detection of a cellular response is the travel time between the agonist containing sample and the laser, which, depending on the pressure and system, is on the order of a few seconds.

Another limitation of flow cytometry is the inability of the technique to measure dynamic Ca^{2+} responses from asynchronous cell populations. In this case, out-of-phase oscillations will be averaged over time, concealing the pattern of Ca^{2+} signaling in individual cells. Flow cytometry is best suited for measurements of the entire cellular response.

B. Nonoptical Techniques for Measuring Ca^{2+}

1. *Electrophysiology*

Changes in intracellular Ca^{2+} can be estimated by monitoring the currents generated by Ca^{2+}-dependent ion channels located in the plasma membrane. Because these are membrane-bound channels, their activation serves as a very sensitive local indicator of $[Ca^{2+}]$. Calcium-activated ion currents have been used in many cell types to investigate the IP_3 signaling pathway, including chromaffin (237), pancreatic (397), and lacrimal cells (240). The Ca^{2+}-activated Cl^- channels in *Xenopus* oocytes, which generate a transient inward current in response to increases in intracellular Ca^{2+}, have also been widely used for this purpose (73, 248, 249). In this system, however, there is a poor temporal correlation between Ca^{2+} signals estimated using Ca^{2+}-activated Cl^- currents and simultaneous measurements using fluorescent Ca^{2+} indicators. Specifically, activation of the Cl^- current is transient, reaching a peak while the fluorescent signal continues to increase (215, 296). Parker and Yao (296) reported that activation of the Cl^- current corresponded better to the rate of rise of intracellular Ca^{2+} rather than to its steady-state level and suggested that the Cl^- channels may show an adaptive response. Interpretation of the changing Ca^{2+} signal is complicated by the fact that the Ca^{2+}-activated Cl^- current exhibits at least two distinct Ca^{2+}-sensitive components (78, 234, 250, 294, 295, 301). The first component is transient and does not depend on extracellular Ca^{2+}, whereas the second component is slower and depends on extracellular Ca^{2+}. Recent evidence suggests that the two components are due to two distinct types of Cl^- currents with different Ca^{2+} sensitivities (142). Further complicating the interpretation of the signal is the fact that Ca^{2+} influx can trigger regenerative Ca^{2+} release from IP_3-sensitive stores (Ca^{2+}-induced Ca^{2+} release or CICR) (434). Additionally, activation of the IP_3-sensitive pathway activates protein kinase C-mediated phosphorylation events, which appear to affect the Ca^{2+} sensitivity Cl^- current (301). Finally, inhomogeneities in the distri-

bution of Cl^- channels may bias the measurements, since the Ca^{2+} signal is integrated over the entire cell (30, 235).

Currents other than those carried by Cl^- channels can also be used to report changes in intracellular Ca^{2+}. These include the Ca^{2+}-activated nonselective cation channels (436) and the Ca^{2+}-activated K^+ channels (237, 293, 436). A very novel application of Ca^{2+}-activated ion channels was developed by Kramer (201), who named the technique "patch cramming." As the name implies, a patch-clamp electrode is used to isolate a patch of membrane containing Ca^{2+}-sensitive ion channels. The patch is excised in the inside-out configuration (137), and the Ca^{2+} dependence of the ion channel open probability is calibrated by exposure to different $[Ca^{2+}]$. Subsequently, the patch is inserted (crammed) into the cell, and the open probability of the channels is used as an indicator of local $[Ca^{2+}]$. The advantage of this technique resides in the utilization of the ion channel as a natural biochemical detector. However, the technique relies on the assumption that the open probability of the channel in the patch does not change over time, an assumption that might not always be valid. For example, reintroduction of the patch into the cell after excision may cause changes in the state of phosphorylation or sensitivity of the channel. Additionally, the application of this technique is more appropriate for large cells that can withstand impalement with a patch electrode.

Overall, Ca^{2+}-activated ion currents are good indicators of changes in intracellular Ca^{2+}. However, this technique would not be the method of choice if estimates of the absolute changes in $[Ca^{2+}]$ were required.

2. *Ca^{2+}-selective electrodes*

Calcium ion concentrations can be measured potentiometrically using ion-selective electrodes. Calcium-selective electrodes have a wider dynamic range (pCa 9 to 1) than fluorescent dye indicators (e.g., indo 1, pCa 7.5 to 5). They are excellent for calibration of Ca^{2+} solutions and can be used in vivo for calibrating signals obtained from fluorescent indicators. However, the response time of an ion-selective electrode to changes in free Ca^{2+} is slower (~0.5–1 s) when compared with that of a fluorescent indicator (ms). Ion-selective electrodes are made by incorporating an ion-complexing agent (ligand) into a liquid lipophilic membrane that imparts an ion selectivity to the membrane itself. The lipophilic membrane separates two aqueous compartments, generally a sample solution from an internal reference solution in the electrode. The role of the ligand is to selectively extract ions from the aqueous solutions, transport them across the lipophilic membrane, and in doing so generate a membrane potential proportional to the concentration difference. The potential difference (ΔV) between an unknown ion concentration (C) and a reference concentration (C_r), assuming that there are no interfering ions, is given by the Nernst equation

$$\Delta V = 28 \log (C/C_r)$$

Neutral-based carriers are the preferred ion-selective ligand for Ca^{2+}-selective electrodes because they exhibit a high preference of Ca^{2+} over Na^+ and K^+ and have much better Ca^{2+}/Mg^{2+} and Ca^{2+}/H^+ selectivities when compared with electrically charged lipophilic ligands (8). ETH-1001 has been used extensively as a Ca^{2+}-selective ligand since its synthesis in 1976 (284). However, this complexing agent has poor sensitivity to Ca^{2+} below 1 μM (8). More recently, new ligands with greatly improved Ca^{2+} selectivity have been synthesized. ETH-129 (343) permits measurements of Ca^{2+} close to pCa 8–9. ETH-5234, an extremely lipophilic Ca^{2+}-selective ionophore (113), permits even lower measurements of Ca^{2+} to pCa 10 at the expense of longer equilibration time for the measurements. Suzuki et al. (382) have recently synthesized the ligand K23E1, which allows accurate estimates of very high $[Ca^{2+}]$ (pCa 5–1).

In addition to neutral carriers, liquid membranes are composed of a resin cocktail containing membrane solvent (e.g., silicon rubber) and a membrane matrix (typically, polyvinylchloride gelled). Premade cocktails containing both the Ca^{2+} ligand and resin are commercially available (e.g., Fluka). Complete Ca^{2+}-selective electrode measuring kits can also be commercially purchased. Alternatively, macroelectrodes can be easily constructed in the laboratory and used with standard laboratory pH meters to monitor potential. Several practical guides to ion-selective electrode construction have been published (8, 24). Typically, a macroelectrode is made from polyethylene tubing (~1–3 mm diameter) that is dipped into a cocktail solution to form a Ca^{2+}-selective membrane, several 100 ms thick, and allowed to dry overnight (24). Dry electrodes can be stored for months in protein-free solution, although a decrease in electrode sensitivity can be expected. Protein concentrations make measurements of low Ca^{2+} (~10 nM) difficult and should be done with freshly prepared electrodes (24).

Minielectrodes must be fabricated in the laboratory to monitor intracellular Ca^{2+} (24, 205, 328, 363). Briefly, glass capillary tubes are pulled on a standard pipette puller to tip diameters of 0.5–10 μm. A complication that is encountered in minielectrode fabrication is the noise that is introduced by the resistance of the pipette tip. A larger tip diameter reduces electrode resistance and increases signal-to-noise ratio, but the tip diameter is practically limited by the tolerance of your experimental preparation. A short electrode shank (similar to a patch electrode) also reduces resistance and reduces capacitance artifacts due to a fluctuating bath level. Pulled

electrodes are dehydrated and silanized to help stabilize the short column of hydrophobic ionophore liquid membrane. Minielectrodes are back-filled with a reference Ca^{2+} electrolyte (plus 0.5% agar) then front-filled with the ionophore membrane. Again, ionophore cocktails can be commercially obtained (e.g., Fluka Calcium Ionophore I, cocktail A, which contains the Ca^{2+}-selective sensor ETH 1001). Electrical contacts are made using Ag/AgCl wires.

3. Vibrating Ca^{2+}-selective probe

A variant of the Ca^{2+}-selective microelectrode technique is the vibrating Ca^{2+}-selective probe. The vibrating probe was originally designed to measure small extracellular ion currents. By vibrating a voltage-sensing probe between two points, the system was self-referencing (which significantly increases signal-to-noise ratio) and was capable of measuring microvolt differences over several microns, which equates to picomolar ion fluxes when the signal is averaged (174). The standard voltage-sensitive probe measures only net current flow, whereas the ion-selective vibrating system measures a current flux attributable to a single ion species. Vibrating ion-selective electrodes are noninvasive (recordings can last for hours or even days) and can be located within microns of the cell surface. Additionally, vibrating probes can easily be moved around the cell to survey current flow from multiple locations. An obvious disadvantage of the technique is that the vibrating probe cannot be used to measure intracellular concentrations. However, this technique has been successfully used in a wide range of preparations to study processes as diverse as Ca^{2+} entry during pollen tube growth in plant cells (303), ACh-induced Ca^{2+} fluxes across the sarcolemma in smooth muscle cells (84), Ca^{2+} entry during oxidative challenges in *Aplysia* neurons (94), and the activation currents during fertilization of various egg species (282, 283).

The underlying principle of the vibrating probe measurement is that steady extracellular currents generate very small voltages in conductive extracellular fluids (363). Jaffe and co-workers (173, 205) refined this approach by developing the Ca^{2+}-selective vibrating probe to measure extracellular Ca^{2+} currents. The same minielectrodes that are used for intracellular Ca^{2+} can be used for the vibrating probe technique. The Ca^{2+}-sensitive electrode can be vibrated by piezoelectrical microstages that are driven by a square wave of low frequency. Because of concerns of mixing of chemical gradients, the ion-selective probe cannot be vibrated as rapidly as a voltage-sensitive probe. Typically, frequencies of 0.3–0.5 Hz are used.

Extracellular Ca^{2+} flux (J) is calculated assuming Ca^{2+} move through the extracellular medium by diffusion according to Fick's law

$$J = -D(\Delta c/\Delta x)$$

where J is the ion flux (in $\mu mol \cdot cm^{-2} \cdot s^{-1}$), D is the diffusion constant (in cm^2/s), and $\Delta c/\Delta x$ is the ion concentration gradient over distance (in $\mu mol/cm^2$). The Ca^{2+} J can be calculated once the value of $\Delta c/\Delta x$ is determined. A Ca^{2+}-selective probe is used to calculate Δc by vibrating the tip over a distance Δx. The ion gradient Δc is calculated by measuring the change in voltage over a known vibrating distance. The spatial resolution is determined by the diameter of the glass electrode tip (~1–5 ms, see above).

A calibration curve should be constructed such that any change in voltage (ΔV) can be converted into a change in Ca^{2+} using the Nernst equation

$$\Delta V = 28 \log (C_2/C_1)$$

where C_2 and C_1 are the Ca^{2+} concentrations at the extreme of the vibration distance (Δx). With the assumption that the difference (ΔC) between C_1 and C_2 is small, ΔC can be estimated according to

$$\Delta V = 12\Delta C/C_b \text{ (mV)}$$

where C_b is the background concentration of Ca^{2+} (205). Substitution into Fick's law (see above) then yields the Ca^{2+} flux.

VIII. CONCLUSIONS

In the past two decades, optical microscopy and Ca^{2+} indicators have become quite common and standard. Moreover, several promising new technologies, including TPLSM and TRFLM, have been developed. Microscopy is no longer an approach to just watch morphological changes but has evolved to allow the observation of real-time cellular physiology. The advent of GFP, which can be used in FRET-based assays, in addition to serving as a marker for genes or proteins, will expand the role of microscopic investigation rapidly. Changes in some important ion concentration such as Ca^{2+} or pH are known to act as a trigger of many cellular events. Developing microscopic methods will enable the investigation of their dynamics and regulation.

Address for reprint requests and other correspondence: B. Herman, Dept. of Cellular and Structural Biology, mail code 7762, Univ. of Texas Health Science Center at San Antonio, 7703 Floyd Curl Dr., San Antonio, TX 78229-3900 (E-mail: hermanb@uthscsa.edu).

REFERENCES

1. ABE, F., M. MITSUI, H. KARAKI, AND M. ENDOH. Calcium compartments in vascular smooth muscle cells as detected by aequorin signal. *Br. J. Pharmacol.* 116: 3000–3004, 1995.

2. AIKENS, R. S., D. A. AGARD, AND J. W. SEDAT. Solid-state imagers for microscopy. *Methods Cell Biol.* 29: 291–313, 1989.
3. ALBOTA, M., D. BELJONNE, J. L. BRÉDAS, J. E. EHRLICH, J. Y. FU, A. A. HEIKAL, S. E. HESS, T. KOGEJ, M. D. LEVIN, S. R. MARDER, D. MCCORD-MAUGHON, J. W. PERRY, H. RÖCKEL, M. RUMI, G. SUBRAMANIAN, W. W. WEBB, X. L. WU, AND C. XU. Design of organic molecules with large two-photon absorption cross section. *Science* 281: 1653–1656, 1998.
4. ALLEN, D. G., AND J. R. BLINKS. The interpretation of light signals from aequorin-injected skeletal and cardiac muscle cells: a new method of calibration. In: *Detection and Measurement of Free Ca^{2+} in Cells*, edited by C. C. Ashley and A. K. Campbell. Amsterdam: Elsevier/North-Holland, 1979, p. 159–174.
5. ALLEN, D. G., J. R. BLINKS, AND F. G. PRENDERGAST. Aequorin luminescence: relation of light emission to calcium concentration. A calcium-independent component. *Science* 195: 996–998, 1977.
6. ALMERS, W., AND E. NEHER. The Ca signal from fura-2 loaded mast cells depends strongly on the method of dye-loading. *FEBS Lett.* 192: 13–18, 1985.
7. ALONSO, M. T., M. J. BARRERO, E. CARNICERO, M. MONTERO, J. GARCIA-SANCHO, AND J. ALVAREZ. Functional measurements of $[Ca^{2+}]$ in the endoplasmic reticulum using a herpes virus to deliver targeted aequorin. *Cell Calcium* 24: 87–96, 1998.
8. AMMANN, D. *Ion-Selective Microelectrodes. Principles, Design and Application.* New York: Springer-Verlag, 1986.
9. ARKHAMMAR, P., T. NILSSON, AND P. O. BERGGREN. Glucose-stimulated efflux of fura-2 in pancreatic β-cells is prevented by probenecid. *Biochem. Biophys. Res. Commun.* 159: 223–228, 1989.
10. ARKHAMMAR, P., T. NILSSON, AND P. O. BERGGREN. Glucose-stimulated efflux of indo-1 in pancreatic β-cells is reduced by probenecid. *FEBS Lett.* 273: 182–184, 1990.
11. ARSLAN, P., F. DI VIRGILIO, AND M. BELTRAME. Cytosolic Ca^{2+} homeostasis in Ehrlich and Yoshida carcinomas: a new, membrane-permeant chelator of heavy metals reveals that ascites tumor cell line have normal cytosolic free Ca^{2+}. *J. Biol. Chem.* 260: 2719–2727, 1985.
12. ASHLEY, C. C., A. K. CAMBPELL, AND D. G. MOISESCU. A demonstration of some of the properties of obelin: a calcium-sensitive luminescent protein. *J. Physiol. (Lond.)* 245: 9P–10P, 1974.
13. ATAR, D., P. H. BACKX, M. M. APPEL, W. D. GAO, AND E. MARBAN. Excitation-transcription coupling mediated by zinc influx through voltage-dependent calcium channels. *J. Biol. Chem.* 270: 2473–2477, 1995.
14. BABCOCK, D. F., J. HERRINGTON, P. C. GOODWIN, Y. B. PARK, AND B. HILLE. Mitochondrial participation in the intracellular Ca^{2+} network. *J. Cell Biol.* 136: 833–844, 1997.
15. BACSKAI, B. J., P. WALLÉN, V. LEV-RAM, S. GRILLNER, AND R. Y. TSIEN. Activity-related calcium dynamics in lamprey motoneurons as revealed by video-rate confocal microscopy. *Neuron* 14: 19–28, 1995.
16. BADMINTON, M. N., A. K. CAMPBELL, AND C. M. REMBOLD. Differential regulation of nuclear and cytosolic Ca^{2+} in HeLa cells. *J. Biol. Chem.* 271: 31210–31214, 1996.
17. BADMINTON, M. N., J. M. KENDALL, C. M. REMBOLD, AND A. K. CAMPBELL. Current evidence suggests independent regulation of nuclear calcium. *Cell Calcium* 23: 79–86, 1998.
18. BADMINTON, M. N., J. M. KENDALL, G. SALA-NEWBY, AND A. K. CAMPBELL. Nucleoplasmin-targeted aequorin provides evidence for nuclear calcium barrier. *Exp. Cell Res.* 216: 236–243, 1995.
19. BAKER, A. J., R. BRANDES, J. H. M. SCHREUR, S. A. CAMACHO, AND M. W. WEINER. Protein and acidosis alter calcium-binding and fluorescence spectra of the calcium indicator indo-1. *Biophys. J.* 67: 1646–1654, 1994.
20. BARBER, K., R. R. MALA, M. P. LAMBERT, R. QIU, R. C. MACDONALD, AND W. L. KLEIN. Delivery of membrane-impermeant fluorescent probes into living neural cell populations by lipotransfer. *Neurosci. Lett.* 207: 17–20, 1996.
21. BARCENAS-RUIZ, L., AND W. G. WIER. Voltage dependence of intracellular $[Ca^{2+}]_i$ transients in guinea pig ventricular myocytes. *Circ. Res.* 61: 148–154, 1987.
22. BARRERO, M. J., M. MONTERO, AND J. ALVAREZ. Dynamics of $[Ca^{2+}]$ in the endoplasmic reticulum and cytoplasm of intact Hela cells: a comparative study. *J. Biol. Chem.* 272: 27694–27699, 1997.
23. BASSNETT, S., L. REINISCH, AND D. C. BEEBE. Intracellular pH measurement using single excitation-dual emission fluorescence ratios. *Am. J. Physiol.* 258 (*Cell Physiol.* 27): C171–C178, 1990.
24. BAUDET, S., L. HOVE-MADSEN, AND D. M. BERS. How to make and use calcium-specific mini- and microelectrodes. *Methods Cell Biol.* 40: 93–113, 1994.
25. BAYLOR, S. M., AND S. HOLLINGWORTH. Fura-2 calcium transients in frog skeletal muscle fiber. *J. Physiol. (Lond.)* 403: 151–192, 1988.
26. BECKER, E. L., AND P. M. HENSON. Biochemical characteristics of ATP-induced secretion of lysosomal enzymes from rabbit polymorphonuclear leukocytes. *Inflammation* 1: 71–84, 1975.
27. BECKER, P. L., AND F. S. FAY. Photobleaching of fura-2 and its effect on determination of calcium concentrations. *Am. J. Physiol.* 253 (*Cell Physiol.* 22): C613–C618, 1987.
28. BECKER, P. L., J. V. WALSH, J. J. SINGER, AND F. S. FAY. Calcium buffering capacity, calcium currents, and $[Ca^{2+}]$ changes in voltage clamped, fura-2 loaded single smooth muscle cells (Abstract). *Biophys. J.* 53: 595a, 1988.
29. BERNAL, S. D., T. J. LAMPIDIS, I. C. SUMMERHAYES, AND L. B. CHEN. Rhodamine-123 selectively reduces clonal growth of carcinoma cells in vitro. *Science* 218: 1117, 1982.
30. BERRIDGE, M. J. Inositol trisphosphate-induced membrane potential oscillations in *Xenopus* oocytes. *J. Physiol. (Lond.)* 403: 589–599, 1988.
31. BERRIDGE, M. J. Inositol triphosphate and calcium signalling. *Nature* 361: 315–325, 1993.
32. BERRIDGE, M. J. The AM and FM of calcium signalling. *Nature* 386: 759–760, 1997.
33. BLATTER, L. A., AND W. G. WIER. Intracellular diffusion, binding, and compartmentalization of the fluorescent calcium indicators indo-1 and fura-2. *Biophys. J.* 58: 1491–1499, 1990.
34. BLINKS, J. R., W. G. WIER, P. HESS, AND F. G. PRENDERGAST. Measurement of Ca^{2+} concentrations in living cells. *Prog. Biophys. Mol. Biol.* 40: 1–114, 1982.
35. BLUMENFELD, H., L. ZABLOW, AND B. SABATINI. Evaluation of cellular mechanisms for modulation of calcium transients using a mathematical model of fura-2 Ca^{2+} imaging in *Aplysia* sensory neurons. *Biophys. J.* 63: 1146–1164, 1992.
36. BOND, J. M., E. CHACON, B. HERMAN, AND J. J. LEMASTERS. Intracellular pH and Ca^{2+} homeostasis in the pH paradox of reperfusion injury to neonatal rat cardiac myocytes. *Am. J. Physiol.* 265 (*Cell Physiol.* 34): C129–C137, 1993.
37. BORLE, A. B., C. C. FREUDENRICH, AND K. W. SNOWDONE. A simple method for incorporating aequorin into mammalian cells. *Am. J. Physiol.* 251 (*Cell Physiol.* 20): C323–C326, 1986.
38. BORLE, A. B., AND K. W. SNOWDONE. Measurement of intracellular free calcium in monkey kidney cells with aequorin. *Science* 217: 252–254, 1982.
39. BORLE, A. B., AND K. W. SNOWDONE. Measurement of intracellular ionized calcium with aequorin. *Methods Enzymol.* 124: 90–116, 1985.
40. BRAIN, K. L., AND M. R. BENNETT. Calcium in sympathetic varicosities of mouse vas deferens during facilitation, augmentation and autoinhibition. *J. Physiol. (Lond.)* 502: 521–536, 1997.
41. BRAKENHOFF, G. J., M. MÜLLER, AND R. I. GHAUHARALI. Analysis of efficiency of two-photon versus single-photon absorption for fluorescence generation in biological objects. *J. Microsc.* 183: 140–144, 1995.
42. BRAKENHOFF, G. J., H. T. M. VAN DE VOORT, E. A. VAN SPRONSEN, W. A. M. LINNEMANS, AND N. NANNINGA. Three-dimensional chromatin distribution in neuroblastoma nuclei shown by confocal scanning laser microscopy. *Nature* 317: 748–749, 1985.
43. BRIGHT, G. R., G. W. FISHER, J. ROGOWSKA, AND D. L. TAYLOR. Fluorescence ratio imaging microscopy: temporal and spatial measurements of cytoplasmic pH. *J. Cell Biol.* 104: 1019–1033, 1987.
44. BRIGHT, G. R., J. E. WHITAKER, R. P. HAUGLAND, AND D. L. TAYLOR. Heterogeneity of the changes in cytoplasmic pH upon serum stimulation of quiescent fibroblasts. *J. Cell. Physiol.* 141: 410–419, 1989.
45. BRINI, M., F. DE GIORGI, M. MURGIA, R. MARSAULT, M. L. MASSIMINO, M. CANTINI, R. RIZZUTO, AND T. POZZAN. Subcellular analysis of Ca^{2+} homeostasis in primary cultures of skeletal muscle myotubes. *Mol. Biol. Cell* 8: 129–143, 1997.

46. BRINI, M., R. MARSAULT, C. BASTIANUTTO, J. ALVAREZ, T. POZZAN, AND R. RIZZUTO. Transfected aequorin in the measurement of cytosolic Ca^{2+} concentration ($[Ca^{2+}]_c$): a critical evaluation. *J. Biol. Chem.* 270: 9896–9903, 1995.
47. BRINI, M., R. MARSAULT, C. BASTIANUTTO, T. POZZAN, AND R. RIZZUTO. Nuclear targeting of aequorin: a new approach for measuring nuclear Ca^{2+} concentration in intact cells. *Cell Calcium* 16: 259–268, 1994.
48. BRINI, M., M. MURGIA, L. PASTI, D. PISCARD, T. POZZAN, AND R. RIZZUTO. Nuclear Ca^{2+} concentration measured with specifically targeted recombinant aequorin. *EMBO J.* 12: 4813–4819, 1993.
49. BURNS, J. M., AND G. K. LEWIS. Improved measurement of calcium mobilization by flow cytometry. *Biotechniques* 23: 1022–1026, 1997.
50. BUSH, D. S., AND R. L. JONES. Measurement of cytoplasmic calcium in aleurone protoplasts using indo-1 and fura-2. *Cell Calcium* 8: 455–472, 1987.
51. BUTTON, D., AND A. EIDSATH. Aequorin targeted to the endoplasmic reticulum reveals heterogeneity in luminal Ca^{2+} concentration and reports agonist- or IP_3-induced release of Ca^{2+}. *Mol. Biol. Cell* 7: 419–434, 1996.
52. BYGRAVE, F. L., AND A. BENEDETTI. What is the concentration of calcium ion in the endoplasmic reticulum? *Cell Calcium* 19: 547–551, 1996.
53. CAMACHO, P., AND J. D. LECHLEITER. Increased frequency of calcium waves in *Xenopus laevis* oocytes that express a calcium-ATPase. *Science* 260: 226–229, 1993.
54. CAMPBELL, A. K. Extraction, partial purification and properties of obelin, the calcium-activated luminescent protein from hydroid *Obelia geniculata*. *Biochem. J.* 143: 411–418, 1974.
55. CAMPBELL, A. K., R. A. DAW, M. B. HALLETT, AND P. LUZIO. Direct measurement of the increase in intracellular free calcium ion concentration in response to the action of complement. *Biochem. J.* 194: 551–560, 1981.
56. CAMPBELL, A. K., AND M. B. HALLETT. Measurement of intracellular calcium ions and oxygen radicals in polymorphonuclear leucocyte-erythrocyte "ghost" hybrids. *J. Physiol. (Lond.)* 338: 537–550, 1983.
57. CANNELL, M. B., J. R. BERLIN, AND W. J. LEDERER. Effect of membrane potential changes on the calcium transient in single rat cardiac cells. *Science* 238: 1419–1423, 1987.
58. CARTER, T. D., AND D. OGDEN. Kinetics of Ca^{2+} release by $InsP_3$ in pig single aortic endothelial cells: evidence for an inhibitory role of cytosolic Ca^{2+} in regulating hormonally evoked Ca^{2+} spike. *J. Physiol. (Lond.)* 504: 17–33, 1997.
59. CHACON, E., H. OHATA, I. S. HARPER, D. R. TROLLINGER, B. HERMAN, AND J. J. LEMASTERS. Mitochondrial free calcium transients during excitation-contraction coupling in rabbit cardiac myocytes. *FEBS Lett.* 382: 31–36, 1996.
60. CHACON, E., J. M. REECE, A. L. NIEMINEN, G. ZAHREBELSKI, B. HERMAN, AND J. J. LEMASTERS. Distribution of electrical potential, pH, free Ca^{2+}, and volume inside cultured adult rabbit cardiac myocytes during chemical hypoxia: a multiparameter digitized confocal microscopic study. *Biophys. J.* 66: 942–952, 1994.
61. CHALFIE, M. Y., Y. TU, G. EUSKIRCHEN, W. W. WARD, AND D. C. PRASHER. Green fluorescent protein as a marker for gene expression. *Science* 263: 802–805, 1994.
62. CHANG, D. C., AND C. MENG. A localized elevation of cytosolic free calcium is associated with cytokinesis in the zebrafish embryo. *J. Cell Biol.* 131: 1539–1545, 1995.
63. CHAREST, R., P. F. BLACKMORE, AND J. H. EXTON. Characterization of responses of isolated rat hepatocytes to ATP and ADP. *J. Biol. Chem.* 260: 15789–15794, 1985.
64. CHENG, H., W. J. LEDERER, AND M. B. CANNELL. Calcium sparks: elementary events underlying excitation-contraction coupling in heart muscle. *Science* 262: 740–744, 1993.
65. CLAFLIN, D. R., D. L. MORGAN, D. G. STEPHENSON, AND F. J. JULIAN. The intracellular Ca^{2+} transient and tension in frog skeletal muscle fibers measures with high temporal resolution. *J. Physiol. (Lond.)* 475: 319–325, 1994.
66. CLAPPER, D. L., AND P. M. CONN. Gonadotropin-releasing hormone stimulation of pituitary gonadotrope cells produces an increase in intracellular calcium. *Biol. Reprod.* 32: 269–278, 1985.
67. COBBOLD, P. H. Cytoplasmic free calcium and amoeboid movement. *Nature* 285: 441–446, 1980.
68. COBBOLD, P. H., K. S. R. CUTHBERSTON, M. H. GOYNS, AND V. RICE. Aequorin measurements of free calcium in single mammalian cells. *J. Cell Sci.* 61: 123–136, 1983.
69. COBBOLD, P. H., AND T. J. RINK. Fluorescence and bioluminescence measurement of cytoplasmic free calcium. *Biochem. J.* 248: 313–328, 1987.
70. COHEN, L. B., B. M. SALZBERG, H. V. DAVILA, W. N. ROSS, D. LANDOWNE, A. S. WAGGONER, AND C. H. WANG. Changes in axon fluorescence during activity: molecular probes of membrane potential. *J. Membr. Biol.* 19: 1–36, 1974.
71. COLLINS, M. L. P., AND M. R. J. SALYON. Solubility characteristics of *Micrococcus lysodeikticus* membrane components in detergents and chaotropic salts analyzed by immunoelectrophoresis. *Biochim. Biophys. Acta* 553: 40–53, 1979.
72. DAHLQUIST, R., AND B. DIAMANT. Interaction of ATP and calcium on the rat mast cell: effect on histamine release. *Acta Pharmacol. Toxicol.* 34: 368–384, 1974.
73. DASCAL, N. The use of *Xenopus* oocytes for the study of ion channels. *CRC Crit. Rev. Biochem.* 22: 317–387, 1987.
74. DAVID, G., J. N. BARRETT, AND E. F. BARRETT. Stimulation-induced changes in $[Ca^{2+}]$ in lizard motor nerve terminals. *J. Physiol. (Lond.)* 504: 83–96, 1997.
75. DAVIES, E. V., AND M. B. HALLETT. Near membrane Ca^{2+} changes resulting from store release in neutrophils: detection by FFP-18. *Cell Calcium* 19: 355–362, 1996.
76. DEBER, C. M., J. TOM-KUN, E. MACK, AND S. GRINSTEIN. Bromo-A23187: a non-fluorescent calcium ionophore for use with fluorescent probes. *Anal. Biochem.* 146: 349–352, 1985.
77. DELAGRAVE, S., R. E. HAWTIN, C. M. SILVA, M. M. YANG, AND D. C. YOUVAN. Red-shifted excitation mutants of the green fluorescent protein. *Biotechnology* 13: 151–154, 1995.
78. DELISLE, S., D. PITTET, B. V. L. POTTER, P. D. LEW, AND M. J. WELSH. $InsP_3$ and $Ins(1,3,4,5)P_4$ act in synergy to stimulate influx of extracellular Ca^{2+} in *Xenopus* oocytes. *Am. J. Physiol.* 262 (*Cell Physiol.* 31): C1456–C1463, 1992.
79. DEMAUREX, N., W. FURUYA, S. D'SOUZA, J. S. BONIFACINO, AND S. GRINSTEIN. Mechanism of acidification of the *trans*-Golgi network (TGN): in situ measurements of pH using retrieval of TGN38 and furin from the cell surface. *J. Biol. Chem.* 273: 2044–2051, 1998.
80. DENK, W. Two-photon scanning photochemical microscopy: mapping ligand gated ion channel distributions. *Proc. Natl. Acad. Sci. USA* 91: 6629–6633, 1994.
81. DENK, W. Two-photon excitation in functional biological imaging. *J. Biomed. Optics* 1: 296–304, 1996.
82. DENK, W., J. H. STRICKLER, AND W. W. WEBB. Two-photon laser scanning fluorescence microscopy. *Science* 248: 73–76, 1990.
83. DENNIS, E. A. Formation and characterization of mixed micelles of the nonionic surfactant Triton X-100 with egg, dipalmitoyl, and dimyristoyl phosphatidylcholines. *Arch. Biochem. Biophys.* 165: 764–773, 1974.
84. DEVLIN, C. L., AND P. J. SMITH. A non-invasive vibrating calcium-selective electrode measures acetylcholine-induced calcium flux across the sarcolemma of a smooth muscle. *J. Comp. Physiol. B Biochem. Syst. Environ. Physiol.* 166: 270–277, 1996.
85. DIGREGORIO, D. A., AND J. L. VERGARA. Localized detection of action potential-induced presynaptic calcium transients at a *Xenopus* neuromuscular junction. *J. Physiol. (Lond.)* 505: 585–592, 1997.
86. DILIBERTO, P. A., AND B. HERMAN. Quantitative estimation of PDGF-induced nuclear free calcium oscillations in single cells performed by confocal microscopy with fluo-3 and fura-red (Abstract). *Biophys. J.* 64: A130, 1993.
87. DILIBERTO, P. A., X. F. WANG, AND B. HERMAN. Confocal imaging of Ca^{2+} in cells. *Methods Cell Biol.* 40: 243–262, 1994.
88. DI VIRGILIO, F., C. FASOLATO, AND T. H. STEINBERG. Inhibitors of membrane transport system for organic anions block fura-2 excretion from PC12 and N2A cells. *Biochem. J.* 256: 959–963, 1988.
89. DI VIRGILIO, F., T. H. STEINBERG, AND S. C. SILVERSTEIN. Organic-anion transport inhibitors to facilitate measurement of

cytosolic free Ca^{2+} with fura-2. *Methods Cell Biol.* 31: 453–462, 1989.
90. DI VIRGILIO, F., T. H. STEINBERG, AND S. C. SILVERSTEIN. Inhibition of fura-2 sequestration and secretion with organic anion transport blockers. *Cell Calcium* 11: 57–62, 1990.
91. DONNADIEU, E., AND L. Y. W. BOURGUIGNON. Ca^{2+} signaling in endothelial cells stimulated by bradykinin: Ca^{2+} measurement in the mitochondria and cytosol by confocal microscopy. *Cell Calcium* 20: 53–61, 1996.
92. DUFFY, S., AND B. A. MACVICAR. Adrenergic calcium signaling in astrocyte networks within the hippocampal slice. *J. Neurosci.* 15: 5535–5550, 1995.
93. DUNNE, J. F. Time window analysis and sorting. *Cytometry* 12: 597–601, 1991.
94. DUTHIE, G. G., A. SHIPLEY, AND P. J. SMITH. Use of a vibrating electrode to measure changes in calcium fluxes across the cell membranes of oxidatively challenged *Aplysia* nerve cells. *Free Radical Res.* 20: 307–313, 1994.
95. EBASHI, S. Calcium binding activity of vesicular relaxing factor. *J. Biochem.* 50: 236–244, 1961.
96. EBASHI, S. Regulatory mechanism of muscle contraction with special reference to Ca-troponin-tripomyosin system. *Essays Biochem.* 10: 1–36, 1974.
97. EBASHI, S., F. EBASHI, AND A. KODAMA. Troponin is the Ca^{2+}-receptive protein in the contractile system. *J. Biochem.* 62: 137–138, 1967.
98. EBASHI, S., AND A. KODAMA. A new protein factor promoting aggregation of tropomyosin. *J. Biochem.* 58: 107–108, 1965.
99. EBASHI, S., AND F. LIPMANN. Adenosine triphosphate-linked concentration of calcium ions in a particulate fraction of rabbit muscle. *J. Cell Biol.* 14: 389–400, 1962.
100. EBERHARD, M., AND P. ERNE. Calcium binding to fluorescent indicators: calcium green, calcium orange and calcium crimson. *Biochem. Biophys. Res. Commun.* 180: 209–215, 1991.
101. EL-FOULY, M. H., J. E. TROSKO, AND C. C. CHANG. Scrape-loading and dye transfer: a rapid and simple technique to study gap junctional intercellular communincation. *Exp. Cell Res.* 168: 422–430, 1987.
102. ELIAS, P. M., J. GOERKE, AND D. S. FRIEND. Freeze-fracture identification of sterol-digitonin complexes in cell and liposome membranes. *J. Cell Biol.* 78: 577–596, 1978.
103. ENDOH, M., AND J. R. BLINKS. Actions of sympathomimetic amines on the Ca^{2+} transients and contractions of rabbit myocardium: reciprocal changes in myofibrillar responsiveness to Ca^{2+} mediated through α- and β-adenoceptors. *Circ. Res.* 62: 247–265, 1988.
104. ESCOBAR, A. L., J. R. MONCK, J. M. FERNANDEZ, AND J. L. VERGARA. Localization of the site of Ca^{2+} release at the level of single sarcomere in skeletal muscle fibers. *Nature* 367: 739–741, 1994.
105. ETTER, E. F., M. A. KUHN, AND F. S. FAY. Detection of changes in near-membrane Ca^{2+} concentration using a novel membrane-associated Ca^{2+} indicator. *J. Biol. Chem.* 269: 10141–10149, 1994.
106. ETTER, E. F., A. MINTA, M. POENIE, AND F. S. FAY. Near-membrane $[Ca^{2+}]$ transients resolved using the Ca^{2+} indicator FFP18. *Proc. Natl. Acad. Sci. USA* 93: 5368–5373, 1996.
107. FABIATO, A., AND F. FABIATO. Calculator programs for computing the composition of the solution containing multiple metals and ligands used for experiments in skinned muscle cells. *J. Physiol. (Paris)* 75: 463–505, 1979.
108. FEWTRELL, C., AND E. SHERMAN. IgE receptor-activated calcium permeability pathway in rat basophilic leukemia cells: measurement of the unidirectional influx of calcium using quin2-buffered cells. *Biochemistry* 26: 6995–7003, 1987.
109. FISKUM, G., S. W. CRAIG, G. L. DECKER, AND A. L. LEHNINGER. The cytoskelton of digitonin-treated rat hepatocytes. *Proc. Natl. Acad. Sci. USA* 77: 3430–3434, 1980.
110. FLOTO, R. A., M. P. MAHAUT-SMITH, B. SOMASUNDARAM, AND J. M. ALLEN. IgG-induced Ca^{2+} oscillations in differentiated U937 cells; a study using laser scanning confocal microscopy and co-loaded Fluo-3 and Fura-Red fluorescent probes. *Cell Calcium* 18: 377–389, 1995.
111. GANITKEVICH, V. Y. Use of indo-1FF for measurements of rapid micromolar cytoplasmic free Ca^{2+} increments in a single smooth muscle cell. *Cell Calcium* 23: 313–322, 1998.
112. GANZ, M. B., J. RASMUSSEN, W. B. BOLLAG, AND H. RASMUSSEN. Effect of buffer systems and pH_i on the measurement of $[Ca^{2+}]_i$ with fura 2. *FASEB J.* 4: 1638–1644, 1990.
113. GEHRIG, P. R. B., AND W. SIMON. Very lipophilic Ca^{2+}-selective ionophore for chemical sensors of high lifetime. *Chimia* 43: 377–379, 1989.
114. GÖPPERT-MAYER, M. Üeber elementarakte miz zwei quantenspruengen. *Ann. Phys.* 9: 273–295, 1931.
115. GEORGE, C. H., J. M. KENDALL, A. K. CAMPBELL, AND W. H. EVANS. Connexin-aequorin chimerae report cytoplasmic calcium environments along trafficking pathways leading to gap junction biogenesis in living COS-7 cells. *J. Biol. Chem.* 273: 29822–29829, 1998.
116. GILCHRIST, J. S. C., C. PALAHNIUK, AND R. BOSE. Spectroscopic determination of sarcoplasmic reticulum Ca^{2+} uptake and Ca^{2+} release. *Mol. Cell. Biochem.* 172: 159–170, 1997.
117. GILROY, S., AND R. L. JONES. Gibberellic acid and abscisic acid coordinately regulate cytoplasmic calcium and secretory activity in barley aleurone protoplasts. *Proc. Natl. Acad. Sci. USA* 89: 3591–3595, 1992.
118. GIRARD, S., AND D. CLAPHAM. Acceleration of intracellular calcium waves in *Xenopus* oocytes by calcium influx. *Science* 260: 229–232, 1993.
119. GIROY, S., N. D. READ, AND A. J. TREWAVAS. Elevation of cytoplasmic calcium by caged calcium or caged inositol triphosphate initiates stomatal closure. *Nature* 346: 769–771, 1990.
120. GIULIANO, K. A., AND R. J. GILLIES. Determination of intracellular pH of BALB/c-373 cells using the fluorescence of pyranine. *Anal. Biochem.* 167: 362–371, 1987.
121. GLENNON, M. C., G. ST. J. BIRD, C. Y. KWAN, AND J. W. PUTNEY, JR. Actions of vasopressin an the Ca^{2+}-ATPase inhibitor, thapsigargin, on Ca^{2+} signaling in hepatocytes. *J. Biol. Chem.* 267: 8230–8233, 1992.
122. GLENNON, M. C., G. S. J. BIRD, H. TAKEMURA, O. THASTRUP, B. A. LESLIE, AND J. W. PUTNEY. In situ imaging of agonist-sensitive calcium pools in AR4–2J pancreatoma cells: evidence for an agonist- and inositol 1,4,5-triphosphate-sensitive calcium pool in or closely associated with the nuclear envelope. *J. Biol. Chem.* 267: 25568–25575, 1992.
123. GOLCONDA, M. S., N. UEDA, AND S. V. SHAH. Evidence suggesting that iron and calcium are interrelated in oxidant-induced DNA damage. *Kidney Int.* 44: 1228–1234, 1993.
124. GOLOVINA, V. A., AND M. P. BLAUSTEIN. Spatially and functionally distinct Ca^{2+} stores in sarcoplasmic and endoplasmic reticulum. *Science* 275: 1643–1648, 1997.
125. GRIFFITHS, E. J., S. WEI, M. C. P. HAIGNEY, C. J. OCAMPO, M. D. STERN, AND H. S. SILVERMAN. Inhibition of mitochondrial calcium effux by conazepam in intact single rat cardiomyocytes and effects on NADH production. *Cell Calcium* 21: 321–329, 1997.
126. GRODEN, D. L., Z. GUAN, AND B. T. STOKES. Determination of fura-2 dissociation constants following adjustment of the apparent Ca-EGTA association constant for temperature and ionic strength. *Cell Calcium* 12: 279–287, 1991.
127. GRYNKIEWICZ, G., M. POENIE, AND R. Y. TSIEN. A new generation of Ca^{2+} indicators with greatly improved fluorescence properties. *J. Biol. Chem.* 260: 3440–3450, 1985.
128. GUNTER, T. E., D. RESTREPO, AND K. K. GUNTER. Conversion of esterified fura-2 and indo-1 to Ca^{2+}-sensitive forms by mitochondria. *Am. J. Physiol.* 255 (*Cell Physiol.* 24): C304–C310, 1988.
129. GURNEY, A. M., P. CHARNET, J. M. PYE, AND J. NARGEOT. Augmentation of cardiac calcium current by flash photolysis of intracellular caged-Ca^{2+} molecules. *Nature* 341: 65–68, 1989.
130. GURNEY, A. M., R. Y. TSIEN, AND H. A. LESTER. Activation of a potassium current by rapid photochemically generated step increases of intracellular calcium in rat sympathetic neurons. *Proc. Natl. Acad. Sci. USA* 84: 3496–3500, 1987.
131. GWATHMEY, J. K., L. COPELAS, R. MACKINNON, F. J. SHOEN, M. D. FELDMAN, W. GROSSMAN, AND J. P. MORGAN. Abnormal intracellular calcium handling in myocardium from patients with end-stage heart failure. *Circ. Res.* 61: 70–76, 1987.
132. HAJN CZKY, G., L. D. ROBB-GASPERS, M. B. SEIZ, AND A. P.

THOMAS. Decoding of calcium oscillations in the mitochondria. *Cell* 82: 415–424, 1995.
133. HAJNÓCZKY, G., AND A. P. THOMAS. Minimal requiements for calcium oscillations driven by the IP_3 receptor. *EMBO J.* 16: 3533–3545, 1997.
134. HALLETT, M. B., AND A. K. CAMPBELL. Uptake of liposomes containing the photoprotein obelin by rat isolated adipocytes: adhesion, endocytosis or fusion? *Biochem. J.* 192: 587–596, 1980.
135. HALLETT, M. B., AND A. K. CAMPBELL. Measurement of changes in cytoplasmic free Ca^{2+} in fused cell hybrids. *Nature* 295: 155–158, 1982.
136. HAMA, T., A. TAKAHASHI, A. ICHIHARA, AND T. TAKAMATSU. Real time in situ confocal imaging of calcium wave in the perfused whole heart of the rat. *Cell. Signal.* 10: 331–337, 1998.
137. HAMILL, O. P., A. MARTY, E. NEHER, AND F. J. SIGWORTH. Improved patch-clamp techniques for high-resolution current recording from cells and cell free patches. *Pflügers Arch.* 391: 85–100, 1981.
138. HARAFUJI, H., AND Y. OGAWA. Re-examination of the apparent binding constant of ethylene glycol bis(β-aminoethyl ether)-*N,N,N′,N′*-tetraacetic acid with calcium around neutral pH. *J. Biochem.* 87: 1305–1312, 1980.
139. HARBIG, K., B. CHANCE, A. G. B. KOVÁCH, AND M. REIVICH. In vivo measurement of pyridine nucleotide fluorescence from cat brain cortex. *J. Appl. Physiol.* 41: 480–488, 1976.
140. HARKINS, A. B., N. KUREBAYASHI, AND S. M. BAYLOR. Resting myoplasmic free calcium in frog skeletal muscle fibers estimated with fluo-3. *Biophys. J.* 65: 865–881, 1993.
141. HARRISON, S. M., AND D. M. BERS. The effect of temperature and ionic strength on the apparent Ca-affinity of EGTA and the analogous Ca-chelators BAPTA and dibromo-BAPTA. *Biochim. Biophys. Acta* 925: 133–143, 1987.
142. HARTZELL, H. C. Activation of different Cl currents in *Xenopus* oocytes by Ca liberated from stores and by capacitative Ca influx. *J. Gen. Physiol.* 108: 157–175, 1996.
143. HAWORTH, R. A., AND D. REDON. Calibration of intracellular Ca transients of isolated adult heart cells labelled with fura-2 by acetoxymethyl ester loading. *Cell Calcium* 24: 263–273, 1998.
144. HEILBRUNN, L. V. *An Outline of General Physiology.* Philadelphia, PA: Saunders, 1937.
145. HEILBRUNN, L. V. The action of calcium on muscle protoplasm. *Physiol. Zool.* 13: 88–94, 1940.
146. HEILBRUNN, L. V. *The Dynamics of Living Protoplasm.* New York: Academic, 1956.
147. HEILBRUNN, L. V., AND F. J. WIERCINSKI. The action of various cations on muscle protoplasm. *J. Cell. Comp. Physiol.* 29: 15–32, 1947.
148. HEIM, R., D. C. PRASHER, AND R. Y. TSIEN. Wavelength mutations and posttranslational autoxidation of green fluorescent protein. *Proc. Natl. Acad. Sci. USA* 91: 12501–12504, 1994.
149. HEPPEL, L. A., G. A. WEISMAN, AND I. FRIEDBERG. Permeabilization of transformed cells in culture by external ATP. *J. Membr. Biol.* 86: 189–196, 1985.
150. HERMAN, B., G. J. GORES, A. L. NIEMINEN, T. KAWANISHI, A. HARMAN, AND J. J. LEMASTERS. Calcium and pH in anoxic and toxic injury. *Crit. Rev. Toxicol.* 21: 127–148, 1990.
151. HERMAN, B., X. F. WANG, A. PERIASAMY, S. KWON, G. GORDON, AND P. WODNICKI. Fluorescence lifetime imaging in cell biology. *SPIE* 2678: 88–97, 1996.
152. HERMAN, B., P. WODNICKI, S. KWON, A. PERIASAMY, G. W. GORDON, N. MAHAJAN, AND W. F. WANG. Recent developments in monitoring calcium and protein interactions in cell using fluorescence lifetime microscopy. *J. Fluorescence* 7: 85–91, 1997.
153. HESKETH, T. R., G. A. SMITH, J. P. MOORE, M. V. TAYLOR, AND J. C. METCALFE. Free cytoplasmic calcium concentration and the mitogenic stimulation of lymphocytes. *J. Biol. Chem.* 258: 4876–4882, 1983.
154. HIBINO, M., M. SHIGEMORI, H. ITOH, K. NAGAYAMA, AND K. J. KINOSITA. Membrane conductance of an electroporated cell analyzed by submicrosecond imaging of transmembrane potential. *Biophys. J.* 59: 209–220, 1991.
155. HOFER, A. M., AND T. E. MACHEN. Technique for in situ measurement of calcium in intracellular inositol 1,4,5-triphosphate-sensitive stores using the fluorescent indicator mag-fura-2. *Proc. Natl. Acad. Sci. USA* 90: 2598–2602, 1993.
156. HOFER, A. M., AND T. E. MACHEN. Direct measurement of free Ca in organelles of gastric epithelial cells. *Am. J. Physiol.* 267 (*Gastrointest. Liver Physiol.* 30): G442–G451, 1994.
157. HOFER, A. M., W. R. SCHLUE, S. CURCI, AND T. E. MACHEN. Spatial distribution and quantitation of free luminal [Ca] within $InsP_3$-sensitive internal store of individual BHK-21 cells: ion dependence of $InsP_3$-induced Ca release and reloading. *FASEB J.* 9: 788–798, 1995.
158. HOFER, A. M., AND I. SCHULZ. Quantification of intraluminal free [Ca] in the agonist-sensitive internal calcium store using compartmentalized fluorescent indicators: some considerations. *Cell Calcium* 20: 235–242, 1996.
159. HOPE, F. W., P. R. TURNER, W. F. J. DENETCLAW, P. REDDY, AND R. A. STEINHARDT. A critical evaluation of resting intracellular free calcium regulation in dystrophic *mdx* muscle. *Am. J. Physiol.* 271 (*Cell Physiol.* 40): C1325–C1339, 1996.
160. HOTH, M., C. M. FANGER, AND R. S. LEWIS. Mitochondrial regulation of store-operated calcium signaling in T lymphocytes. *J. Cell Biol.* 137: 633–648, 1997.
161. HOVE-MADSEN, L., AND D. M. BERS. Indo-1 binding to protein in permeabilized ventricular myocytes alters its spectral and Ca binding properties. *Biophys. J.* 63: 89–97, 1992.
162. HURLEY, T. W., M. P. RYAN, AND R. W. BRINCK. Changes of cytosolic Ca^{2+} interfere with measurements of cytosolic Mg^{2+} using mag-fura-2. *Am. J. Physiol.* 263 (*Cell Physiol.* 32): C300–C307, 1992.
163. HYRC, K., S. D. HANDRAN, S. M. ROTHMAN, AND M. P. GOLDBERG. Ionized intracellular calcium concentration predicts excitotic neuronal death: observations with low-affinity fluorescent calcium indicator. *J. Neurosci.* 17: 6669–6677, 1997.
164. HYRC, K. L., J. M. BOWNIK, AND M. P. GOLDBERG. Neuronal free calcium measurement using BTC/AM, a low affinity calcium indicator. *Cell Calcium* 24: 165–175, 1998.
165. IATRIDOU, H., E. FOUKARAKI, M. A. KUHN, E. M. MARCUS, R. P. HAUGLAND, AND H. E. KATERINOPOULOS. The development of a new family of intracellular calcium probes. *Cell Calcium* 15: 190–198, 1994.
166. IKENOUCHI, H., G. A. PEETERS, AND W. H. BARRY. Evidence that binding of indo-1 to cardiac myocyte protein does not markedly change K_d for Ca^{2+}. *Cell Calcium* 12: 415–422, 1991.
167. ILLNER, H., J. A. S. MCGUIGAN, AND D. LÜTHI. Evaluation of mag-fura-5, the new fluorescent indicator for free magnesium measurements. *Pflügers Arch.* 422: 179, 1992.
168. INOUYE, S., S. AOYAMA, T. MIYATA, F. I. TSUJI, AND Y. SAKAKI. Overexpression and purification of the recombinant Ca^{2+}-binding protein, apoaequorin. *J. Biochem.* 105: 473–477, 1989.
169. INOUYE, S., M. NOGUCHI, Y. SAKAKI, Y. TAKAGI, T. MIYATA, S. IWANAGA, T. MIYATA, AND F. I. TSUJI. Cloning and sequence analysis of cDNA for luminescent protein aequorin. *Proc. Natl. Acad. Sci. USA* 82: 3154–3158, 1985.
170. INOUYE, S., AND F. I. TSUJI. Aequorea green fluorescent protein: expression of the gene and fluorescence characteristics of recombinant protein. *FEBS Lett.* 341: 277–280, 1994.
171. ISHINO, Y., J. MINENO, T. INOUE, H. FUJIMIYA, K. YAMAMOTO, T. TAMURA, M. HOMMA, K. TANAKA, AND I. KATO. Practical applications in molecular biology of sensitive fluorescence detection by laser-excited fluorescence image analyzer. *Biotechniques* 13: 936–943, 1992.
172. ITO, K., Y. MIYASHITA, AND H. KASAI. Micromolar and submicromolar Ca^{2+} spikes regulating distinct cellular functions in pancreatic acinar cells. *EMBO J.* 16: 242–251, 1997.
173. JAFFE, L. F., AND S. LEVY. Calcium gradients measured with a vibrating calcium-selective electrode. *IEEE Conf.* 9: 779–781, 1987.
174. JAFFE, L. F., AND R. NUCCITELLI. An ultrasensitive vibrating probe for measuring steady extracellular currents. *J. Cell Biol.* 63: 614–628, 1974.
175. JEFFERSON, J. R., J. B. HUNT, AND A. GINSBURG. Characterization of indo-1 and quin-2 as spectroscopic probes for Zn^{2+}-protein interactions. *Anal. Biochem.* 187: 328–336, 1990.
176. JOHANSSON, J. S., AND D. H. HAYNES. Deliberate quin2 overload as a method for in situ characterization of active calcium extrusion

systems and cytoplasmic calcium binding: application to the human platelet. *J. Membr. Biol.* 104: 147–163, 1988.
177. JOHNSON, L. V., M. L. WALSH, B. J. BOCKUS, AND L. B. CHEN. Monitoring of relative mitochondrial membrane potential in living cells by fluorescence microscopy. *J. Cell Biol.* 88: 526–535, 1981.
178. JOHNSON, L. V., M. L. WALSH, AND L. B. CHEN. Localization of mitochondria in living cells with rhodamine 123. *Proc. Natl. Acad. Sci. USA* 77: 990–994, 1980.
179. JOU, M. J., T. I. PENG, AND S. S. SHEU. Histamine induces oscillations of mitochondrial free Ca^{2+} concentration in single cultured rat brain astrocytes. *J. Physiol. (Lond.)* 497: 299–308, 1996.
180. JUNE, C. H., AND P. S. RABINOVITCH. Flow cytometric measurement of intracellular ionized calcium in single cells with indo-1 and fluo-3. *Methods Cell Biol.* 33: 37–58, 1990.
181. KAISER, W., AND C. B. G. GARRETT. Two-photon excitation in CaF_2:Eu^{2+}. *Phys. Rev. Lett.* 7: 229–231, 1961.
182. KAKIUCHI, S., K. SOBUE, AND M. FUJITA. Purification of a 240,000 M_r calmodulin-binding protein from a microsomal fraction of brain. *FEBS Lett.* 132: 144–148, 1981.
183. KAKIUCHI, S., K. SOBUE, R. YAMAZAKI, J. KAMBAYASHI, M. SAKON, AND G. KOSAKI. Lack of tissue specificity of calmodulin: a rapid and high-yield purification method. *FEBS Lett.* 126: 203–207, 1981.
184. KAMADA, T., AND H. KINOSITA. Disturbances initiated from naked surface on muscle protoplasm. *Jpn. J. Zool.* 10: 469–493, 1943.
185. KAO, J. P., A. T. HAROOTUNIAN, AND R. Y. TSIEN. Photochemically generated cytosolic calcium pulses and their detection by fluo-3. *J. Biol. Chem.* 264: 8179–8184, 1989.
186. KAO, J. P. Y. Practical aspects of measuring [Ca^{2+}] with fluorescent indicators. *Methods Cell Biol.* 40: 155–181, 1994.
187. KASAI, H., AND G. J. AUGUSTINE. Cytosolic Ca^{2+} gradients triggering unidirectional fluid secretion from exocrine pancreas. *Nature* 348: 735–738, 1990.
188. KAWANISHI, T., T. KATO, H. ASOH, C. UNEYAMA, K. TOYODA, K. MOMOSE, M. TAKAHASHI, AND Y. HAYASHI. Hepatocyte growth factor-induced calcium waves in hepatocytes as revealed with rapid scanning confocal microscopy. *Cell Calcium* 18: 495–504, 1995.
189. KEATING, S. M., AND T. G. WENSEL. Nanosecond fluorescence microscopy: emission kinetics of Fura-2 in single cells. *Biophys. J.* 59: 186–202, 1991.
190. KELLY, K. A. Very early detection of changes associated with cellular activation using a modified flow cytometer. *Cytometry* 12: 464–468, 1991.
191. KENDALL, J. M., R. L. DORMER, AND A. K. CAMPBELL. Targeting aequorin to the endoplasmic reticulum of living cells. *Biochem. Biophys. Res. Commun.* 189: 1008–1016, 1992.
192. KIHARA, Y., M. INOKO, AND S. SASAYAMA. L-Methionine augments mammalian myocardial contraction by sensitizing the myofilament to Ca^{2+}. *Circ. Res.* 77: 80–87, 1995.
193. KIHARA, Y., AND J. P. MORGAN. A comparative study of three methods for intracellular loading of the calcium indicator aequorin in ferret papillary muscle. *Biochem. Biophys. Res. Commun.* 162: 402–407, 1988.
194. KINOSITA, K. J., I. ASHIKAWA, N. SAITA, H. YOSHIMURA, H. ITOH, K. NAGAYAMA, AND A. IKEGAMI. Electroporation of cell membrane visualized under a pulsed-laser fluorescence microscope. *Biophys. J.* 53: 1015–1019, 1988.
195. KITAGAWA, T., AND Y. AKAMATSU. Control of passive permeability of Chinese hamster ovary cells by external and intracellular ATP. *Biochim. Biophys. Acta* 649: 76–82, 1981.
196. KNEEN, M., J. FARINAS, Y. LI, AND A. S. VERKMAN. Green fluorescent protein as a noninvasive intracellular pH indicator. *Biophys. J.* 74: 1591–1599, 1998.
197. KNIGHT, M. R., N. D. READ, A. K. CAMPBELL, AND A. J. TREWAVAS. Imaging calcium dynamics in living plants using semi-synthetic recombinant aequorins. *J. Cell Biol.* 121: 83–90, 1993.
198. KONISHI, M., S. HOLLINGWORTH, A. B. HARKINS, AND S. M. BAYLOR. Myoplasmic calcium transients in intact frog skeletal muscle fibers monitored with the fluorescent indicator furaptra. *J. Gen. Physiol.* 97: 271–301, 1991.
199. KONISHI, M., A. OLSON, S. HOLLIGWORTH, AND S. M. BAYLOR. Myoplasmic binding of fura-2 investigated by steady-state fluorescence and absorbance measurements. *Biophys. J.* 54: 1089–1104, 1988.
200. KONISHI, M., N. SUDA, AND S. KURIHARA. Fluorescence signals from the Mg^{2+}/Ca^{2+} indicator furaputa in frog skeletal muscle fibers. *Biophys. J.* 64: 223–239, 1993.
201. KRAMER, R. H. Patch cramming: monitoring intracellular messengers in intact cells with membrane patches containing detector ion channels. *Neuron* 2: 335–341, 1990.
202. KRETSINGER, R. H. Calcium-binding proteins. *Annu. Rev. Biochem.* 45: 239–266, 1976.
203. KUDO, Y. Saibounai calcium noudo kenkyuuno kisochisiki. In: *Saibounai Calcium Jikken Protocol*, edited by Y. Kudo. Tokyo: Youdosya, 1996, p. 14–22.
204. KUDO, Y., K. AKITA, T. NAKAMURA, A. OGURA, T. MAKINO, A. TAMAGAWA, K. OZAKI, AND A. MIYAKAWA. A single optical fiber fluorometric device for measurement of intracellular Ca^{2+} concentration: its application to hippocampal neurons in vitro and in vivo. *Neuroscience* 50: 619–625, 1992.
205. KUHTREIBER, W. M., AND L. F. JAFFE. Detection of extracellular calcium gradients with a calcium-specific vibrating electrode. *J. Cell Biol.* 110: 1565–1573, 1990.
206. KUREBAYASHI, N., A. B. HARKINS, AND S. M. BAYLOR. Use of fura red as an intracellular calcium indicator in frog skeletal muscle fibers. *Biophys. J.* 64: 1934–1960, 1993.
207. KWAN, C. Y., AND J. W. J. PUTNEY. Uptake and intracellular sequestration of divalent cations in resting and methacholine-stimulated mouse lacrimal acinar cells: dissociation by Sr^{2+} and Ba^{2+} of agonist-stimulated divalent cation entry from the refilling of the agonist-sensitive intracellular pool. *J. Biol. Chem.* 265: 678–684, 1990.
208. LAKOWICZ, J. R., H. SZMACINSKI, AND M. L. JOHNSON. Calcium imaging using fluorescence lifetimes and long-wavelength probes. *J. Fluorescence* 2: 47–62, 1992.
209. LAKOWICZ, J. R., H. SZMACINSKI, K. NOWACZYK, AND M. L. JOHNSON. Fluorescence lifetime imaging of calcium using quin-2. *Cell Calcium* 13: 131–147, 1992.
210. LAKOWICZ, J. R., H. SZMACINSKI, K. NOWACZYK, AND M. L. JOHNSON. Fluorescence lifetime imaging of free and protein-bound NADH. *Proc. Natl. Acad. Sci. USA* 89: 1271–1275, 1992.
211. LAKOWICZ, J. R., H. SZMACINSKI, K. NOWACZYK, W. J. LEDERER, M. S. KIRBY, AND M. L. JOHNSON. Fluorescence lifetime imaging of intracellular calcium in COS cells using quin-2. *Cell Calcium* 15: 7–27, 1994.
212. LAMPIDIS, T. J., S. D. BERNAL, I. C. SUMMERHAYES, AND L. B. CHEN. Rhodamine-123 is selectively toxic and preferentially retained in carcinoma cells in vitro. *Ann. NY Acad. Sci.* 397: 299–302, 1982.
213. LATTANZIO, F. A. J. The effects of pH and temperature on fluorescent calcium indicators as determined with Chelex-100 and EDTA buffer systems. *Biochem. Biophys. Res. Commun.* 171: 102–108, 1990.
214. LATTANZIO, F. A. J., AND D. K. BARTSHAT. The effects of pH on rate constant, ion selectivity and thermodynamic properties of fluorescent calcium and magnesium indicators. *Biochem. Biophys. Res. Commun.* 177: 184–191, 1991.
215. LECHLEITER, J., S. GIRARD, D. CLAPHAM, AND E. PERALTA. Subcellular patterns of calcium release determined by G protein-specific residues of muscarinic receptors. *Nature* 350: 505–508, 1991.
216. LECHLEITER, J., S. GIRARD, E. PERALTA, AND D. CLAPHAN. Spiral calcium wave propagation and annihilation in *Xenopus laevis* oocytes. *Science* 252: 123–126, 1991.
217. LEE, H., R. MOHABIR, N. SMITH, M. R. FRANZ, AND W. T. CLUSIN. Effect of ischemia on calcium-dependent fluorescence transients in rabbit hearts containing indo-1: correlation with monophasic action potentials and contraction. *Circulation* 78: 1047–1059, 1988.
218. LEE, H. C., N. SMITH, R. MOHABIR, AND W. T. CLUSIN. Cytosolic calcium transients from the beating mammalian heart. *Proc. Natl. Acad. Sci. USA* 84: 7793–7797, 1987.
219. LEMASTERS, J. J., J. DIGUISEPPI, A. L. NIEMINEN, AND B. HERMAN. Blebbing, free Ca^{2+} and mitochondrial membrane potential preceding cell death in hepatocytes. *Nature* 325: 78–81, 1987.
220. LEMASTERS, J. J., G. J. GORES, A. L. NIEMINEN, T. L. DAWSON,

B. E. WRAY, AND B. HERMAN. Multiparameter digitized video microscopy of toxic and hypoxic injury in single cells. *Environ. Health Perspect.* 84: 83–94, 1990.
221. LEMASTERS, J. J., A. L. NIEMINEN, E. CHACON, J. M. BOND, I. HARPER, J. M. REECE, AND B. HERMAN. Single-cell microscopic techniques for studying toxic injury. *Methods Toxicol.* 1B: 438–455, 1994.
222. LI, Q., R. A. ALTSCHULD, AND B. T. STOKES. Quantitation of intracellular free calcium in single adult cardiomyocytes by fura-2 fluorescence microscopy: calibration of fura-2 ratio. *Biochem. Biophys. Res. Commun.* 147: 120–126, 1987.
223. LIPP, P., AND M. D. BOOTMAN. To quark or to spark, that is the question. *J. Physiol. (Lond.)* 502: 1, 1997.
224. LIPP, P., C. LÜSCHER, AND E. NIGGLI. Photolysis of caged compounds characterized by ratiometric confocal microscopy: a new approach to homogeneously control and measure the calcium concentration in cardiac myocytes. *Cell Calcium* 19: 255–266, 1996.
225. LIPP, P., AND E. NIGGLI. Ratiometric confocal Ca^{2+}-measurements with visible wavelength indicators in isolated cardiac myocytes. *Cell Calcium* 14: 359–372, 1993.
226. LIPP, P., AND E. NIGGLI. Modulation of Ca^{2+} release in cultured neonatal rat cardiac myocytes: insight from subcellular release patterns revealed by confocal microscopy. *Circ. Res.* 74: 979–990, 1994.
227. LIU, C., AND T. E. HERMANN. Characterization of ionomycin as a calcium ionophore. *J. Biol. Chem.* 253: 5892–5894, 1978.
228. LIVINGSTON, F. R., E. M. K. LUI, G. A. LOEB, AND H. J. FORMAN. Sublethal oxidant stress induces a reversible increase in intracellular calcium dependent on NAD(P)H oxidation in rat alveolar macrophages. *Arch. Biochem. Biophys.* 299: 83–91, 1992.
229. LLINÁS, R., M. SUGIMORI, AND R. B. SILVER. Microdomains of high calcium concentration in a presynaptic terminal. *Science* 256: 677–679, 1992.
230. LLOPIS, J., J. M. MCCAFFERY, A. MIYAWAKI, M. G. FARQUHAR, AND R. TSIEN. Measurement of cytosolic, mitochondrial, and Golgi pH in single living cells with green fluorescent proteins. *Proc. Natl. Acad. Sci. USA* 95: 6803–6808, 1998.
231. LLOYD, Q. P., M. A. KUHN, AND C. V. GAY. Characterization of calcium translocation across the plasma membrane of primary osteoblasts using a lipophilic calcium-sensitive fluorescent dye, calcium green C_{18}. *J. Biol. Chem.* 270: 22445–22451, 1995.
232. LOEW, L. M., W. CARRINGTON, R. A. TUFT, AND F. S. FAY. Physiological cytosolic Ca^{2+} transients evoke concurrent mitochondrial depolarizations. *Proc. Natl. Acad. Sci. USA* 91: 12579–12583, 1994.
233. LUKÁCS, G. L., AND A. KAPUS. Measurement of matrix free Ca^{2+} concentration in heart mitochondria by entrapped fura-2 and quin2. *Biochem. J.* 248: 609–613, 1987.
234. LUPPU-MEIRI, M., H. SHAPIRA, AND Y. ORON. Hemispheric asymmetry of rapid chloride responses to inositol trisphosphate and calcium in *Xenopus* oocytes. *FEBS Lett.* 240: 83–87, 1988.
235. MACHACA, K., AND H. C. HARTZELL. Asymmetrical distribution of Ca-activated Cl channels in *Xenopus* oocytes. *Biophys. J.* 74: 1286–1295, 1998.
236. MALGAROLI, A., D. MILANI, J. MELDOLESI, AND T. POZZAN. Fura-2 measurement of cytosolic free Ca^{2+} in monolayers and suspensions of various types of animal cells. *J. Cell Biol.* 105: 2145–2155, 1987.
237. MARTY, A. Ca-dependent K channels with large unitary conductance in chromaffin cell membranes. *Nature* 291: 497–500, 1981.
238. MARTÍNEZ-ZAGUILÁN, R., G. M. MARTÍNEZ, F. LATTANZIO, AND R. J. GILLIES. Simultaneous measurement of intracellular pH and Ca^{2+} using the fluorescence of SNARF-1 and fura-2. *Am. J. Physiol.* 260 (*Cell Physiol.* 29): C297–C307, 1991.
239. MARTÍNEZ-ZAGUIL[ACTUE]AN, R., G. PARNAMI, AND R. M. LYNCH. Selection of fluorescent ion indicators for simultaneous measurements of pH and Ca^{2+}. *Cell Calcium* 19: 337–349, 1996.
240. MARTY, A., Y. P. TAN, AND A. TRAUTMANN. Three types of calcium-dependent channel in rat lacrimal glands. *J. Physiol. (Lond.)* 357: 293–325, 1984.
241. MARUYAMA, I., T. HASEGAWA, T. YAMAMOTO, AND K. MOMOSE. Effects of Pluronic F-127 on loading of fura 2/AM into single smooth muscle cells isolated from guinea pig taenia coli. *J. Toxicol. Sci.* 14: 153–163, 1989.
242. MCDONOUGH, P. M., AND D. C. BUTTON. Measurement of cytoplasmic calcium concentration in cell suspensions: correction for extracellular Fura-2 through use of Mn^{2+} and probenecid. *Cell Calcium* 10: 171–180, 1989.
243. MCGUIGAN, J. A. S., D. LÜTHI, AND A. BURI. Calcium buffer solution and how to make them: a do it yourself guide. *Can. J. Physiol. Pharmacol.* 69: 1733–1749, 1991.
244. MCNEIL, P. L. Incorporation of macromolecules into living cells. *Methods Cell Biol.* 29: 153–173, 1989.
245. MCNEIL, P. L., R. F. MURPHY, F. LANNI, AND D. L. TAYLOR. A method for incorporating macromolecules into adherent cells. *J. Cell Biol.* 98: 1556–1564, 1984.
246. MEYER, T., T. WENSEL, AND L. STRYER. Kinetics of calcium channel opening by inositol 1,4,5-triphosphate. *Biochemistry* 29: 32–37, 1990.
247. MIESENBÖCK, G., D. A. DE ANGELIS, AND J. E. ROTHMAN. Visualizing secretion and synaptic transmission with pH-sensitive green fluorescent proteins. *Nature* 394: 192–195, 1998.
248. MILEDI, R. A calcium-dependent transient outward current in *Xenopus laevis* oocytes. *Proc. R. Soc. Lond. B Biol. Sci.* 215: 491–497, 1982.
249. MILEDI, R., AND I. PARKER. Chloride current induced by injection of calcium into *Xenopus* oocytes. *J. Physiol. (Lond.)* 357: 173–183, 1984.
250. MILEDI, R., I. PARKER, AND R. M. WOODWARD. Membrane currents elicited by divalent cations in *Xenopus* oocytes. *J. Physiol. (Lond.)* 417: 173–195, 1989.
251. MINAMIKAWA, T., S. H. CODY, AND D. A. WILLIAMS. In situ visualization of spontaneous calcium waves within perfused whole rat heart by confocal imaging. *Am. J. Physiol.* 272 (*Heart Circ. Physiol.* 41): H236–H243, 1997.
252. MINAMIKAWA, T., A. TAKAHASHI, AND S. FUJITA. Differences in features of calcium transients between the nucleus and the cytosol in cultured heart muscle cells: analyzed by confocal microscopy. *Cell Calcium* 17: 167–176, 1995.
253. MINAMIKAWA, T., T. TAKAMATSU, S. KASHIMA, S. FUSHIKI, AND S. FUJITA. Confocal calcium imaging with an ultraviolet laser-scanning microscope and indo-1. *Micron* 24: 551–556, 1993.
254. MINTA, A., J. P. KAO, AND R. Y. TSIEN. Fluorescent indicators for cytosolic calcium based on rhodamine and fluorescein chromophores. *J. Biol. Chem.* 264: 8171–8178, 1989.
255. MITANI, A., F. KADOYA, AND K. KATAOKA. Temperature dependence of hypoxia-induced calcium accumulation in gerbil hippocampal slices. *Brain Res.* 562: 159–163, 1991.
256. MITANI, A., S. TAKEYASU, H. YANASE, Y. NAKAMURA, AND K. KATAOKA. Changes in intracellular Ca^{2+} and energy levels during in vitro ischemia in the gerbil hippocampal slice. *J. Neurochem.* 62: 626–634, 1994.
257. MITSUI, M., A. ABE, M. TAJIMI, AND H. KARAKI. Leakage of the fluorescent Ca^{2+} indicator fura-2 in smooth muscle. *Jpn. J. Pharmacol.* 61: 165–170, 1993.
258. MIYATA, H., H. S. SILVERMAN, S. J. SOLLOTT, E. G. LAKATTA, M. D. STERN, AND R. G. HANSFORD. Measurement of mitochondrial free Ca^{2+} concentration in living single rat cardiac myocytes. *Am. J. Physiol.* 261 (*Heart Circ. Physiol.* 30): H1123–H1134, 1991.
259. MIYAWAKI, A., J. LLOPSI, R. HEIM, J. M. MCCAFFERY, J. A. ADAMS, M. IKURA, AND R. Y. TSIEN. Fluorescent indicators for Ca^{2+} based on green fluorescent proteins and calmodulin. *Nature* 388: 882–887, 1997.
260. MOHR, F. C., AND C. FEWTRELL. The effect of mitochondrial inhibitors on calcium homeostasis in tumor mast cells. *Am. J. Physiol.* 258 (*Cell Physiol.* 27): C217–C226, 1990.
261. MOISESCU, D. G., C. C. ASHLEY, AND A. K. CAMPBELL. Comparative aspects of the calcium-sensitive photoproteins aequorin and obelin. *Biochim. Biophys. Acta* 396: 133–140, 1975.
262. MONCK, J. R., I. M. ROBINSON, A. L. ESCOBAR, J. L. VERGARA, AND J. M. FERNANDEZ. Pulsed laser imaging of rapid Ca^{2+} gradients in excitable cells. *Biophys. J.* 67: 505–514, 1994.
263. MONTERO, M., M. J. BARRERO, AND J. ALVAREZ. $[Ca^{2+}]$ microdomains control agonist-induced Ca^{2+} release in intact HeLa cells. *FASEB J.* 11: 881–885, 1997.

264. MONTERO, M., M. BRINI, R. MARSAULT, J. ALVAREZ, R. SITIA, T. POZZAN, AND R. RUZZUTO. Monitoring dynamic changes in free Ca^{2+} concentration in the endoplasmic reticulum of intact cells. *EMBO J.* 14: 5467–5475, 1995.
265. MOONEY, R. A. Use of digitonin-permeabilized adipocytes for cAMP studies. *Methods Enzymol.* 159: 193–202, 1988.
266. MORGAN, J. P., T. T. DEFEO, AND K. G. MORGAN. A chemical procedure for loading the calcium indicator aequorin into mammalian working myocardium. *Pflügers Arch.* 400: 338–340, 1984.
267. MORGAN, J. P., AND K. G. MORGAN. Vascular smooth muscle: the first recorded Ca^{2+} transients. *Pflügers Arch.* 395: 75–78, 1982.
268. MUNSCH, T., AND J. W. DEITMER. Maintenance of Fura-2 fluorescence in glial cells and neurones of the leech central nervous system. *J. Neurosci. Methods* 57: 195–204, 1995.
269. MUNSCH, T., W. NETT, AND J. W. DEITMER. Fura-2 signals evoked by kainate in leech glial cells in the presence of different divalent cations. *Glia* 11: 345–353, 1994.
270. MURPHY, E., C. C. FREUDENRICH, L. A. LEVY, R. E. LONDON, AND M. LIEBERMAN. Monitoring cytosolic free magnesium in cultured chicken heart cells by use of the fluorescent indicator Furaptra. *Proc. Natl. Acad. Sci. USA* 86: 2981–1984, 1989.
271. NARAGHI, M. T-jump study of calcium binding kinetics of calcium chelators. *Cell Calcium* 22: 255–268, 1997.
272. NEHER, E. The use of fura-2 for estimating Ca buffers and Ca fluxes. *Neuropharmacology* 34: 1423–1442, 1995.
273. NEHER, E., AND W. ALMERS. Patch pipettes used for loading small cells with fluorescent indicator dyes. *Adv. Exp. Med. Biol.* 211: 1–5, 1986.
274. NEHER, E., AND G. AUGUSTINE. Calcium gradients and buffers in bovine chromaffin cells. *J. Physiol. (Lond.)* 450: 273–301, 1992.
275. NEWMAN, E. A., AND K. R. ZAHS. Calcium waves in retinal glial cells. *Science* 275: 844–847, 1997.
276. NIEMINEN, A. L., A. I. BYRNE, AND J. J. LEMASTERS. Confocal microscopic studies of oxidative stress in hepatocytes. *Cell Vision* 4: 176–177, 1997.
277. NIEMINEN, A. L., G. B. E. WRAY, Y. TANAKA, B. HERMAN, AND J. J. LEMASTERS. Calcium dependence of bleb formation and cell death in hepatocytes. *Cell Calcium* 9: 237–246, 1988.
278. NIGGLI, E., AND W. J. LEDERER. Real-time confocal microscopy and calcium measurements in heart muscle cells: towards the development of a fluorescence microscope with high temporal and spatial resolution. *Cell Calcium* 11: 121–130, 1990.
279. NIGGLI, E., AND W. J. LEDERER. Restoring forces in cardiac myocytes: insight from relaxations induced by photolysis of caged ATP. *Biophys. J.* 59: 1123–1135, 1991.
280. NIGGLI, E., D. W. PISTON, M. S. KIRBY, H. CHENG, D. R. SANDISON, W. W. WEBB, AND W. J. LEDERER. A confocal laser scanning microscope designed for indicators with ultraviolet excitation wavelength. *Am. J. Physiol.* 266 (*Cell Physiol.* 35): C303–C310, 1994.
281. NOVAK, E. J., AND P. S. RABINOVITCH. Improved sensitivity in flow cytometric intracellular ionized calcium measurement using fluo-3/fura red fluorescence ratios. *Cytometry* 17: 135–141, 1994.
282. NUCCITELLI, R. The wave of activation current in the egg of the medaka fish. *Dev. Biol.* 122: 522–534, 1987.
283. NUCCITELLI, R., D. KLINE, W. B. BUSA, R. TALEVI, AND C. CAMPANELLA. A highly localized activation current yet widespread intracellular calcium increase in the egg of the frog, *Discoglossus pictus*. *Dev. Biol.* 130: 120–132, 1988.
284. OEHME, M., M. KESSLER, AND W. SIMON. Neutral carrier Ca^{2+}-microelectrodes. *Chimia* 30: 204–206, 1976.
285. OHEIM, M., M. NARAGHI, T. H. MÜLLER, AND E. NEHER. Two dye two wavelength excitation calcium imaging: results from bovine adrenal chromaffin cells. *Cell Calcium* 24: 71–84, 1998.
286. OVERLY, C. C., K. D. LEE, E. BERTHIAUME, AND P. J. HOLLENBECK. Quantitative measurement of intraorganelle pH in the endosomal-lysosomal pathway in neurons by using ratiometric imaging with pyranine. *Proc. Natl. Acad. Sci. USA* 92: 3156–3160, 1995.
287. OWEN, C. S. Phorobol ester (12-*O*-tetradecanoylphorbol 13-acetate) partially inhibits rapid intracellular free calcium transients triggered by anti-immunogloblin in murine lymphocytes. *J. Biol. Chem.* 263: 2732–2737, 1988.
288. OWEN, C. S. Spectra of intracellular Fura-2. *Cell Calcium* 12: 385–393, 1991.
289. OWEN, C. S., N. L. SYKES, R. L. SHULER, AND D. OST. Non-calcium environmental sensitivity of intracellular indo-1. *Anal. Biochem.* 192: 142–148, 1991.
290. OZAKI, H., K. SATO, T. SATOH, AND H. KARAKI. Simultaneous recording of calcium signals and mechanical activity using fluorescent dye Fura 2 in isolated strips of vascular smooth muscle. *Jpn. J. Pharmacol.* 45: 429–433, 1987.
291. OZAKI, H., T. SSTOH, H. KARAKI, AND Y. ISHIDA. Regulation of metabolism and contraction by cytoplasmic calcium in the intestinal smooth muscle. *J. Biol. Chem.* 263: 14074–14079, 1988.
292. PADDLE, B. M. A cytoplasmic component of pyridine nucleotide fluorescence in rat diaphragm: evidence from comparisons with flavoprotein fluorescence. *Pflügers Arch.* 404: 326–331, 1985.
293. PALLOTTA, B. S., K. L. MAGLEBY, AND J. N. BARRETT. Single channel recordings of Ca^{2+} activated K^+ currents in rat muscle cell culture. *Nature* 293: 471–474, 1981.
294. PARKER, I., C. B. GUNDERSEN, AND R. MILEDI. A transient inward current elicited by hyperpolarization during serotonin activation in *Xenopus* oocytes. *Proc. R. Soc. Lond. B Biol. Sci.* 223: 279–292, 1985.
295. PARKER, I., AND R. MILEDI. Inositol trisphosphate activates a voltage-dependent calcium influx in *Xenopus* oocytes. *Proc. R. Soc. Lond. B Biol. Sci.* 231: 27–36, 1987.
296. PARKER, I., AND Y. YAO. Relation between intracellular Ca^{2+} signals and Ca^{2+}-activated Cl^- current in *Xenopus* oocytes. *Cell Calcium* 15: 276–288, 1994.
297. PATTERSON, G. H., S. M. KNOBEL, W. D. SHARIF, S. R. KAIN, AND D. W. PISTON. Use of the green fluorescent protein and its mutants in quantitative fluorescence microscopy. *Biophys. J.* 73: 2782–2780, 1997.
298. PEETERS, G. A., V. HLADY, J. H. B. BRIDGE, AND W. H. BARRY. Simultaneous measurement of calcium transients and motion in cultured heart cells. *Am. J. Physiol.* 253 (*Heart Circ. Physiol.* 22): H1400–H1408, 1987.
299. PERSECHINI, A., J. A. LYNCH, AND V. A. ROMOSER. Novel fluorescent indicator proteins for monitoring free intracellular Ca^{2+}. *Cell Calcium* 22: 209–216, 1997.
300. PETERS, S. M. A., M. J. H. TIJSEN, R. J. M. BINDELS, C. H. VAN OS, AND J. F. M. WEITZELS. Rise in cytosolic Ca^{2+} and collapse of mitochondrial potential in anoxic, but not hypoxic, rat proximal tubules. *J. Am. Soc. Nephrol.* 7: 2348–2356, 1996.
301. PETERSEN, C., AND M. BERRIDGE. The regulation of capacitative calcium entry by calcium and protein kinase C in *Xenopus* oocytes. *J. Biol. Chem.* 269: 32246–32253, 1994.
302. PETERSEN, O. H., C. C. H. PETERSEN, AND H. KASAI. Calcium and hormone action. *Annu. Rev. Physiol.* 56: 297–319, 1994.
303. PIERSON, E. S., D. D. MILLER, D. A. CALLAHAM, J. VAN AKEN, G. HACKETT, AND P. K. HEPLER. Tip-localized calcium entry fluctuates during pollen tube growth. *Dev. Biol.* 174: 160–173, 1996.
304. PINTON, P., T. POZZAN, AND R. RIZZUTO. The Golgi apparatus is an inositol 1,4,5-triphosphate-sensitive Ca^{2+} store, with functional properties distinct from those of the endoplasmic reticulum. *EMBO J.* 17: 5298–5308, 1998.
305. PISTON, D. W., M. S. KIRBY, H. CHENG, W. J. LEDERER, AND W. W. WEBB. Two-photon-excitation fluorescence imaging of three-dimensional calcium-ion activity. *Appl. Optics* 33: 662–669, 1994.
306. POENIE, M., J. ALDERTON, R. STEINHARDT, AND R. TSIEN. Calcium rises abruptly and briefly throughout the cell at the onset of anaphase. *Science* 233: 886–889, 1986.
307. POULI, A. E., N. KARAGENC, C. WASMEIER, J. C. HUTTON, N. BRIGHT, S. ARDEN, J. G. SCHOFIELD, AND G. A. RUTTER. A phogrin-aequorin chimera to image free Ca^{2+} in the vicinity of secretory granules. *Biochem. J.* 330: 1399–1404, 1998.
308. PRASHER, D. C., V. K. ECKENRODE, W. W. WARD, F. G. PRENDERGAST, AND M. J. CORMIER. Primary structure of *Aequorea victoria* green-fluorescent protein. *Gene* 111: 229–233, 1992.
309. QIAN, T., B. HERMAN, AND J. J. LEMASTERS. Confocal microscopy of the mitochondrial permeability transition in calcium ionophore toxicity and ischemia/reperfusion injury to cultured rat hepatocytes. *Cell Vision* 4: 166–167, 1997.

310. RAJDEV, S., AND I. J. REYNOLDS. Calcium green-5N, a novel fluorescent probe for monitoring high intracellular free Ca^{+} concentrations associated with glutamate excitotoxicity in cultured rat brain neurons. *Neurosci. Lett.* 162: 149–152, 1993.
311. RAJU, B., E. MURPHY, L. A. LEVY, R. D. HALL, AND R. E. LONDON. A fluorescent indicator for measuring cytosolic free magnesium. *Am. J. Physiol.* 256 (*Cell Physiol.* 25): C540–C548, 1989.
312. REGEHR, W. G., AND P. P. ATLURI. Calcium transients in cerebellar granule cell presynaptic terminals. *Biophys. J.* 68: 2156–2170, 1995.
313. REMBOLD, C. M., J. M. KENDALL, AND A. K. CAMPBELL. Measurement of changes in sarcoplasmic reticulum $[Ca^{2+}]$ in rat tail artery with targeted apoaequorin delivered by an adenoviral vector. *Cell Calcium* 21: 69–79, 1997.
314. RIDGEWAY, E. B., AND C. C. ASHLEY. Calcium transients in single muscle fibers. *Biochem. Biophys. Res. Commun.* 29: 229–234, 1967.
315. RIJKERS, G. T., L. B. JUSTEMENT, A. W. GRIFFIOEN, AND J. C. CAMBIER. Improved method for measuring intracellular Ca^{2+} with fluo-3. *Cytometry* 11: 923–927, 1990.
316. RINGER, S. Concerning the influence exerted by each of the constituents of the blood on the contraction of the ventricle. *J. Physiol. (Lond.)* 3: 380–393, 1882.
317. RINGER, S. A further contribution regarding the influence of the different constituents of the blood on the contraction of the heart. *J. Physiol. (Lond.)* 4: 29–42, 1883.
318. RINGER, S. A third contribution regarding the influence of the inorganic constituents of the blood on the ventricular contraction. *J. Physiol. (Lond.)* 4: 222–225, 1883.
319. RINGER, S. Further observations regarding the antagonism between calcium salts and sodium potassium and ammonium salts. *J. Physiol. (Lond.)* 18: 425–429, 1895.
320. RINGER, S., AND H. S. INSBURY. The action of potassium, sodium and calcium salts on tubifex rivulorum. *J. Physiol. (Lond.)* 16: 1–9, 1894.
321. RINGER, S., AND H. SAINSBURY. The influence of certain salts upon the act of clotting. *J. Physiol. (Lond.)* 11: 369–383, 1890.
322. RIZZUTO, R., C. BASTIANUTTO, M. BRINI, M. MURGIA, AND T. POZZAN. Mitochondrial Ca^{2+} homeostasis in intact cells. *J. Cell Biol.* 126: 1183–1194, 1994.
323. RIZZUTO, R., M. BRINI, M. MURGIA, AND T. POZZAN. Microdomines with high Ca^{2+} close to IP_3-sensitive channels that are sensed by neighboring mitochondria. *Science* 262: 744–747, 1993.
324. RIZZUTO, R., P. PINTON, W. CARRINGTON, F. S. FAY, K. E. FOGARTY, L. M. LIFSHITZ, R. A. TUFT, AND T. POZZAN. Close contacts with the endoplasmic reticulum as determinants of mitochondrial Ca^{2+} responses. *Science* 280: 1763–1766, 1998.
325. RIZZUTO, R., A. W. M. SIMPSON, M. BRINI, AND T. POZZAN. Rapid changes of mitochondrial Ca^{2+} revealed by specifically targeted recombinant aequorin. *Nature* 358: 325–327, 1992.
326. ROBERT, V., F. DE GIORGI, M. L. MASSIIMINO, M. CANTINI, AND T. POZZAN. Direct monitoring of the calcium concentration in the sarcoplasmic and endoplasmic reticulum of skeletal muscle myotubes. *J. Biol. Chem.* 273: 30372–30378, 1998.
327. ROBINSON, I. M., J. M. FINNEGAN, J. R. MONCK, R. M. WIGHTMAN, AND J. M. FERNANDEZ. Colocalization of calcium entry and exocytotic release sites in adrenal chromaffin cells. *Proc. Natl. Acad. Sci. USA* 92: 2474–2478, 1995.
328. RODRIGO, G. C., AND R. A. CHAPMAN. A novel resin-filled ion-sensitive micro-electrode suitable for intracellular measurements in isolated cardiac myocytes. *Pflügers Arch.* 416: 196–200, 1990.
329. ROE, M. W., J. J. LEMASTERS, AND B. HERMAN. Assessment of Fura-2 for measurements of cytosolic free calcium. *Cell Calcium* 11: 63–73, 1990.
330. ROMOSER, V. A., P. M. HINKLE, AND A. PERSECHINI. Detection in living cells of Ca^{2+}-dependent changes in the fluorescence emission of an indicator composed of two green fluorescent protein variants linked by a calmodulin-binding sequence. *J. Biol. Chem.* 272: 13270–13274, 1997.
331. ROONEY, T. A., E. J. SASS, AND A. P. THOMAS. Agonist-induced cytosolic calcium oscillations originate from a specific locus in single hepatocytes. *J. Biol. Chem.* 265: 10792–10796, 1990.
332. RUTTER, G. A., P. BURNETT, R. RIZZUTO, M. BRINI, M. MURGIA, T. POZZAN, J. M. TAVARÉ, AND R. M. DENTON. Subcellular imaging of intramitochondrial Ca^{2+} with recombinant targeted aequorin: significance for the regulation of pyruvate dehydrogenase activity. *Proc. Natl. Acad. Sci. USA* 93: 5489–5494, 1996.
333. RUTTNER, Z., L. LIGETI, L. REINLIB, K. HINES, AND A. C. MCLAUGHLIN. Monitoring of intracellular free calcium in perfused rat liver. *Cell Calcium* 14: 465–472, 1993.
334. SAKO, Y., A. SEKIHATA, Y. YANAGISAWA, M. YAMAMOTO, Y. SHIMADA, K. OZAKI, AND A. KUSUMI. Comparison of two-photon excitation laser scanning microscopy with UV-confocal laser scanning microscopy in three-dimensional calcium imaging using the fluorescence indicator Indo-1. *J. Microsc.* 185: 9–20, 1997.
335. SANDERS, R., A. DRAAIJER, H. C. GERRITSEN, P. M. HOUPT, AND Y. K. LEVEINE. Quantitative pH imaging in cells using confocal fluorescence lifetime imaging microscopy. *Anal. Biochem.* 227: 302–308, 1995.
336. SANDERS, R., H. C. GERRITSEN, A. DRAAIJER, P. M. HOUPT, AND Y. K. LEVINE. Fluorescence lifetime imaging of free calcium in single cells. *Bioimaging* 1994: 131–138, 1994.
337. SANDLER, V. M., AND W. N. ROSS. Serotonin modulates spike backpropagation and associated $[Ca^{2+}]_i$ changes in the apical dendrites of hippocampal CA1 pyramidal neurons. *J. Neurophysiol.* 81: 216–224, 1999.
338. SATO, K., H. OZAKI, AND H. KARAKI. Changes in cytosolic calcium level in vascular smooth muscle strip measured simultaneously with contraction using fluorescent calcium indicator Fura 2. *J. Pharmacol. Exp. Ther.* 246: 294–300, 1988.
339. SCALLEN, T. J., AND S. E. DIETERT. The quantitative retention of cholesterol in mouse liver prepared for electron microscopy by fixation in digitonin-containing aldehyde solution. *J. Cell Biol.* 40: 802–813, 1969.
340. SCANLON, M., D. A. WILLIAMS, AND F. S. FAY. A Ca^{2+}-insensitive form of fura-2 associated with polymorphonuclear leukocytes. *J. Biol. Chem.* 262: 6308–6312, 1987.
341. SCHEENEN, W. J. J. M., B. G. JENKS, R. J. A. M. VAN DINTER, AND E. W. ROUBOS. Spatial and temporal aspects of Ca^{2+} oscillations in *Xenopus laevis* melanotrope cells. *Cell Calcium* 19: 219–227, 1996.
342. SCHEENEN, W. J. J. M., L. R. MAKINGS, L. R. GROSS, T. POZZAN, AND R. Y. TSIEN. Photodegradation of indo-1 and its effects on apparent Ca^{2+} concentrations. *Chem. Biol.* 3: 765–774, 1996.
343. SCHEFER, U., D. AMMANN, E. PRETSCH, U. OESCH, AND W. SIMON. Neutral carrier based Ca^{2+}-selective electrode with detection limit in the subnanomolar range. *Anal. Chem.* 58: 2282–2285, 1986.
344. SCHILD, D., A. JUNG, AND H. A. SCHULTENS. Localization of calcium entry through calcium channels in olfactory receptor neurones using a laser scanning microscope and the calcium indicator dyes Fluo-3 and Fura-Red. *Cell Calcium* 15: 341–348, 1994.
345. SCHLATTERER, C., G. KNOLL, AND D. MALCHOW. Intracellular calcium during chemotaxis of *Dictyostelium descoideum*: a new fura-2 derivative avoids sequestration of the indicator and allows long-term calcium measurements. *Eur. J. Cell Biol.* 58: 172–181, 1992.
346. SCHLIEPER, P., AND E. DE ROBERTIS. Triton X-100 as a channel-forming substance in artificial lipid bilayer membrane. *Arch. Biochem. Biophys.* 184: 204–208, 1977.
347. SETO, M., K. SHINDO, K. ITO, AND Y. SASAKI. Selective inhibition of myosin phosphorylation and tension of hyperplastic arteries by the kinase inhibitor HA1077. *Eur. J. Pharmacol.* 276: 27–33, 1995.
348. SHEA, C. R., N. CHEN, J. WIMBERLY, AND T. HASAN. Rhodamine dyes as potential agents for photochemotherapy of cancer in human bladder carcioma cells. *Cancer Res.* 49: 3961–3965, 1989.
349. SHEAR, J. B., E. B. BROWN, AND W. W. WEBB. Multiphoton-excited fluorescence of fluorogen-labeled neurotransmitters. *Anal. Chem.* 68: 1778–1783, 1996.
350. SHIMADA, K., AND H. C. BERG. Response of the flagellar rotary motor to abrupt changes in extracellular pH. *J. Mol. Biol.* 193: 585–589, 1987.
351. SHIMOMURA, O. Bioluminescence in the sea: photoprotein systems. *Symp. Soc. Exp. Biol.* 39: 351–372, 1985.
352. SHIMOMURA, O., AND F. H. JOHNSON. Regeneration of the photoprotein aequorin. *Science* 256: 236–238, 1975.
353. SHIMOMURA, O., F. H. JHONSON, AND Y. SAIGA. Microdetermi-

nation of calcium by aequorin luminescence. *Science* 140: 1339–1340, 1963.
354. SHIMOMURA, O., Y. KISHI, AND S. INOUYE. The relative rate of aequorin regeneration from apoaequorin and coelenerazine analogues. *Biochem. J.* 296: 549–551, 1993.
355. SHIMOMURA, O., B. MUSICKI, AND Y. KISHI. Semi-synthetic aequorin: an improved tool for the measurement of calcium ion concentration. *Biochem. J.* 251: 405–410, 1988.
356. SHIMOMURA, O., B. MUSICKI, Y. KISHI, AND S. INOUYE. Light-emitting properties of recombinant semi-synthetic aequorins and recombinant fluorescein-conjugated aequorin for measuring cellular calcium. *Cell Calcium* 14: 373–378, 1993.
357. SHOJI, K., J. WIKMAN-COFFELT, S. T. WU, AND W. W. PARMLEY. Nature of $[Ca^{2+}]_i$ transients during ventricular fibrillation and quinidine treatment in perfused rat heart. *Am. J. Physiol.* 266 (*Heart Circ. Physiol.* 35): H1473–H1484, 1994.
358. SICK, T. J., AND M. ROSENTHAL. Indo-1 measurement of intracellular free calcium in the hippocampal slice: complications of labile NADH fluorescence. *J. Neurosci. Methods* 28: 125–132, 1989.
359. SIMONS, T. J. B. Measurement of free Zn^{2+} ion concentration with fluorescent probe Mag-fura-2 (Furaptra). *J. Biochem. Biophys. Methods* 27: 25–37, 1993.
360. SIMPSON, P. B., AND J. T. RUSSELL. Mitochondrial support inositol 1,4,5-triphosphate-mediated Ca^{2+} waves in cultured oligodendrocytes. *J. Biol. Chem.* 271: 33493–33501, 1996.
361. SIPIDO, K. R., AND G. CALLEWAERT. How to measure intracellular $[Ca^{2+}]$ in single cardiac cells with fura-2 or indo-1. *Cardiovasc. Res.* 29: 717–726, 1995.
362. SLAVÍK, J. Anilinonaphthalene sulfonate as a probe of membrane composition and function. *Biochim. Biophys. Acta* 694: 1–25, 1982.
363. SMITH, P. J., R. H. SANGER, AND L. F. JAFFE. The vibrating Ca^{2+} electrode: a new technique for detecting plasma membrane regions of Ca^{2+} influx and efflux. *Methods Cell Biol.* 40: 115–134, 1994.
364. SMITH, T. C., J. T. HERLIHY, AND S. C. ROBINSON. The effect of fluorescent probe, 3,3′-dipropylthiadicarbocyanine iodide, on the energy metabolism of Ehrlich ascites tumor cells. *J. Biol. Chem.* 256: 1108–1110, 1981.
365. SNITSAREV, V. A., T. J. MCNULTY, AND C. W. TAYLOR. Endogenous heavy metal ions perturb fura-2 measurements of basal and hormone-evoked Ca^{2+} signals. *Biophys. J.* 71: 1048–1056, 1996.
366. SOLLOTT, S. J., B. D. ZIMAN, AND E. G. LAKATTA. Novel technique to load indo-1 free acid into single adult cardiac myocytes to assess cytosolic Ca^{2+}. *Am. J. Physiol.* 262 (*Heart Circ. Physiol.* 31): H1941–H1949, 1992.
367. SOMMER, F., S. BISCHOF, M. RÖLLINGHOFF, AND M. LOHOFF. Demonstration of organic anion transport in T lymphocytes: L-lactate and fluo-3 are target molecules. *J. Immunol.* 153: 3523–3532, 1994.
368. SPENCER, I. C., AND J. R. BERLIN. Control of sarcoplasmic reticulum calcium release during calcium loading in isolated rat ventricular myocytes. *J. Physiol. (Lond.)* 488: 267–279, 1995.
369. SPENCER, I. C., AND J. R. BERLIN. A method for recording intracellular $[Ca^{2+}]$ transients in cardiac myocytes using calcium green-2. *Pflügers Arch.* 430: 579–583, 1995.
370. SPRING, K. R., AND R. J. LOWY. Characteristics of low light level television cameras. *Methods Cell Biol.* 29: 269–289, 1989.
371. SRIVASTAVA, S. K., L. F. WANG, N. H. ANSARI, AND A. BHATNAGAR. Calcium homeostasis of isolated single cortical fibers of rat lens. *Invest. Ophthamol. Vis. Sci.* 38: 2300–2312, 1997.
372. STEFENELLI, T., J. WIKMAN-COFFELT, S. T. WU, AND W. W. PARMLEY. Calcium-dependent fluorescence transients during ventricular fibrillation. *Am. Heart J.* 120: 590–597, 1990.
373. STEINBERG, S. F., J. P. BILEZIKIAN, AND Q. AL-AQWATI. Fura-2 fluorescence is localized to mitochondria in endothelial cells. *Am. J. Physiol.* 253 (*Cell Physiol.* 22): C744–C747, 1987.
374. STEINBERG, T. H., A. S. NEWMAN, J. A. SWANSON, AND S. C. SILVERSTEIN. ATP^{4-} permeabilizes the plasma membrane of mouse macrophages to fluorescent dyes. *J. Biol. Chem.* 262: 8884–8888, 1987.
375. STEINBERG, T. H., A. S. NEWMAN, J. A. SWANSON, AND S. C. SILVERSTEIN. Macrophages possess probenecid-inhibitable organic anion transporters that remove fluorescent dyes from the cytoplasmic matrix. *J. Cell Biol.* 105: 2695–2702, 1987.
376. STEINBERG, T. H., AND S. C. SILVERSTEIN. ATP permeabilization of the plasma membrane. *Methods Cell Biol.* 31: 45–61, 1989.
377. STEPHENSON, D. G., AND P. J. SUTHERLAND. Studies on the luminescent response of the Ca^{2+}-activated photoprotein obelin. *Biochim. Biophys. Acta* 678: 65–75, 1981.
378. STRICKER, S. A., V. E. CENTONZE, S. W. PADDOCK, AND G. SCHATTEN. Confocal microscopy of fertilization-induced calcium dynamics in sea urchin eggs. *Dev. Biol.* 149: 370–380, 1992.
379. SUGIYAMA, T., AND W. F. GOLDMAN. Measurement of SR free Ca^{2+} and Mg^{2+} in permeabilized smooth muscle cells with use of furaptra. *Am. J. Physiol.* 269 (*Cell Physiol.* 38): C698–C705, 1995.
380. SUMMERHAYES, I. C., T. LAMPIDISS, S. D. BERNAL, J. J. NADAKAVUKAREN, K. K. NADAKAVUKAREN, E. L. SHEPHERD, AND L. B. CHEN. Unusual retention of rhodamine 123 by mitochondria in muscle and carcinoma cell. *Proc. Natl. Acad. Sci. USA* 79: 5259–5296, 1982.
381. SUN, W. C., K. R. GEE, D. H. KLAUBERT, AND R. P. HAUGLAND. Synthesis of fluorinated fluoresceins. *J. Org. Chem.* 62: 6469–6475, 1997.
382. SUZUKI, K., K. WATANABE, Y. MATSUMOTO, M. KOBAYASHI, S. SATO, D. SISWANTA, AND H. HISAMOTO. Design and synthesis of calcium and magnesium ionophores based on double-armed diazacrown ether compounds and their application to an ion-sensing component for an ion-selective electrode. *Anal. Chem.* 67: 324–334, 1995.
383. SVOBODA, K., W. DENK, D. KLEINFELD, AND D. W. TANK. In vivo dendritic calcium dynamics in neocortical pyramidal neurons. *Nature* 385: 161–165, 1997.
384. SZMACINSKI, H., I. GRYCZYNSKI, AND J. R. LAKOWICZ. Calcium-dependent fluorescence lifetimes of indo-1 for one- and two-photon excitation of fluorescence. *Photochem. Photobiol.* 58: 341–345, 1993.
385. SZMACINSKI, H., AND J. R. LAKOWICZ. Optical measurements of pH using fluorescence lifetimes and phase-modulation fluorometry. *Anal. Chem.* 65: 1668–1674, 1993.
386. SZMACINSKI, H., AND J. R. LAKOWICZ. Possibility of simultaneously measuring low and high calcium concentrations using Fura-2 and lifetime-based sensing. *Cell Calcium* 18: 64–75, 1995.
387. TAKAHASHI, A., AND T. TAKAMATSU. Effects of basal $[Ca^{2+}]_i$ on calcium handling in Ca^{2+}-overloaded rat cultured heart muscle cells. *Cell. Signal.* 9: 617–625, 1997.
388. TAKAHASHI, M. P., M. SUGIYAMA, AND T. TSUMOTO. Laminar difference in tetanus-induced increase of intracellular Ca^{2+} in visual cortex of young rats. *Neurosci. Res.* 17: 217–228, 1993.
389. TAKAHASHI, M. P., M. SUGIYAMA, AND T. TSUMOTO. Contribution of NMDA receptors to tetanus-induced increase in postsynaptic Ca^{2+} in visual cortex of young rats. *Neurosci. Res.* 17: 229–239, 1993.
390. TAKAMATSU, T., T. MINAMIKAWA, H. KAWACHI, AND S. FUJITA. Imaging of calcium wave propagation in guinea-pig ventricular cell pairs by confocal laser scanning microscopy. *Cell Struct. Funct.* 16: 341–346, 1991.
391. TAKAMATSU, T., AND W. G. WIER. Calcium waves in mammalian heart: quantification of origin, magnitude, waveform, and velocity. *FASEB J.* 4: 1519–1525, 1990.
392. TANAKA, H., K. NISHIMURA, T. SEKINE, T. KAWANISHI, R. NAKAMURA, K. YAMAGAKI, AND K. SHIGENOBU. Two-dimensional millisecond analysis of intracellular Ca^{2+} sparks in cardiac myocytes by rapid scanning confocal microscopy: increase in amplitude by isoproterenol. *Biochem. Biophys. Res. Commun.* 233: 413–418, 1997.
393. TAO, J., AND D. H. HAYNES. Actions of thapsigargin on the Ca^{2+}-handling system of the human platelet: incomplete inhibition of the dense tubular Ca^{2+} uptake, partial inhibition of the Ca^{2+} extrusion pump, increase in plasma membrane Ca^{2+} permeability, and consequent elevation of resting cytoplasmic Ca^{2+}. *J. Biol. Chem.* 267: 24972–24982, 1992.
394. TARNOK, A. Rare-event sorting by fixed-time flow cytometry based on changes in intracellular free calcium. *Cytometry* 27: 65–70, 1997.
395. TERRY, B. R., E. K. MATTHEWS, AND J. HASELOFF. Molecular characterization of recombinant green fluorescent protein by fluorescence correlation microscopy. *Biochem. Biophys. Res. Commun.* 217: 21–27, 1995.

396. TERTYSHNIKOVA, S., AND A. FEIN. Inhibition of inositol 1,4,5-triphosphate-induced Ca^{2+} release by cAMP-dependent protein kinase in a living cell. *Proc. Natl. Acad. Sci. USA* 95: 1613–1617, 1998.
397. THORN, P., A. M. LAWRIE, P. M. SMITH, D. V. GALLACHER, AND O. H. PETERSEN. Local and global cytosolic Ca^{2+} oscillations in exocrine cells evoked by agonists and inositol trisphosphate. *Cell* 74: 661–668, 1993.
398. TROLLINGER, D. R., W. E. CASCIO, AND J. J. LEMASTERS. Selective loading of rhod-2 into mitochondria shows mitochondrial Ca^{2+} transients during the contractile cycle in adult rabbit cardiac myocytes. *Biochem. Biophys. Res. Commun.* 236: 738–742, 1997.
399. TSE, F. W., A. TSE, AND B. HILLE. Cyclic Ca^{2+} changes in intracellular stores of gonadotropes during gonadotropin-releasing hormone-stimulated Ca^{2+} oscillations. *Proc. Natl. Acad. Sci. USA* 91: 9750–9754, 1994.
400. TSIEN, R., AND T. POZZAN. Measurement of cytosolic free Ca^{2+} with quin2. *Methods Enzymol.* 172: 230–262, 1989.
401. TSIEN, R. Y. New calcium indicators and buffers with high selectivity against magnesium and protons: design, synthesis, and properties of prototype structures. *Biochemistry* 19: 2396–2404, 1980.
402. TSIEN, R. Y. A non-disruptive technique for loading calcium buffers and indicators into cells. *Nature* 290: 527–528, 1981.
403. TSIEN, R. Y. Fluorescence probes of cell signalling. *Annu. Rev. Neurosci.* 12: 227–253, 1989.
404. TSIEN, R. Y. The green fluorescent protein. *Annu. Rev. Biochem.* 67: 509–544, 1998.
405. TSIEN, R. Y., T. POZZAN, AND T. J. RINK. Calcium homeostasis in intact lymphocytes: cytoplasmic free calcium monitored with a new, intracellularly trapped fluorescent indicator. *J. Cell Biol.* 94: 325–334, 1982.
406. TSIEN, R. Y., AND R. S. ZUCKER. Control of cytoplasmic calcium with photolabile tetracarboxylate 2-nitrobenzhydrol chelators. *Biophys. J.* 50: 843–853, 1986.
407. TSUJI, F. I., Y. OHMIYA, T. F. FAGAN, H. TOH, AND S. INOUYE. Molecular evolution of the Ca^{2+}-binding photoproteins of the hydrozoa. *Photochem. Photobiol.* 62: 657–661, 1995.
408. TUCKER, T., AND R. FETTIPLACE. Confocal imaging of calcium microdomains and calcium extrusion in turtle hair cells. *Neuron* 15: 1323–1335, 1995.
409. TURAN, B., H. FLISS, AND M. DESILETS. Oxidants increase intracellular free Zn^{2+} concentration in rabbit ventricular myocytes. *Am. J. Physiol.* 272 (*Heart Circ. Physiol.* 41): H2095–H2106, 1997.
410. VALANT, P. A., P. N. ADJEI, AND D. H. HAYNES. Rapid Ca^{2+} extrusion via the Na^+/Ca^{2+} exchanger of human platelet. *J. Membr. Biol.* 130: 63–82, 1992.
411. VALANT, P. A., AND D. H. HAYNES. The Ca^{2+}-extruding ATPase of the human platelet creates and responds to cytoplasmic pH changes, consistent with a $2Ca^{2+}/nH^+$ exchange mechanism. *J. Membr. Biol.* 136: 215–230, 1993.
412. VALDEOMILLOS, M., S. C. O'NEIL, G. L. SMITH, AND D. A. EISNER. Calcium-induced calcium release activates contraction in intact cardiac cells. *Pflügers Arch.* 413: 676–678, 1989.
413. VENTURA, C., M. C. CAPOGROSSI, H. A. SPURGEON, AND E. G. LAKATTA. κ-Opioid peptide receptor stimulation increases cytosolic pH and myofilament responsiveness to Ca^{2+} in cardiac myocytes. *Am. J. Physiol.* 261 (*Heart Circ. Physiol.* 30): H1671–H1674, 1991.
414. VERGNE, I., P. CONSTANT, AND G. LANEELLE. Phagosomal pH determination by dual fluorescence flow cytometry. *Anal. Biochem.* 255: 127–132, 1998.
415. VORNDRAN, C., A. MINTA, AND M. POENIE. New fluorescent calcium indicators designed for cytosolic retention or measuring calcium near membranes. *Biophys. J.* 69: 2112–2124, 1995.
416. WAHL, M., M. J. LUCHERINI, AND E. GRUENSTEIN. Intracellular Ca^{2+} measurement with Indo-1 in substrate-attached cells: advantages and special considerations. *Cell Calcium* 11: 487–500, 1990.
417. WAMPLER, J. E., AND K. KUTZ. Quantitative fluorescence microscopy using photomultiplier tubes and imaging detectors. *Methods Cell Biol.* 29: 239–267, 1989.
418. WANG, X. F., A. PERIASAMY, B. HERMAN, AND D. M. COLEMAN. Fluorescence lifetime imaging microscopy (FLIM): instrumentation and applications. *Crit. Rev. Anal. Chem.* 23: 369–395, 1992.
419. WARD, W. W., AND S. H. BOKMAN. Reversible denaturation of *Aequorea* green-fluorescent protein: physical separation and characterization of renatured protein. *Biochemistry* 21: 4535–4540, 1982.
420. WARD, W. W., C. W. CODY, R. C. HART, AND M. J. CORMIER. Spectrophotometric identity of the energy transfer chromophores in *Renilla* and *Aequorea* green-fluorescent protein. *Photochem. Photobiol.* 31: 611–615, 1980.
421. WARD, W. W., H. J. PRENTICE, A. F. ROTH, C. W. CODY, AND S. C. REEVES. Spectral perturbations of the *Aequorea* green-fluorescent protein. *Photochem. Photobiol.* 35: 803–808, 1982.
422. WESTERBLAD, H., AND D. G. ALLEN. Intracellular calibration of the calcium indicator indo-1 in isolated fibers of *Xenopus* muscle. *Biophys. J.* 71: 908–917, 1996.
423. WHITAKER, M., AND R. PATEL. Calcium and cell cycle control. *Development* 108: 525–542, 1990.
424. WHITE, J. G., W. B. AMOS, AND M. FORDHAM. An evaluation of confocal versus conventional imaging of biological structures by fluorescence light microscopy. *J. Cell Biol.* 105: 41–48, 1987.
425. WIJNAENDTS VAN RESANDT, R. W., H. J. B. MARSMAN, R. KAPLAN, J. DAVOUST, E. H. K. STELZER, AND R. STRICKER. Optical fluorescence microscopy in three dimensions: microtomoscopy. *J. Microsc.* 138: 29–34, 1985.
426. WILLIAMS, D. A., AND F. S. FAY. Intracellular calibration of fluorescent calcium indicator Fura-2. *Cell Calcium* 11: 75–83, 1990.
427. WILLIAMS, D. A., K. E. FOGARTY, R. Y. TSIEN, AND F. S. FAY. Calcium gradients in single smooth muscle cells revealed by the digital imaging microscope using Fura-2. *Nature* 318: 558–561, 1985.
428. WILLIAMS, R. M., D. W. PISTON, AND W. W. WEBB. Two-photon molecular excitation provides intrinsic 3-dimensional resolution for laser-based microscopy and microphotochemistry. *FASEB J.* 8: 804–813, 1994.
429. WOODS, N. W., K. S. R. CUTHBERTSON, AND P. H. COBBOLD. Agonist-induced oscillations in cytoplasmic free calcium concentration in single rat hepatocytes. *Cell Calcium* 8: 79–100, 1987.
430. XU, C., J. B. SHEAR, AND W. W. WEBB. Hyper-Rayleigh and hyper-Raman scattering background of lipid water in two-photon excited fluorescence detection. *Anal. Chem.* 69: 1285–1287, 1997.
431. XU, C., AND W. W. WEBB. Measurement of two-photon excitation cross sections of molecular fluorophores with data from 690 to 1050 nm. *J. Opt. Soc. Am.* 13: 481–491, 1996.
432. XU, C., W. ZIPFEL, J. B. SHEAR, R. M. WILLIAMS, AND W. W. WEBB. Multiphoton fluorescence excitation: new spectral windows for biological nonlinear microscopy. *Proc. Natl. Acad. Sci. USA* 93: 10763–10768, 1996.
433. YAKUBU, M. A., S. MAJUMDER, AND F. KIERSZENBAUM. Changes in *Trypanosoma cruzi* infectivity by treatments that affect calcium ion levels. *Mol. Biochem. Parasitol.* 66: 119–125, 1994.
434. YAO, Y., AND I. PARKER. Inositol trisphosphate-mediated Ca^{2+} influx into *Xenopus* oocytes triggers Ca^{2+} liberation from intracellular stores. *J. Physiol. (Lond.)* 468: 275–296, 1993.
435. YEAGER, M. D., AND G. W. FEIGENSON. Direct determination of the dissociation constant for calcium sensitive indicators (Abstract). *Biophys. J.* 53: 332a, 1988.
436. YELLEN, G. Single Ca^{2+}-activated nonselective cation channel in neuroblastoma. *Nature* 296: 357–359, 1982.
437. ZHAO, M., S. HOLLINGWORTH, AND S. M. BAYLOR. Properties of tri- and tetracarboxylate Ca^{2+} indicators in frog skeletal muscle fibers. *Biophys. J.* 70: 896–916, 1996.
438. ZOREC, R., J. HOYLAND, AND W. T. MASON. Simultaneous measurements of cytosolic pH and calcium interactions in bovine lactotrophs using optical probes and four-wavelength quantitative video microscopy. *Pflügers Arch.* 423: 41–50, 1993.
439. ZUCKER, R. S. Effects of photolabile calcium chelators on fluorescent calcium indicators. *Cell Calcium* 13: 29–40, 1992.
440. ZUURENDONK, P. F., AND J. M. TAGER. Rapid separation of particulate components and soluble cytoplasm of isolated rat-liver cells. *Biochim. Biophys. Acta* 333: 393–399, 1974.